arXiv:1712.04064v5 [math.AT] 14 Feb 2022

Extracting Persistent Clusters in Dynamic Data via Möbius inversion

Woojin Kim[1] and Facundo Mémoli[2]

[1]Department of Mathematics, Duke University, woojin@math.duke.edu
[2]Department of Mathematics and Department of Computer Science and Engineering, The Ohio State University, facundo.memoli@gmail.com

February 15, 2022

Abstract

Identifying and representing *clusters* in time-varying network data is of particular importance when studying collective behaviors emerging in nature, in mobile device networks or in social networks. Based on combinatorial, categorical, and persistence theoretic viewpoints, we establish a stable functorial pipeline for the summarization of the evolution of clusters in a time-varying network.

We first construct a complete summary of the evolution of clusters in a given time-varying network over a set of entities X of which takes the form of a *formigram*. This formigram can be understood as a certain Reeb graph $\mathscr{R}$ which is labeled by subsets of X. By applying Möbius inversion to the formigram in two different manners, we obtain two dual notions of diagram: the *maximal group diagram* and the *persistence clustergram*, both of which are in the form of an 'annotated' barcode. The maximal group diagram consists of time intervals annotated by their corresponding *maximal groups* — a notion due to Buchin et al., implying that we recognize the notion of maximal groups as a special instance of *generalized persistence diagram* by Patel. On the other hand, the persistence clustergram is mostly obtained by annotating the intervals in the zigzag barcode of the Reeb graph $\mathscr{R}$ with certain merging/disbanding events in the given time-varying network.

We show that both diagrams are complete invariants of formigrams (or equivalently of *trajectory grouping structure* by Buchin et al.) and thus contain more information than the Reeb graph $\mathscr{R}$.

Contents

1 Introduction **2**
2 Preliminaries **5**
3 From dynamic graphs to formigrams, Reeb graphs, and zigzag barcodes **12**
4 Interleavings between dynamic graphs and between formigrams **16**
5 Categorical aspects of $\mathrm{SubPart}(X)$, Part and set **20**
6 Summarizing formigrams via Möbius inversion **23**
7 Analysis of dynamic metric spaces (DMSs) **35**
8 Conclusion **39**
A Details and Proofs **39**
B Distance between weighted Reeb graphs **44**
C Smoothing formigrams **45**
D About the 0-slack interleaving distance between DMSs **47**
E Higher dimensional persistent homology barcodes of dynamic metric spaces. **49**

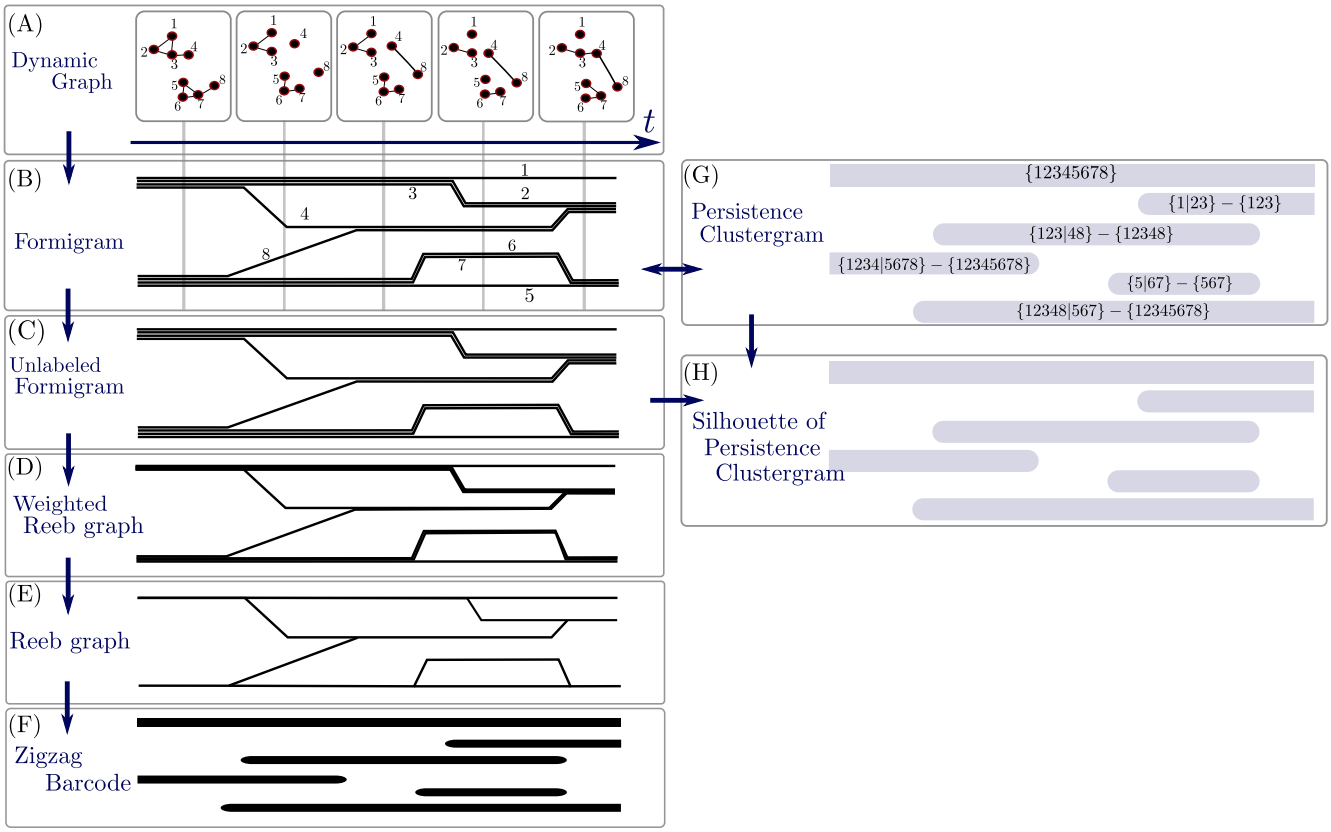


Figure 1: **Summarization process of a dynamic graph.** The evolution of connected components in a dynamic graph (A) is encoded in a formigram (B). A summarization procedure of the formigram yields invariants depicted in (C), (D), (E), and (F) in order. On the other hand, a persistence clustergram (G) is obtained from the formigram via Möbius inversion. Persistence clustergrams are complete invariants of formigrams, i.e. persistence clustergrams permit reconstructing formigrams (hence the two-way arrow between (B) and (G)). When a given formigram satisfies a certain property, the silhouette of persistence clustergram (H) is isomorphic to the zigzag barcode (F). Observe from (B), (G), and (F) that the label on an interval in the persistence clustergram indicates which merging and disbanding events in the formigram account for the corresponding interval in the zigzag barcode. In (F), (G), and (H) a rounded ending on an interval indicates an open endpoint while a straight ending indicates a closed endpoint.

1 Introduction

One of the most frequent tasks in data analysis consists of finding clusters in datasets. Since data in the real world are often *spatiotemporal* (i.e. data encode for both space and time), identifying and analyzing clusters in such data is of critical importance. Spatiotemporal data includes flocking, swarming, or herding behavior of animals [7, 43, 44, 46, 57, 65, 77, 82], sensor networks [1, 2, 31, 32, 40], swarm robots [73], convoys [49], moving clusters [50], or mobile groups [47, 83]. Furthermore, with the development of tracking and mobile devices with positioning capabilities, numerous object trajectory data are being collected, which makes the task of identifying and analyzing clusters in spatiotemporal datasets increasingly more important.

Buchin et al. [15] introduced a formal definition of *groups* in a given set $\mathbf{X}$ of trajectories and introduced a notion of *trajectory grouping structure* which encodes all groups in $\mathbf{X}$ represented as a Reeb graph along the timeline that is decorated by *maximal groups*.

The **first** goal of this work is to make clear identification of the trajectory grouping structure (and similar

concepts that appeared in applications; e.g. [71, 81])) as a mathematical object, which we call *formigrams* [52].[1] A formigram is a *constructible cosheaf* over the real line [30, 29] valued in *the category of partitions*; in plain language, a formigram is a 'zigzag' diagram of partitions. This category can be seen as either a lattice (when an underlying set is specified) or a category whose morphisms are monic (when an underlying set is *not* specified). This identification allows us to put formigrams into the context of the theories of persistence [17, 37], lattices [8], and categories [14, 58]. The **second** goal is to exploit this established identity of formigrams for metrizing the space of formigrams, summarizing formigrams, and smoothing formigrams. In particular, the metrization of the space of formigrams addresses a question formulated by Buchin et al. regarding the quantification of the difference between two collective motions via trajectory grouping structures [15, Section 6]. In order to achieve our second goal, we deploy recent ideas from zigzag or multiparameter persistence [9, 11, 18, 34], constructible cosheaves [29, 33], and generalized persistence diagrams [53, 67].

Contributions. In a nutshell, we establish a stable and (mostly) functorial summarization process illustrated in Figures 1 and 2. This entails appropriate identification of categories (Table 1), functors (Table 2), and metrics (Table 3), as well as appropriate usage of *generalized rank* and *Möbius inversion* (Table 4). More details follow:

- We adapt recent ideas from generalized persistence diagrams and Möbius inversion [72] in order to define the *persistence clustergram* of a formigram (cf. Figure 1 (B),(G)). The persistence clustergram is a *finer* invariant than the Reeb graph of a formigram and thus it is also finer than the zigzag barcode of the Reeb graph (cf. Figure 1 (E),(F)). In fact, the persistence clustergram is a *complete invariant* of formigrams. See **Definition 6.27** and **Remark 6.28**.
- We show that the maximal groups [15] of a set $\mathbf{X}$ of trajectories can be obtained from the formigram $\theta_{\mathbf{X}}$ associated to $\mathbf{X}$. More specifically, to obtain the maximal groups, we use the Möbius inversion of a suitable notion of *rank invariant* associated to the formigram. This leads us to the fact that the collection of all maximal groups (which we call the *maximal group diagram*) is another complete invariant of formigrams. This also implies that the collection of all maximal groups defined by Buchin et al. [15] is not just an invariant of collections of trajectories but it is also an invariant of formigrams. See **Definition 6.16** and **Remark 6.20**.
- By utilizing the join operation on the lattice of (sub)partitions, we metrize the space of formigrams with a distance function $d_{\mathrm{I}}^{\mathrm{F}}$ (the interleaving distance between formigrams). $d_{\mathrm{I}}^{\mathrm{F}}$ dovetails with celebrated metrics in topological data analysis, which makes the summarization pipeline that is illustrated in Figure 1 is entirely stable. See **Proposition 4.13, Corollary 4.16, Theorems 4.17** and **6.35**.

Several subsidiary contributions follow:

- We define *dynamic graphs* as constructible cosheaves over $\mathbf{R}$ valued in the lattice of all subgraphs of a given complete graph. By doing this, we are able to harness machinery from applied topology which allows us to both quantify the difference between dynamic graphs and induce the invariants of dynamic graphs illustrated in Figure 1. See **Definition 3.1.**
- We identify a sufficient condition on a dynamic metric space γ_X [54] so that its dynamic *Rips graph* $\mathscr{R}_\delta^1(\gamma_X)$, $\delta \geq 0$ (1-skeleton of Rips complexes), define a dynamic graph as described in the previous item. For example, our result implies that a finite collection of piecewise linear trajectories in Euclidean space induces a dynamic graph via the Rips graph functor. See **Proposition 7.5.**
- We show that the λ-slack interleaving distance between dynamic metric spaces [54] is a metric. Also we show that different choice of $\lambda > 0$ does not change the topology of the metric space of dynamic metric spaces. See **Theorem 7.12** and **Proposition A.15.**

[1] The name formigram is a combination of the words formicarium and diagram. A formicarium or ant farm is an enclosure for keeping ants under semi-natural conditions [84]. Visually, a formigram is reminiscent of a formicarium (cf. Figure 1 (B)).

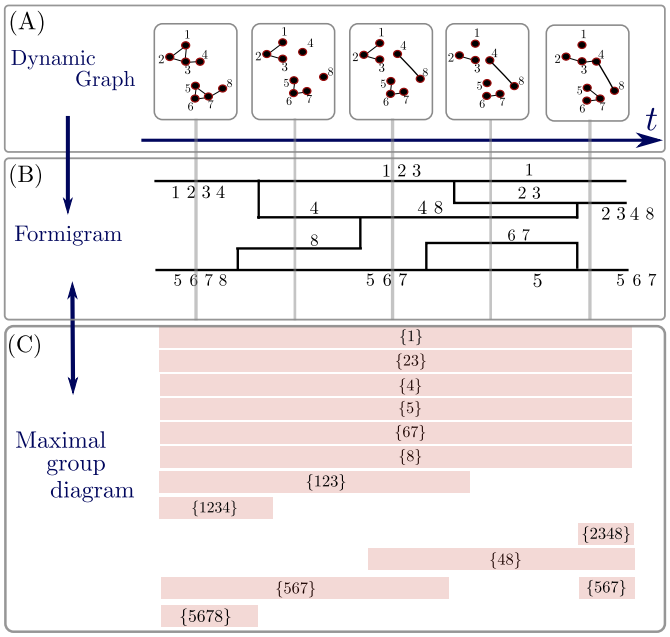


Figure 2: The *maximal groups* introduced by Buchin et al. [15] can be obtained via the Möbius inversion of the $\bigwedge$-rank function of a formigram (cf. Definition 6.16). NB: In panel (C), commas are omitted in each set, e.g. {23} means the set $\{2,3\}$.

- We observe that *robust grouping structure* by Buchin et al. [15] can be formulated as an *intrinsic* smoothing operation on formigrams. Smoothing operations on formigrams is entirely compatible with the Reeb graph smoothing operation. We also clarify the effect of smoothing operations on the zigzag barcode of an input formigram. See **Remark C.1, Propositions C.2 and C.5.**
- We clarify the computational complexity of every metric that is introduced in this paper. See **Theorem 4.7, Remark 6.37 ((ii))**, and **Theorems 7.15** and **A.7** (Theorem A.7 appeared in the conference paper by the same authors [52]).

Other related work. In [55], a collection of dynamic graphs that naturally arise from an artificial life program, called *Boids* [69], were successfully classified by the bottleneck distance on their zigzag barcodes (cf. Figure 1 (F)). An implementation is available in [26].

In [79], van Goethem et al. presented algorithms and data structures that support the interactive analysis of the trajectory grouping structure. In [80, 85], Van Kreveld et al. proposed an alternative to the aforementioned definition of *groups* of [15] together with experimental evaluation related to identifying groups from real or simulated pedestrian data.

Sinhuber and Ouellette carried out statistical analysis on time-varying connectivity graphs in order to characterize swarms of midges [76]. Munch established stability of time-varying persistence diagrams derived from dynamic point clouds in $\mathbf{R}^d$ [64]. Kim and Mémoli proposed a method to encode spatiotemporal topology of dynamic metric spaces into multiparameter persistence modules [54]. While [54] provides useful tools for characterizing and classifying dynamic metric spaces according to their spatiotemporal homological features [27], no visualizable summary was provided which is one of the novel contributions of the present work.

We remark that, in this paper, only clustering features of dynamic *graphs* [1, 31, 40, 45] are studied (i.e. the zeroth order homological features), whereas [54] considers arbitrary order homological features of dynamic *metric spaces* [76, 78, 86].

R. González-Díaz et al. devised the so-called spatiotemporal barcode as a visual tool to encode the lifespan of connected components on an image sequence over time [42]. Dey and Hou proposed efficient algorithms for computing zigzag persistent homology of dynamic graphs [34]. Kim, Mémoli, and Stefanou showed in [56] that

the aforementioned distance $d_{\mathrm{I}}^{\mathrm{F}}$ between formigrams is closely related to both the Hausdorff distance [16] and the erosion distance [67]. Rolle and Scoccola considered a variation of $d_{\mathrm{I}}^{\mathrm{F}}$ for comparisons of multiparameter hierarchical clusterings [70]. Ghrist and Riess studied a Hodge theory for cellular sheaves valued in lattices (i.e. functors from the face posets of cell complexes to lattices) [41].

Acknowledgements. This work was partially supported by NSF grants IIS-1422400, CCF-1526513, DMS-1723003, and CCF-1740761. We thank Zane Smith for providing an example of non-planar formigram in Example 3.14. Also, we thank Michael Lesnick for useful comments about the paper. WK thanks Amit Patel for beneficial discussions regarding topics related to Section 6.

Outline. Section 2 includes preliminaries from category theory, poset theory, and persistence theory. Section 3 introduces notions of dynamic graphs, formigrams, and invariants of formigrams that are relevant to an algebraic structure of zigzag persistence. Section 4 introduces interleaving distances between dynamic graphs and between formigrams. Also, the stability of algebraic invariants that were introduced in the previous section is shown therein. Section 5 establishes a few categorical results that will be useful in later sections. Section 6 is the core of this paper. We introduce several combinatorial invariants of formigrams such as *maximal group diagrams* and *persistence clustergrams* and discuss their stability. Section 7 we discuss how to convert dynamic metric spaces into dynamic graphs via the Rips graph functor and its stability. Section 8 concludes this work. For readability we have relegated some proofs, remarks, and examples to an appendix: Sections A, B, C, D, and E.

2 Preliminaries

In Sections 2.1 and 2.2 we introduce the posets, categories, and functors that are considered throughout the paper. In Section 2.3 we review the notion of interval decomposable persistence modules. In Section 2.4 we recall both the notion of constructible cosheaf over the real line and a suitable notion of interleaving.

2.1 Poset theory elements

Any nonempty set with a partial order determines a *poset*. Given a poset $\mathbf{P}$, we call any subset $\mathbf{Q}$ of $\mathbf{P}$ with the partial order obtained by restricting that of $\mathbf{P}$ to $\mathbf{Q}$ a *subposet of* $\mathbf{P}$. We introduce posets that are considered in this paper. First, the following posets will be used as domain posets of order-preserving maps or indexing posets of functors.

1. A poset $\mathbf{P}$ is said to be a *join-semilattice* (resp. *meet-semilattice*) if $\mathbf{P}$ contains the least upper bound $p \vee q$ (resp. greatest lower bound $p \wedge q$) of any pair of points $p, q \in \mathbf{P}$. If $\mathbf{P}$ is both join- and meet-semilattice, then $\mathbf{P}$ is said to be a *lattice*.
2. The poset $\mathbf{R}^n$ with order $(a_1, a_2, \cdots, a_n) \leq (b_1, b_2, \cdots, b_n)$ if and only if $a_i \leq b_i$ for all $1 \leq i \leq n$.
3. $\mathbf{Z}_+$ and $\mathbf{R}_+$ will denote the sets of nonnegative integers and nonnegative real numbers, respectively.
4. Let $\mathbf{P}$ be a poset. By $\mathbf{P}^{\mathrm{op}}$ we mean the opposite poset of $\mathbf{P}$, i.e. for any $p, q \in \mathbf{P}$, $p \leq q$ in $\mathbf{P}^{\mathrm{op}}$ if and only if $q \leq p$ in $\mathbf{P}$.
5. The poset $\mathbf{R}^{\mathrm{op}} \times \mathbf{R}$ where $(a_1, a_2) \leq (b_1, b_2)$ if and only if $a_1 \geq b_1$ and $a_2 \leq b_2$ for the usual order $\leq$ on $\mathbf{R}$.
6. The poset $\mathbf{Int}$ consists of nonempty finite closed real intervals ordered by inclusion. $\mathbf{Int}$ will be identified with the subposet of $\mathbf{R}^{\mathrm{op}} \times \mathbf{R}$ consisting of (a, b) with $a \leq b$ in $\mathbf{R}$ via the bijection $[a, b] (\in \mathbf{Int}) \leftrightarrow (a, b) (\in \mathbf{R}^{\mathrm{op}} \times \mathbf{R})$ (cf. Figure 4 (A)).

Lattices of subgraphs and subpartitions. In the rest of this section, X will stand for some nonempty finite sets. We review lattice structures on the collection of subgraphs of the complete graph on X and on the collection of (sub)partitions of X.

Categories	Objects	Morphisms	
Graph(X)	Subgraphs of the complete graph on X	Inclusion	Def. 2.1
SubPart(X)	Subpartitions of X	Refinement	Def. 2.2
Part	Pairs (X, P_X) where X is a finite set and P_X is a partition of X	Block-preserving injective maps	Def. 2.7
ω**set**	Pairs (X, w_X) where X is a finite set and a weight function $w_X : X \to \mathbb{N}$	Weight-observing maps	Def. 2.8
set	Finite sets	Set maps	
vec	Fin. dim. vector spaces	Linear maps	

Table 1: Categories that are considered throughout the paper. Those are connected by the functors in Table 2.

$$\text{Graph}(X) \xrightarrow[\text{Def. 2.4}]{\pi_0} \text{SubPart}(X) \xrightarrow[\text{Def. 2.9 (i)}]{\mathscr{U}_L^X} \textbf{Part} \xrightarrow[\text{Def. 2.9 (ii)}]{\mathscr{A}} \omega\textbf{set} \xrightarrow[\text{Def. 2.9 (iii)}]{\mathscr{U}_\omega} \textbf{set} \xrightarrow[\text{Def. 2.6}]{\mathscr{F}} \textbf{vec}$$

Table 2: Functors that connect the categories in Table 1.

Definition 2.1 (Lattice of subgraphs)**.** By Graph(X) we denote the lattice of subgraphs of the complete graph on the vertex set X ordered by inclusion. For any $G, H \in \text{Graph}(X)$, the union of G and H is the join $G \vee H$, i.e. the graph whose vertex set (resp. edge set) is the union of the vertex sets (resp. edge sets) of G and H. The intersection of G and H is the meet $G \wedge H$.

Definition 2.2 (Lattice of subpartitions)**.** We call any partition P of a subset X' of X a *subpartition* of X. In this case we call X' the *underlying set of* P, i.e. $X' = \bigcup P$. Each element of P is called a *block*. A partition of the empty set is defined as the empty set. By SubPart(X), we denote the set of *all subpartitions of* X. By **Part**(X), we denote the subcollection of SubPart(X) consisting solely of partitions of the entire X.

For example, for $X := \{x_1, x_2, x_3\}$, both $\{\{x_1\}, \{x_2\}\}$ and $\{\{x_1, x_2, x_3\}\}$ belong to SubPart(X). These subpartitions will henceforth be written simply as $\{x_1|x_2\}$ and $\{x_1x_2x_3\}$ respectively.

The collection SubPart(X) forms a lattice. Given $P, Q \in \text{SubPart}(X)$, by $P \leq Q$ we mean "P is finer than or equal to Q", i.e. for all $B \in P$, there exists $C \in Q$ such that $B \subset C$. Given any $P, Q \in \text{SubPart}(X)$, the join $P \vee Q$ is the finest common coarsening of P and Q. The meet $P \wedge Q$ is the coarsest common refinement of P and Q.

Example 2.3. Let $X := \{x_1, x_2, x_3, x_4\}$. For $P_1 = \{x_1|x_2\}, P_2 = \{x_2x_3\}$, and $P_3 = \{x_1x_4\}$ in SubPart(X), we have: $\bigwedge_{i=1}^2 P_i = \{x_2\}$, $\bigwedge_{i=1}^3 P_i = \emptyset$, $\bigvee_{i=1}^2 P_i = \{x_1|x_2x_3\}$, and $\bigvee_{i=1}^3 P_i = \{x_1x_4|x_2x_3\}$.

We define the *path components functor* (i.e. order-preserving map) $\pi_0 : \text{Graph}(X) \to \text{SubPart}(X)$, which is utilized for the summarization process depicted as the arrow (A)→(B) in Figure 1.

Definition 2.4. Given any graph $G_X = (X, E_X)$, define the partition $\pi_0(X, E_X) := X/\sim$ of X where $\sim$ stands for the equivalence relation on X defined by $x \sim x'$ if and only if there exists a sequence $x = x_1, x_2, \ldots, x_n = x'$ of points in X such that $\{x_i, x_{i+1}\} \in E_X$ for each $i \in \{1, \ldots, n-1\}$.

Whenever $G_X \leq H_X$ in Graph(X), we have that $\pi_0(G_X) \leq \pi_0(H_X)$ in SubPart(X).

2.2 Category theory elements

In this section we introduce categories and functors that appear in Tables 1 and 2 respectively. Consult [58] for general definitions related to category theory. Given any category **C**, we will denote the collection of objects in **C** by Ob(**C**).

Remark 2.5 (Posets as categories)**.** (i) Any poset $\mathbf{P}$ will be regarded as a category: Objects are elements in $\mathbf{P}$. For any $p, q \in \mathbf{P}$, there exists a unique morphism $p \to q$ if and only if $p \leq q$. Therefore, $p \leq q$ in $\mathbf{P}$ will denote the unique morphism $p \to q$. In this perspective, any order-preserving map between posets is a functor. Any subposet $\mathbf{Q}$ of $\mathbf{P}$ is a full subcategory of $\mathbf{P}$.

(ii) Since $\mathrm{Graph}(X)$ is a poset, given *any* poset $\mathbf{P}$ and *any* functor $F : \mathbf{P} \to \mathrm{Graph}(X)$ (i.e. order-preserving map), the limit and colimit of F are $\bigcup_{p\in\mathbf{P}} F_p$ and $\bigcap_{p\in\mathbf{P}} F_p$, respectively. Similarly, since $\mathrm{SubPart}(X)$ is a poset, given *any* poset $\mathbf{P}$ and *any* functor $F : \mathbf{P} \to \mathrm{SubPart}(X)$, the limit and colimit of F are $\bigwedge_{p\in\mathbf{P}} F_p$ and $\bigvee_{p\in\mathbf{P}} F_p$, respectively.

The category **set** consists of finite sets with set maps. The category **vec** consists of finite-dimensional vector spaces over a fixed field $\mathbb{F}$ with linear maps.

Definition 2.6. The *free functor* $\mathscr{F} :$ **set** $\to$ **vec** sends any set S to the vector space $\mathscr{F}(S)$ which consists of formal linear combinations $\sum_i a_i s_i$ ($a_i \in \mathbb{F}$, $s_i \in S$) of finite terms of elements in S over the field $\mathbb{F}$. Also, given a set map $f : S \to T$, $\mathscr{F}(f)$ is the linear map from $\mathscr{F}(S)$ to $\mathscr{F}(T)$ obtained by linearly extending f.

For two categories $\mathbf{C}$ and $\mathbf{D}$, the category $\mathbf{C}^{\mathbf{D}}$ stands for the category of functors from $\mathbf{D}$ to $\mathbf{C}$ with objects being functors $\mathbf{C} \to \mathbf{D}$ and arrows being natural transformations. For two functors $F, G : \mathbf{C} \to \mathbf{D}$, we write $F \cong G$ whenever F and G are *naturally isomorphic*, i.e. there exists a natural transformation $\tau : F \to G$ such that $\tau_c : F(c) \to G(c)$ is invertible for each $c \in \mathrm{Ob}(\mathbf{C})$.

We introduce the category of partitions (without specifying a set to partition) and the category of weighted sets. These categories appear in Figure 1 (B) and (C).

Definition 2.7. In the *category of partitions*, denoted by **Part**, an object is a pair (X, P_X) of a finite set X and a partition P_X of X. A morphism $f : (X, P_X) \to (Y, P_Y)$ is an *injective* map $f : X \hookrightarrow Y$ which preserves the equivalence relation on X induced by P_X, i.e. if x and x' belong to the same block in P_X, then so do $f(x)$ and $f(x')$ in P_Y.

Note that f induces the map $f_* : P_X \to P_Y$ that sends each block B to the unique block C containing the image $f(B)$. The morphism f is an isomorphism if both f and f_* are bijective. For example, let $X := \{x_1, x_2, x_3\}$. Whereas $P_X = \{x_1x_2|x_3\}$ and $Q_X = \{x_1|x_2x_3\}$ are non-isomorphic objects in $\mathrm{SubPart}(X)$, the pairs (X, P_X) and (X, Q_X) are isomorphic in **Part**.

Next we define the category ω**set** of *weighted sets*.

Definition 2.8. In ω**set**, an object is a pair (X, w_X) of a finite set X and a positive-integer-valued *weight* map $w_X : X \to \mathbb{N}$. A morphism $f : (X, w_X) \to (Y, w_Y)$ is a weight-observing set map $f : X \to Y$, i.e. for all $y \in Y$, $\sum_{x\in f^{-1}(y)} w_X(x) \leq w_Y(y)$.

Notice the following: (1) If there exists a morphism from (X, w_X) to (Y, w_Y), then the *total weight* of (Y, w_Y) is at least that of (X, w_X), i.e. $\sum_{x\in X} w_X(x) \leq \sum_{y\in Y} w_Y(y)$. (2) Two objects (X, w_X) and (Y, w_Y) are isomorphic if and only if there exists a weight-*preserving* bijection $X \to Y$. (3) If there exists a pair of morphisms in the opposite directions between two objects in ω**set**, then the two object must be isomorphic.

We introduce the following three functors which are utilized for the summarization procedure depicted as the arrows (B) $\to$ (C) $\to$ (D) $\to$ (E) in Figure 1. See also Table 2. Let X be any nonempty finite set.

Definition 2.9 (Three functors)**.** (i) The *unlabeling functor* $\mathscr{U}_L^X$ sends each $P \in \mathrm{SubPart}(X)$ to the pair $(\bigcup P, P)$. For any pair $P \leq Q$ in $\mathrm{SubPart}(X)$, the corresponding morphism $\mathscr{U}_L^X(P \leq Q) : (\bigcup P, P) \to (\bigcup Q, Q)$ is the inclusion map $\bigcup P \hookrightarrow \bigcup Q$.

(ii) The *agglomerating functor* $\mathscr{A}$ sends each $(X, P_X) \in \mathrm{ob}$(**Part**) to the pair $(P_X, |-|) \in \mathrm{ob}(\omega$**set**$)$ where $|-| : P_X \to \mathbf{N}$ is the size function, i.e. any block in P_X is sent to its size (i.e. cardinality). Since any morphism $f : (X, P_X) \to (Y, P_Y)$ in **Part** is an injective set map $X \hookrightarrow Y$, the induced map $f_* : P_X \to P_Y$ is a weight-observing map.

(iii) The *unweighting functor* $\mathscr{U}_\omega$ simply forgets the weight function (i.e. the second entry) from each object in ω**set**.

2.3 Interval decomposable persistence modules

In this section we review the notion of interval decomposability of persistence modules.

Let $\mathbf{P}$ be a poset. Any functor $F : \mathbf{P} \to \mathbf{vec}$ will be called a $\mathbf{P}$-*indexed module*. This means that each $p \in \mathbf{P}$ is sent to a finite dimensional vector space $F(p)$ and each $p \leq q$ in $\mathbf{P}$ is sent to a linear map $F(p \leq q) : F(p) \to F(q)$. In particular, for any $p \in \mathbf{P}$, $p \leq p$ is sent to the identity map on $F(p)$. Also, for any $p \leq q \leq r$ in $\mathbf{P}$, we have $F(p \leq r) = F(q \leq r) \circ F(p \leq q)$.

Definition 2.10 (Intervals [11])**.** Given a poset $\mathbf{P}$, an *interval* $\mathcal{J}$ of $\mathbf{P}$ is any subset $\mathcal{J} \subset \mathbf{P}$ such that

(i) $\mathcal{J}$ is nonempty.
(ii) If $p, r \in \mathcal{J}$ and $p \leq q \leq r$, then $q \in \mathcal{J}$.
(iii) (connectivity) For any $p, q \in \mathcal{J}$, there is a sequence $p = p_0, p_1, \cdots, p_l = q$ of elements of $\mathcal{J}$ with p_i and p_{i+1} comparable for $0 \leq i \leq l-1$.

For $\mathcal{J}$ an interval in $\mathbf{P}$, the *interval module* $I^{\mathcal{J}} : \mathbf{P} \to \mathbf{vec}$ is the $\mathbf{P}$-indexed module where

$$I^{\mathcal{J}}(p) = \begin{cases} \mathbb{F} & \text{if } p \in \mathcal{J}, \\ 0 & \text{otherwise.} \end{cases} \qquad I^{\mathcal{J}}(p \leq q) = \begin{cases} \mathrm{id}_{\mathbb{F}} & \text{if } p, q \in \mathcal{J}, \\ 0 & \text{otherwise.} \end{cases}$$

The direct sums of $\mathbf{P}$-indexed modules are defined pointwise at each index $t \in \mathbf{P}$. We say that a $\mathbf{P}$-indexed module F is *decomposable* if F is naturally isomorphic to $G_1 \bigoplus G_2$ for some non-trivial $\mathbf{P}$-indexed modules G_1 and G_2. Otherwise, we say that F is *indecomposable*. Any interval module is indecomposable [11, Proposition 2.2]. A $\mathbf{P}$-indexed module F is *interval decomposable* if there exists a multiset $\mathrm{barc}(F)$ of intervals in $\mathbf{P}$ such that

$$F \cong \bigoplus_{\mathcal{J} \in \mathrm{barc}(F)} I^{\mathcal{J}}.$$

By Azumaya-Krull-Remak-Schmidt [3], the multiset $\mathrm{barc}(F)$ is unique if F is interval decomposable. In this case, we call $\mathrm{barc}(F)$ the *barcode* of F.

2.4 Constructible cosheaves over R, their interleavings, and their smoothing operations

In this section we review the notion of constructible cosheaves over $\mathbf{R}$, their interleavings, and their smoothing operations. Constructible cosheaves over $\mathbf{R}$ are fully characterized by "zigzag diagrams over $\mathbf{R}$" [29, 33].

Definition 2.11 (Zigzag poset)**.** Let $\mathbf{ZZ}$ be the subposet of $\mathbf{R}^{\mathrm{op}} \times \mathbf{R}$ given by $\mathbf{ZZ} := \{(k, l) : k \in \mathbf{Z},\ l \in \{k, k-1\}\}$ (cf. Figure 3). By $\mathbf{Int}(\mathbf{ZZ})$ we denote the poset of all *finite* intervals in $\mathbf{ZZ}$ ordered by inclusion.

Notation 2.12 ([11])**.** Letting $<$ denote the strict partial order on $\mathbf{Z}^2$ (not on $\mathbf{Z}^{\mathrm{op}} \times \mathbf{Z}$), every interval in $\mathbf{ZZ}$ falls into one of the four types below:

$$\begin{aligned}
(b,d)_{\mathbf{ZZ}} &:= \{(i,j) \in \mathbf{ZZ} : (b,b) < (i,j) < (d,d)\} && \text{for } b < d \in \mathbf{Z}, \\
[b,d)_{\mathbf{ZZ}} &:= \{(i,j) \in \mathbf{ZZ} : (b,b) \leq (i,j) < (d,d)\} && \text{for } b < d \in \mathbf{Z}, \\
(b,d]_{\mathbf{ZZ}} &:= \{(i,j) \in \mathbf{ZZ} : (b,b) < (i,j) \leq (d,d)\} && \text{for } b < d \in \mathbf{Z}, \\
[b,d]_{\mathbf{ZZ}} &:= \{(i,j) \in \mathbf{ZZ} : (b,b) \leq (i,j) \leq (d,d)\} && \text{for } b \leq d \in \mathbf{Z}.
\end{aligned}$$

See Figure 3 for examples. We let $\langle b, d \rangle_{\mathbf{ZZ}}$ denote any of the above sets without specifying its type. Also, by $\langle b, d \rangle$ for $b \in \{-\infty\} \cup \mathbf{R}$ and $d \in \mathbf{R} \cup \{\infty\}$, we denote any of the intervals $(b,d), [b,d), (b,d]$ or $[b,d]$ in $\mathbf{R}$.

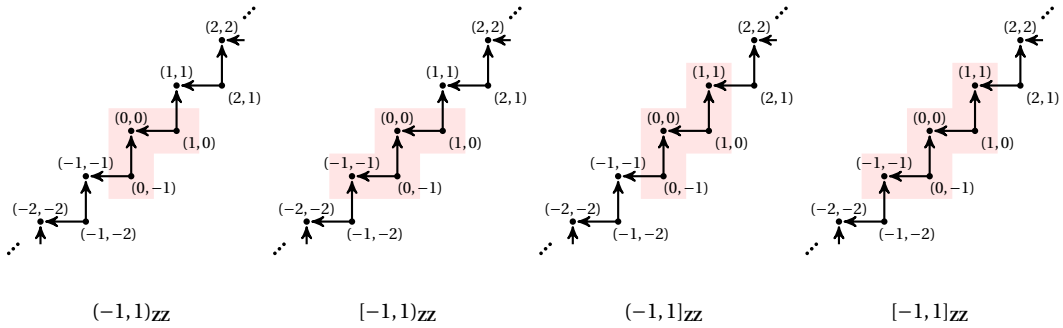


Figure 3: The points falling into the shaded regions comprise the intervals $(-1,1)_{\mathbf{ZZ}}, [-1,1)_{\mathbf{ZZ}}, (-1,1]_{\mathbf{ZZ}}$ and $[-1,1]_{\mathbf{ZZ}}$ of the poset **ZZ**, respectively in order.

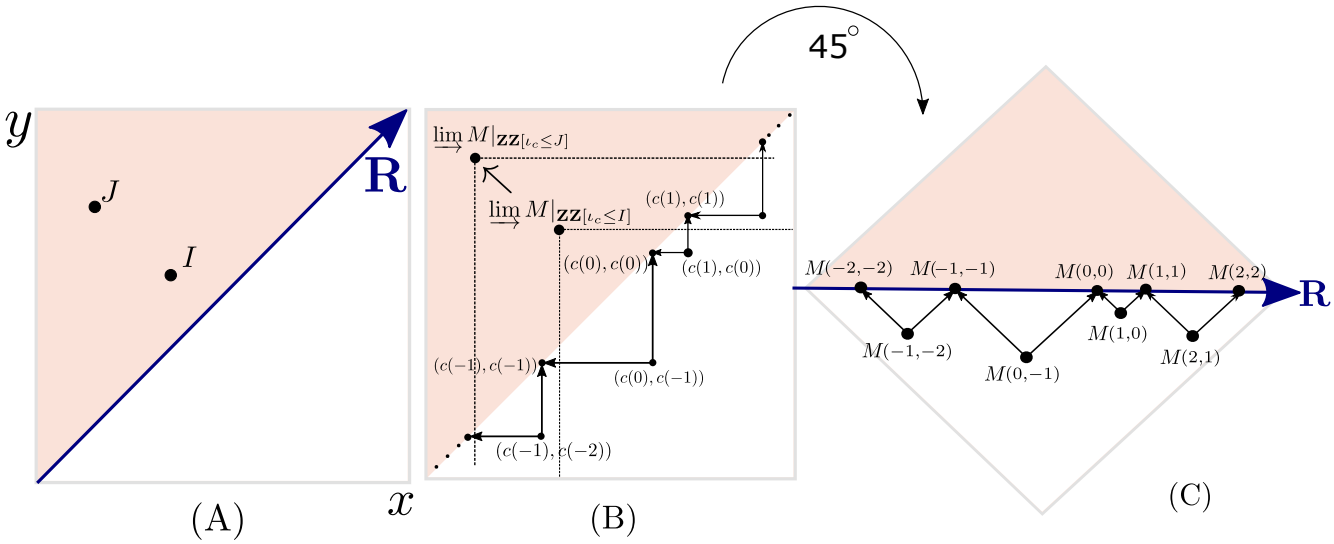


Figure 4: **Illustration for Definition 2.14.** (A) The shaded region stands for the poset **Int**. We have $I \le J$ for the intervals $I, J \in \mathbf{Int}$ shown in the figure. The diagonal line is identified with the real line via the bijection $(t,t) \leftrightarrow t$. (B) The canonical morphism $F(I) \to F(J)$ for $I \le J$ in **Int**. (C) The zigzag diagram anchored over the real line completely determines the cosheaf $F : \mathbf{Int} \to \mathbf{C}$ defined by $I \mapsto \varinjlim M|_{\mathbf{ZZ}[\iota_c \le I]}$.

Interleavings between Int-indexed functors [11]. For $\varepsilon \ge 0$, and $I = [b,d] \in \mathbf{Int}$, let $I^\varepsilon := [b-\varepsilon, d+\varepsilon] \in \mathbf{Int}$.

Definition 2.13 (Interleaving distance)**.** Let $\varepsilon \ge 0$ and **C** be an arbitrary category. Two functors $F, G : \mathbf{Int} \to \mathbf{C}$ are said to be *ε-interleaved* if there exist collections of morphisms $f = (f_I : F(I) \to G(I^\varepsilon))_{I \in \mathbf{Int}}$ and $g = (g_J : G(J) \to F(J^\varepsilon))_{J \in \mathbf{Int}}$ satisfying the following:

1. For all $I, J \in \mathbf{Int}$, $\quad g_{I^\varepsilon} \circ f_I = F(I \le I^{2\varepsilon})$ and $f_{J^\varepsilon} \circ g_J = G(J \le J^{2\varepsilon})$.
2. For all $I \le J \in \mathbf{Int}$, $G(I^\varepsilon \le J^\varepsilon) \circ f_I = f_J \circ F(I \le J)$ and $F(I^\varepsilon \le J^\varepsilon) \circ g_I = g_J \circ G(I \le J)$.

In this case, we call (f,g) an *ε-interleaving pair*. For $F, G \in \mathrm{Ob}(\mathbf{C}^{\mathbf{Int}})$, the interleaving distance between them is

$$d_{\mathrm{I}}(F,G) := \inf\{\varepsilon \ge 0 : F \text{ and } G \text{ are } \varepsilon\text{-interleaved}\}.$$

If F and G are not ε-interleaved for any $\varepsilon \ge 0$, then $d_{\mathrm{I}}(F,G) = +\infty$ by definition.

	C	Name of constructible cosheaves **Int** $\to$ **C**	Metric	
(A)	Graph(X)	Dynamic graph*	$d_{\mathrm{I}}^{\mathrm{dynG}}$	Def. 4.4
(B)	SubPart(X)	Formigram*	$d_{\mathrm{I}}^{\mathrm{F}}$	Def. 4.11
(C)	**Part**	Unlabeled formigram	$d_{\mathrm{I}}^{\mathrm{F}}$	Def. 4.11 and Rem. 4.12 (i)
(D)	ω**set**	Weighted Reeb graph	$d_{\mathrm{I}}^{\omega\mathrm{R}}$	Def. B.2
(E)	**set**	Reeb graph [11, 33]	$d_{\mathrm{I}}^{\mathrm{R}}$	Def. 2.13 and Rem. 2.21
(F)	**vec**	Interlevelset persistence module**	$d_{\mathrm{I}}^{\mathbf{vec}}$ or d_{B}	Def. 2.13 and A.1

Table 3: **Objects in panels (A),(B),(C),(D),(E),(F) of Figure 1 and their corresponding metrics.** Metrics in this table are totally ordered, i.e. in Figure 1, each process in (A)$\to$(B)$\to$(C)$\to$(D)$\to$(E)$\to$(F) is stable. * Extra assumptions are necessary that are given in Definitions 3.1 and 3.5. **Visualized by zigzag barcode (Definition 2.20).

Constructible cosheaves over R [29, 30, 33]. We describe constructible cosheaves over **R** by adapting notation from [11]. In a nutshell, a constructible cosheaf over **R** is a cosheaf over **R** [13] which is fully determined by a certain "zigzag diagram" over **R**.

Given a strictly increasing function $c : \mathbf{Z} \to \mathbf{R}$ such that $\lim_{i\to\pm\infty} c(i) = \pm\infty$ and $I := [b, d] \in$ **Int**, we define

$$\mathbf{ZZ}[\iota_c \le I] := \{(i, j) \in \mathbf{ZZ} : (c(i), c(j)) \le (b, d) \text{ in } \mathbf{R}^{\mathrm{op}} \times \mathbf{R}\}.$$

The following definition is depicted in Figure 4.

Definition 2.14 (Constructible cosheaves and critical points)**.** A functor $F : \mathbf{Int} \to \mathbf{C}$ is called a *constructible cosheaf* over **R** valued in **C**, if there exist a strictly increasing function $c : \mathbf{Z} \to \mathbf{R}$ such that $\lim_{i\to\pm\infty} c(i) = \pm\infty$ and a functor $M : \mathbf{ZZ} \to \mathbf{C}$ such that for all $I \in$ **Int**, $F(I) = \varinjlim M|_{\mathbf{ZZ}[\iota_c \le I]}$ (cf. Figure 4 (B)). For all $I \le J$ in **Int**, the morphism $F(I) \to F(J)$ is specified by the initial property of the colimit $F(I)$. We call $\mathrm{im}(c)$ a set of *critical points* of F.[2]

Constructible cosheaves over **R** are fully characterized by "zigzag diagrams over **R**" (cf. Figure 4 (C)).

Definition 2.15 (Names of cosheaves)**.** We call a constructible cosheaf $F : \mathbf{Int} \to \mathbf{C}$ as given in Table 3, depending on the target category **C**.

Convention 2.16. In the rest of the paper, every functor **Int** $\to$ **C** will be assumed to be a constructible cosheaf and thus will be often simply called a cosheaf.

About cosheaves Int $\to$ C when C is a join-semilattice, vec, or set. Next we provide several remarks and review known results about constructible cosheaves **Int** $\to$ **C** when **C** is either a join-semilattice, **vec**, or **set**.

Definition 2.17 (Cosheaf-inducing map)**.** Let **C** be a join-semilattice (Item 1 in Section 2.1 and Remark 2.5 (i)). A map $f : \mathbf{R} \to \mathrm{ob}(\mathbf{C})$ is said to *be cosheaf-inducing* if the following hold: There exists a locally finite set $C \subset \mathbf{R}$ of 'critical points' such that (1) f is constant between any two consecutive points in C, and (2) for every $c \in C$, $f(c)$ is *locally maximal*, i.e. there exists $r_c > 0$ with $f(c-\varepsilon) \le f(c) \ge f(c+\varepsilon)$ for all $\varepsilon \in [0, r_c)$.

[2] The function c associated to F is not unique and thus we refer to $\mathrm{im}(c)$ as 'a' set of critical points and not as 'the' set of critical points.

Remark 2.18. Let $\mathbf{C}$ be a join-semilattice. Then

(i) A constructible cosheaf $F : \mathbf{Int} \to \mathbf{C}$ induces the map $f : \mathbf{R} \to \mathrm{ob}(\mathbf{C})$ defined by $t \mapsto F([t,t])$. Then, f is cosheaf-inducing. Note also that F is recovered from f via the formula $F(I) = \bigvee\{f(t) : t \in I\}$ for $I \in \mathbf{Int}$.[3]

(ii) Conversely, assume that a map $g : \mathbf{R} \to \mathrm{ob}(\mathbf{C})$ is cosheaf-inducing. Then, $G : \mathbf{Int} \to \mathbf{C}$ defined by $I \to \bigvee\{G(t) : t \in I\}$ is a constructible cosheaf.

For $t \in \mathbf{R}$ and $\varepsilon \geq 0$, let $[t]^\varepsilon := [t-\varepsilon, t+\varepsilon]$.

(iii) For any two constructible cosheaves $F, G : \mathbf{Int} \to \mathbf{C}$, the interleaving distance between them is:

$$\begin{aligned} d_{\mathrm{I}}(F,G) &= \inf\left\{\varepsilon \geq 0 : \text{for all } I \in \mathbf{Int},\, F(I) \leq G(I^\varepsilon) \text{ and } G(I) \leq F(I^\varepsilon)\right\}. \\ &= \inf\left\{\varepsilon \geq 0 : \text{for all } t \in \mathbf{R},\, F([t,t]) \leq G([t]^\varepsilon) \text{ and } G([t,t]) \leq F([t,t]^\varepsilon)\right\}. \end{aligned}$$

.

The following proposition follows from the fact that any $\mathbf{ZZ}$-indexed module is interval decomposable [12, 39].

Proposition 2.19 ([11])**.** Any constructible cosheaf $F : \mathbf{Int} \to \mathbf{vec}$ is interval decomposable.

Let $\mathbf{R}_{\ell:y=x}$ be the diagonal line $y = x$ in $\mathbf{R}^2$. By Proposition 2.19, we have:

Definition 2.20. Given any constructible cosheaf $F : \mathbf{Int} \to \mathbf{vec}$, the *zigzag barcode* of F is defined as

$$\mathrm{barc}_{\mathbf{ZZ}}(F) := \mathrm{barc}(F) \cap \mathbf{R}_{\ell:y=x}.$$

$\mathrm{barc}_{\mathbf{ZZ}}(F)$ will be regarded as a multiset of real intervals by identifying $\mathbf{R}_{\ell:y=x}$ with $\mathbf{R}$ via the bijection $(t,t) \leftrightarrow t$.

Remark 2.21. In Definition 2.13, when $\mathbf{C} = \mathbf{set}$ and M, N are constructible, we obtain the interleaving distance $d_{\mathrm{I}}^{\mathrm{R}}$ between Reeb graphs M and N [11, 33].

Bauer, Ge and Wang [4] observed that the 0-th levelset barcode of a Reeb graph encodes all non-trivial persistent homology information of the Reeb graph. A recent theorem on stability of the 0-th levelset barcode of a Reeb graph is the following (see also [4, 6, 11, 33, 36] and cf. the arrow (E) → (F) in Figure 1).

Theorem 2.22 ([9, 11])**.** For any two Reeb graphs $M, N : \mathbf{Int} \to \mathbf{set}$, we have that

$$d_{\mathrm{B}}(\mathrm{barc}_{\mathbf{ZZ}}(\mathscr{F} \circ M), \mathrm{barc}_{\mathbf{ZZ}}(\mathscr{F} \circ N)) \leq 2 \cdot d_{\mathrm{I}}^{\mathrm{R}}(M,N),$$

where $\mathscr{F}$ is the free functor $\mathbf{Set} \to \mathbf{Vec}$ (Definition 2.6) and d_{B} is the bottleneck distance (Definition A.1).

Smoothing of cosheaves. The following definition is a straightforward adaptation of the notion of *Reeb graph smoothing* [33, Section 4.4].

Definition 2.23. For any $\varepsilon \geq 0$, the *ε-smoothing* of a functor $F : \mathbf{Int} \to \mathbf{C}$ is the functor $S_\varepsilon F : \mathbf{Int} \to \mathbf{C}$ defined by $I \mapsto F(I^\varepsilon)$ and $(I \leq J) \mapsto F(I^\varepsilon \leq J^\varepsilon)$.

In Appendix C we study basic properties of this smoothing operation on formigrams.

Remark 2.24. For $\varepsilon_1, \varepsilon_2 \geq 0$ and $I \in \mathbf{Int}$, since $I^{\varepsilon_1+\varepsilon_2} = (I^{\varepsilon_1})^{\varepsilon_2}$, we have $S_{\varepsilon_1+\varepsilon_2}F = S_{\varepsilon_1}S_{\varepsilon_2}F$. This is a straightforward generalization of [33, Proposition 4.13].

Proposition 2.25 ([33, Propositions 4.16 and 4.17])**.** If a given functor $F : \mathbf{Int} \to \mathbf{C}$ is constructible, then $S_\varepsilon F$ is also constructible. In particular, if C is a set of critical points of F, then one set of critical points of $S_\varepsilon F$ is $(C-\varepsilon) \cup (C+\varepsilon)$ where $C \pm \varepsilon := \{c \pm \varepsilon \in \mathbf{R} : c \in C\}$.

[3] $F([t,t])$ is said to be the *costalk* of F at t in the literature (e.g. [13, 30]).

3 From dynamic graphs to formigrams, Reeb graphs, and zigzag barcodes

In this section we define objects that appear in Figure 1 (A)–(F). In Sections 3.1 and 3.2 we provide rigorous definitions of dynamic graphs and formigrams respectively. Formigrams are used to encode the evolution of connected components of dynamic graphs. In Section 3.3 we define several invariants of formigrams. Throughout this section X and Y are nonempty finite sets.

3.1 Dynamic graphs (DGs)

In this section we define the notion of *dynamic graphs* (cf. Figure 1 (A)) and also a suitable notion of isomorphism.

Definition 3.1 (Dynamic graphs)**.** A *dynamic graph (DG)* over X is any cosheaf-inducing map $\mathscr{G}_X : \mathbf{R} \to \mathrm{Graph}(X)$ (cf. Definition 2.17) which, in addition, also satisfies the condition that every $x \in X$ admits a closed interval lifespan $I_x \subset \mathbf{R}$, i.e. x belongs to the vertex set of $\mathscr{G}_X(t)$ if and only if $t \in I_x$. When all $x \in X$ have the same lifespan, the dynamic graph $\mathscr{G}_X$ is said to be *saturated* (e.g. the DG illustrated in Figure 1 (A)).

Remark 2.18 (ii) allows us to view any DG as a constructible cosheaf over $\mathbf{R}$ valued in the lattice $\mathrm{Graph}(X)$. This will in turn allow us to quantify the difference between DGs using the interleaving distance (Remark 2.18 (iii)).

Example 3.2. Let us consider the two dynamic point clouds depicted in Figure 5 (A) and (B). For $\delta = 1$, their time-varying δ-Rips complexes are the DGs depicted in Figure 5 (A') and (B') (see Proposition 7.13 for a general statement).[4]

We now specify a suitable notion of isomorphism in the class of DGs.

Definition 3.3 (Isomorphism for DGs)**.** Two DGs $\mathscr{G}_X$ and $\mathscr{G}_Y$ over X and Y respectively are *isomorphic* if there exists a bijection $\varphi : X \to Y$ such that for all $t \in \mathbf{R}$, the map φ serves as a graph isomorphism between $\mathscr{G}_X(t)$ and $\mathscr{G}_Y(t)$. Namely, for all $t \in \mathbf{R}$, φ restricted to the vertex set of $\mathscr{G}_X(t)$ is a graph isomorphism from $\mathscr{G}_X(t)$ to $\mathscr{G}_Y(t)$.

Example 3.4. Let $\mathscr{G}_X$ and $\mathscr{G}_Y$ be the two DGs in Example 3.2. Although the two graphs $\mathscr{G}_X(t)$ and $\mathscr{G}_Y(t)$ are isomorphic for each $t \in \mathbf{R}$, it is not difficult to see that $\mathscr{G}_X$ and $\mathscr{G}_Y$ *are not isomorphic as DGs*. It is important to point out that d_1^{dynG} and also all the invariants of DGs which we consider in this paper (see Figures 1 and 2) are able to discriminate these two DGs.

3.2 Formigrams

We introduce a notion of *formigram* to encode the evolution of connected components in dynamic graphs.

Definition 3.5. A *formigram*[5] over a finite set X is any cosheaf-inducing map $\theta_X : \mathbf{R} \to \mathrm{SubPart}(X)$ (cf. Definition 2.17) which, in addition, also satisfies that every $x \in X$ admits a closed interval lifespan $I_x \subset \mathbf{R}$, i.e. x belongs to $\bigcup \theta_X(t)$ if and only if $t \in I_x$. By the *support* of θ_X, denoted by $\mathrm{supp}(\theta_X)$, we mean the union $\bigcup_{x \in X} I_x$ of all lifespans of points in X.

Remark 2.18 (ii) allows us to view any formigram as a constructible cosheaf over $\mathbf{R}$ valued in the lattice $\mathrm{SubPart}(X)$. We will interchangeably write both $\theta_X : \mathbf{R} \to \mathrm{SubPart}(X)$ and $\theta_X : \mathbf{Int} \to \mathrm{SubPart}(X)$ as needed.

Recall the unlabeling functor $\mathscr{U}_L^X : \mathrm{SubPart}(X) \to \mathbf{Part}$ from Definition 2.9 (i).

[4] In [76], this type of DGs was utilized for topological characterization of insect swarms. A sensor network [31, 32] is another example of such DGs arising from viewing each sensor as a point in the dynamic metric space of sensors.

[5] The name formigram is a combination of the words formicarium and diagram.

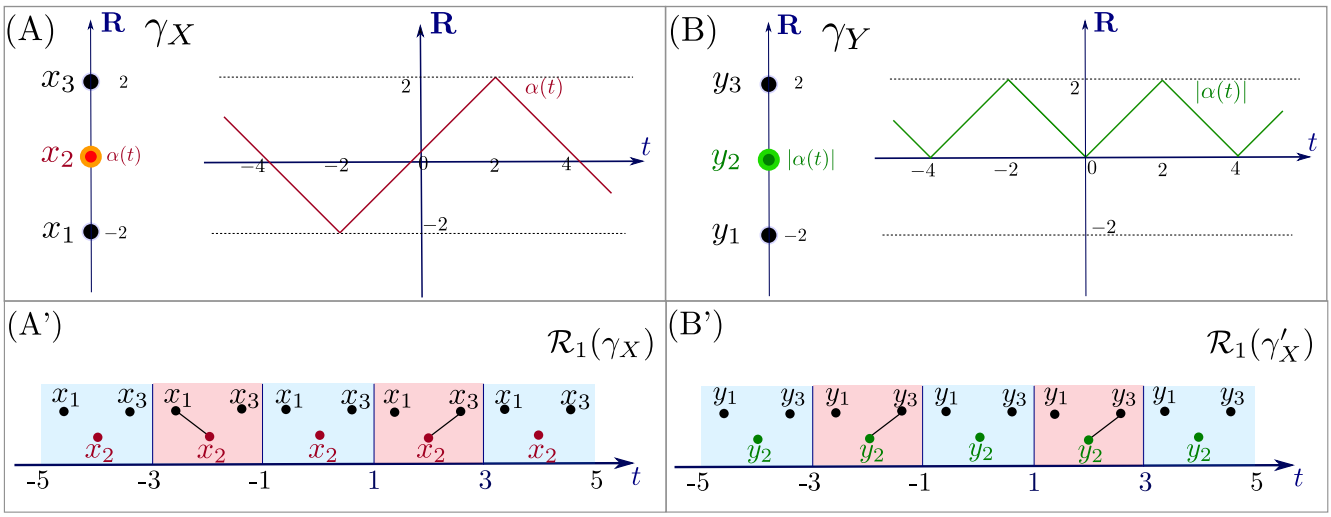


Figure 5: An illustration for Example 3.2. (A) and (B): Two dynamic point clouds γ_X and γ_Y each consisting of three points x_1, x_2, x_3 and y_1, y_2, y_3, respectively. While the two points x_1 and x_3 (resp. y_1 and y_3) are fixed at vertical coordinate values -2 and 2, the other point x_2 (resp. y_2) moves according to $\alpha(t)$ (resp. $|\alpha(t)|$). (A') and (B') show the 1-Rips complexes $\mathscr{R}_1(\gamma_X(t))$ and $\mathscr{R}_1(\gamma_Y(t))$ for $t \in [-5,5]$.

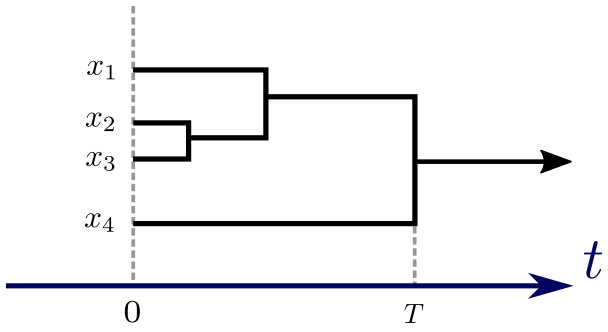


Figure 6: An example of a dendrogram over the set $X = \{x_1, x_2, x_3, x_4\}$.

Remark 3.6 (Essentially unique labeling)**.** Given any unlabeled formigram $\theta : \mathbf{Int} \to \mathbf{Part}$ (cf. Definition 2.15), one can always find a formigram θ_X such that $\mathscr{U}_L^X \circ \theta_X$. For example, in Figure 1 (C), by labeling the eight 'orbits' using any set X of eight elements, we obtain such a formigram θ_X. Assuming that the colimit of θ is isomorphic to a pair $(A, P_A) \in \mathrm{ob}(\mathbf{Part})$, the size of A equals the size of the labeling set.

Remark 3.7. Formigrams generalize the classical notion of *dendrogram*, a 1-parameter nested family of partitions [19, 48]. Namely, any formigram $\theta_X : \mathbf{R} \to \mathrm{SubPart}(X)$ is called a dendrogram if the following properties hold: (1) every $x \in X$ has the lifespan $[0, \infty)$, (2) if $t_1 \leq t_2$, then $\theta_X(t_1) \leq \theta_X(t_2)$, (3) there exists $T > 0$ such that $\theta_X(t) = \{X\}$ for $t \geq T$. See Figure 6 for an illustrative example.

Definition 3.8. Given a formigram $\theta_X : \mathbf{R} \to \mathrm{SubPart}(X)$, we call θ_X *saturated* if all $x \in X$ have the same lifespan (e.g. any dendrogram or the formigram that is depicted in Figure 1 (B)).

Definition 3.9. Two formigrams θ_X and θ_Y over X and Y, respectively, are *isomorphic* if there exists a bijection $\varphi : X \to Y$ such that for all $t \in \mathbf{R}$, $\theta_X(t) = \varphi_*(\theta_Y(t)) := \{\varphi^{-1}(B) \subset X : B \in \theta_Y(t)\}$.

We remark that θ_X and θ_Y are isomorphic if and only if their unlabeled counterparts $\mathscr{U}_L^X \circ \theta_X, \mathscr{U}_L^X \circ \theta_Y : \mathbf{Int} \to \mathbf{Part}$ are naturally isomorphic.

3.3 Functorial summarization of dynamic graphs and formigrams

We can summarize a dynamic graph at different levels by post-composing the functors from Table 2. First of all, a formigram serves as a summary of the evolution of connected components in a DG via the path components functor $\pi_0 : \mathrm{Graph}(X) \to \mathrm{SubPart}(X)$ (cf. Definition 2.4):

Definition 3.10. Given a DG $\mathscr{G}_X : \mathbf{R} \to \mathrm{Graph}(X)$, the formigram of $\mathscr{G}_X$ is defined as $\pi_0 \circ \mathscr{G}_X : \mathbf{R} \to \mathrm{SubPart}(X)$ (cf. Figure 1 (A) and (B)).

Remark 3.11. We remark that the lifespan of any $x \in X$ in $\mathscr{G}_X$ is inherited by the formigram $\pi_0 \circ \mathscr{G}_X$. In particular, the formigram of a saturated DG is itself saturated (Definitions 3.1 and 3.8).

Figure 1 (B)–(F) illustrates the following definition. Recall the three functors in Definition 2.9.

Definition 3.12 (Summaries of formigrams)**.** Let $\theta_X : \mathbf{Int} \to \mathrm{SubPart}(X)$ be a formigram

(i) The *unlabeled formigram* of θ_X is the cosheaf obtained by post-composing the unlabeling functor $\mathscr{U}_L^X : \mathrm{SubPart}(X) \to \mathbf{Part}$ to θ_X.
(ii) The *(underlying) weighted Reeb graph* of θ_X, denoted by $\omega(\theta_X)$, is the cosheaf obtained by post-composing the agglomeration functor $\mathscr{A} : \mathbf{Part} \to \omega\mathbf{set}$ to the unlabeled formigram of θ_X.
(iii) The *(underlying) Reeb graph* of θ_X, denoted by $\mathrm{Reeb}(\theta_X)$, is the cosheaf obtained by post-composing the unweighting functor $\mathscr{U}_\omega : \omega\mathbf{set} \to \mathbf{set}$ to the weighted Reeb graph of θ_X.

The above three items can sometimes be difficult to visualize for example due to possible non-planarity (cf. Example 3.14 below). This motivates us to further summarize formigrams into more easily visualizable invariants. One such invariant is the (zigzag) barcode [18]:

(iv) The *(zigzag) barcode* of θ_X is the zigzag barcode of the cosheaf $\mathbf{Int} \to \mathbf{vec}$ obtained by post-composing the free functor $\mathscr{F} : \mathbf{set} \to \mathbf{vec}$ to the underlying Reeb graph of θ_X. In other words, $\mathrm{barc}_{\mathbf{ZZ}}(\theta_X)$ is the 0-th levelset barcode of the underlying Reeb graph of θ_X.

We now describe how to visualize a formigram and its underlying weighted/unweighted Reeb graphs. The results of the visualization are topological graphs over the real line with or without labels; see Figure 7 for an example. Let us fix a formigram $\theta_X : \mathbf{R} \to \mathrm{SubPart}(X)$ with a set $C \subset \mathbf{R}$ of critical points (cf. Remark 2.18 (ii)).

Step 1. for each $c \in C$, we specify the vertex set $V_c := \theta_X(c)$, which lie over $c \in \mathbf{R}$.

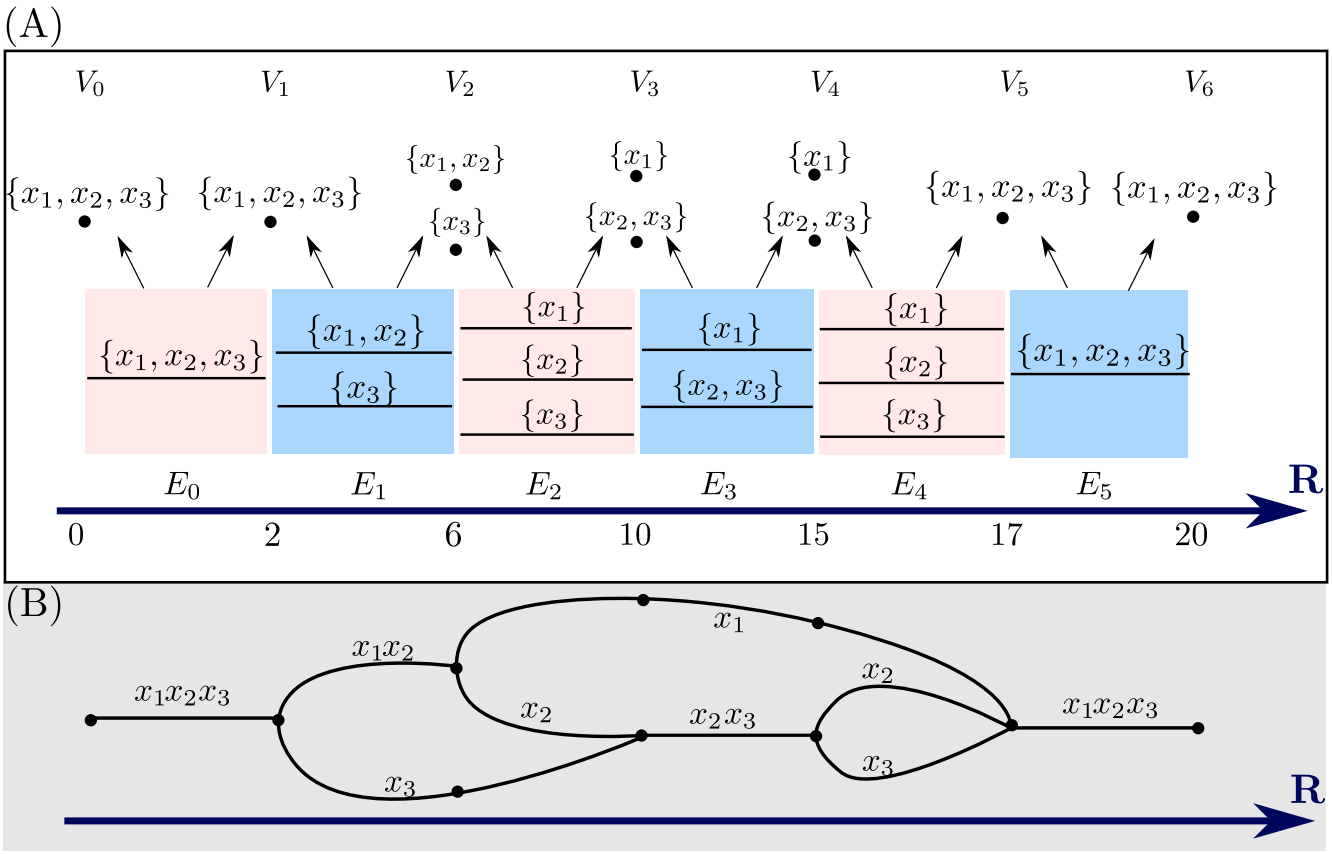


Figure 7: Visualization of the Reeb graph of a formigram $\theta_X : \mathbf{R} \to \mathrm{SubPart}(X)$. (A) The formigram θ_X is defined as follows over the interval $[0,20]$: Let $X := \{x_1, x_2, x_3\}$. $\theta_X(t)$ is $\{x_1x_2x_3\}$ for $t \in [0,2] \cup [17,20]$, it is $\{x_1x_2|x_3\}$ for $t \in (2,6]$, it is $\{x_1|x_2|x_3\}$ for $t \in (6,10) \cup (15,17)$, and it is $\{x_1|x_2x_3\}$ for $t \in [10,15]$. (B) depicts the Reeb graph of θ_X (with labels).

Step 2. for each pair of consecutive critical points $c_1 < c_2$ in C, we specify the edge set $E_{c_1,c_2} := \theta_X(t)$ for any $t \in (c_1, c_2)$, which lie over the interval (c_1, c_2),

Step 3. for each pair of consecutive critical points $c_1 < c_2$ in C, we define left and right attaching maps $l_{c_1,c_2} : E_{c_1,c_2} \to V_{c_1}$ and $r_{c_1,c_2} : E_{c_1,c_2} \to V_{c_2}$ by sending each block $B \in E_{c_1,c_2}$ to the blocks in V_{c_1} and V_{c_2} which contain B, respectively.

As a result, we obtain a topological graph along the real line such as the one depicted in Figure 7 (B). By replacing the labeling of the elements of vertex sets and edge sets by their cardinalities, we obtain the weighted Reeb graph of θ_X. Alternatively, weights can be represented by the thickness of nodes and edges as in Figure 1 (D). By forgetting those weights, we obtain the Reeb graph of θ_X.

The following example shows that two different non-isomorphic formigrams (Definition 3.9) can have the same underlying weighted/unweighted Reeb graph.

Example 3.13. For the sets $X := \{x_1, x_2, x_3\}$ and $Y := \{y_1, y_2, y_3\}$, we consider the following two formigrams θ_X and θ_Y over X and Y respectively:

$$\theta_X(t) := \begin{cases} \{x_1 x_2 | x_3\}, & t \in (-3,-1) \cup (1,3) \\ \{x_1 x_2 x_3\}, & \text{otherwise,} \end{cases} \qquad \theta_Y(t) := \begin{cases} \{y_1 y_2 | y_3\}, & t \in (-3,-1) \\ \{y_1 | y_2 y_3\}, & t \in (1,3) \\ \{y_1 y_2 y_3\}, & \text{otherwise.} \end{cases}$$

It is clear that θ_X and θ_Y are not isomorphic (cf. Definition 3.9) whereas their weighted Reeb graphs are both isomorphic to the weighted Reeb graph depicted in Figure 8 (A). This also implies that their *unweighted* Reeb graphs are isomorphic.

Reeb graphs of formigrams are not always planar, which can make the visualization of a formigram difficult [81]:

Example 3.14. Consider the formigram θ_X over the set $X = \{x_i\}_{i=1}^3 \cup \{y_i\}_{i=1}^3 \cup \{z_i\}_{i=1}^3$ given by:

$$\theta_X(t) := \begin{cases} \{x_1 x_2 x_3 | y_1 y_2 y_3 | z_1 z_2 z_3\}, & t \in (-\infty, 1] \\ \{x_1 | x_2 | x_3 | y_1 | y_2 | y_3 | z_1 | z_2 | x_3\}, & t \in (1,2) \\ \{x_1 y_1 z_1 | x_2 y_2 z_2 | x_3 y_3 z_3\}, & t \in [2,\infty). \end{cases}$$

See Figure 8 (B) for the Reeb graph of θ_X: this graph has the complete bipartite graph $K_{3,3}$ as a minor, which implies that it is not planar by Kuratowski's theorem [10].

4 Interleavings between dynamic graphs and between formigrams

Given any nonempty finite set X, recall that $\mathrm{Graph}(X)$ and $\mathrm{SubPart}(X)$ are lattices. Therefore, we readily have the interleaving distance between two DGs over the *same underlying set* X or between two formigrams over the *same underlying set* X (cf. Remark 2.18 (iii)). However, we often wish to quantify the difference between two given DGs (or between two formigrams) over possibly *different* underlying sets. For achieving this, we blend ideas related to the Gromov-Hausdorff distance (Definition A.2) with the interleaving distance. This type of idea has already appeared in the literature e.g. [20, 54, 61, 70].

Tripods and their compositions. We recall the notion of *tripod* from [61] as a preliminary to blending the Gromov-Hausdorff distance with the interleaving distance.

Definition 4.1 (Tripods)**.** Let X and Y be any two sets. A *tripod* R between X and Y is a pair of surjections from another set Z to X and Y, respectively. Namely, R can be expressed as a diagram $R : X \xleftarrow{\varphi_X} Z \xrightarrow{\varphi_Y} Y$.

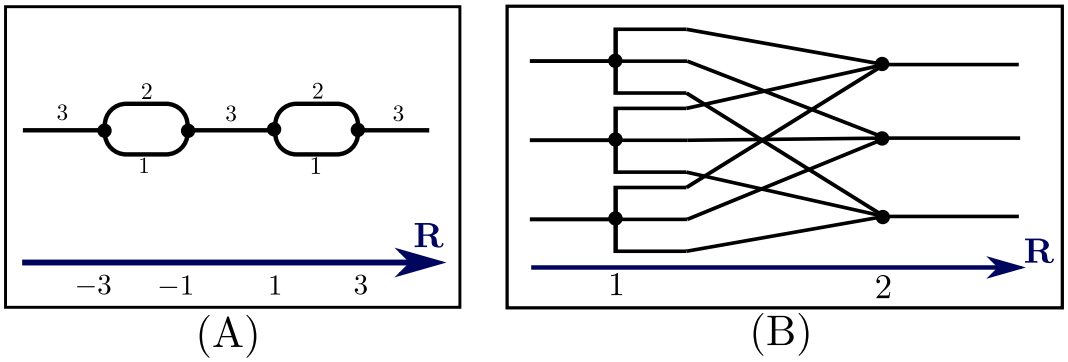
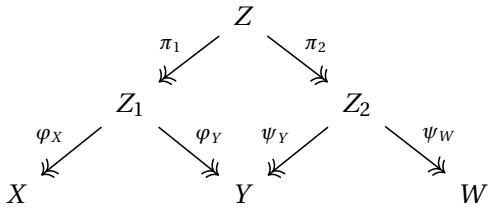


Figure 8: (A) The underlying weighted Reeb graph of the two formigrams from Example 3.13. (B) The underlying Reeb graph of the formigram from Example 3.14.

For any sets X, Y and W, consider any two tripods $R_1 : X \xleftarrow{\varphi_X} Z_1 \xrightarrow{\varphi_Y} Y$ and $R_2 : Y \xleftarrow{\psi_Y} Z_2 \xrightarrow{\psi_W} W$. Consider the set $Z := \{(z_1, z_2) \in Z_1 \times Z_2 : \varphi_Y(z_1) = \psi_Y(z_2)\}$ and let $\pi_1 : Z \to Z_1$ and $\pi_2 : Z \to Z_2$ be the canonical projections to the first and the second coordinate, respectively. We define the composite tripod $R_2 \circ R_1$ as follows:

$$R_2 \circ R_1 : X \xleftarrow{\omega_X} Z \xrightarrow{\omega_W} W, \text{ where } \omega_X := \varphi_X \circ \pi_1, \ \omega_W := \psi_W \circ \pi_2. \tag{1}$$



Notation 4.2. Given a tripod $R : X \xleftarrow{\varphi_X} Z \xrightarrow{\varphi_Y} Y$, for $x \in X$ and $y \in Y$, we write $(x, y) \in R$ whenever there exists $z \in Z$ such that $\varphi_X(z) = x$ and $\varphi_Y(z) = y$.

4.1 Interleaving distance between dynamic graphs

In this section we introduce the interleaving distance between DGs. Let $G_X = (X, E_X)$ be any graph and let Z be any set. For any map $\varphi : Z \to X$, the pullback $G_Z := \varphi^* G_X$ of G_X via φ is the graph on the vertex set Z with the edge set $E_Z = \{\{z, z'\} : \{\varphi(z), \varphi(z')\} \in E_X\}$. Let $\mathscr{G}_X = (V_X(\cdot), E_X(\cdot))$ be a DG over X. The *pullback* $\mathscr{G}_Z := \varphi^* \mathscr{G}_X$ of $\mathscr{G}_X$ via φ is a DG over Z defined as follows: for all $t \in \mathbf{R}$, $\mathscr{G}_Z(t)$ is the graph on the vertex set $V_Z(t) = \varphi^{-1}(V_X(t))$ with the edge set $E_Z(t) = \{\{z, z'\} : \{\varphi(z), \varphi(z')\} \in E_X(t)\}$.

Let $\mathscr{G}_X$ and $\mathscr{G}_Y$ be two DGs. Given a tripod $R : X \xleftarrow{\varphi_X} Z \xrightarrow{\varphi_Y} Y$, we write $\mathscr{G}_X \leq_R \mathscr{G}_Y$ if for all $t \in \mathbf{R}$ $\varphi_X^* \mathscr{G}_X(t) \leq \varphi_Y^* \mathscr{G}_Y(t)$ in the poset $\mathrm{Graph}(Z)$.

Remark 4.3. Let $\mathscr{G}_X$, $\mathscr{G}_Y$, and $\mathscr{G}_W$ be any three DGs. Let R_1 be any tripod between X and Y and let R_2 be any tripod between Y and W. If $\mathscr{G}_X \leq_{R_1} \mathscr{G}_Y$ and $\mathscr{G}_Y \leq_{R_2} \mathscr{G}_W$, then it is easy to check that $\mathscr{G}_X \leq_{R_2 \circ R_1} \mathscr{G}_W$ as well.

Recall that a DG $\mathscr{G}_X$ can be viewed as a constructible cosheaf $\mathbf{Int} \to \mathrm{Graph}(X)$ (Definition 3.1 and Remark 2.18 (ii)). This cosheaf sends each $I \in \mathbf{Int}$ to $\bigvee_I \mathscr{G}_X := \bigvee\{\mathscr{G}_X(t) : t \in I\} = \bigcup\{\mathscr{G}_X(t) : t \in I\}$. Therefore, we can utilize the interleaving distance between cosheaves (Definition 2.13) and tripods for quantifying the difference between two DGs over possibly different underlying sets.

Definition 4.4. Let $\mathscr{G}_X : \mathbf{Int} \to \mathrm{Graph}(X)$ and $\mathscr{G}_Y : \mathbf{Int} \to \mathrm{Graph}(Y)$ be two DGs. A tripod $R : X \xleftarrow{\varphi_X} Z \xrightarrow{\varphi_Y} Y$ is called an *ε-tripod between $\mathscr{G}_X$ and $\mathscr{G}_Y$* if $d_1^{\mathrm{Graph}(Z)}(\varphi_X^* \mathscr{G}_X, \varphi_Y^* \mathscr{G}_Y) \leq \varepsilon$. The interleaving distance between DGs

$\mathscr{G}_X$ and $\mathscr{G}_Y$ is defined as

$$d_{\mathrm{I}}^{\mathrm{dynG}}(\mathscr{G}_X,\mathscr{G}_Y)=\min\{\varepsilon\geq 0 : \text{there exists an } \varepsilon\text{-tripod between } \mathscr{G}_X \text{ and } \mathscr{G}_Y\}.$$

If there is no ε-tripod between $\mathscr{G}_X$ and $\mathscr{G}_Y$ for any $\varepsilon\geq 0$, then we declare $d_{\mathrm{I}}^{\mathrm{dynG}}(\mathscr{G}_X,\mathscr{G}_Y)=+\infty$.

Theorem 4.5. $d_{\mathrm{I}}^{\mathrm{dynG}}$ in Definition 4.4 is an extended pseudo metric on DGs.

We need the following lemma for proving Theorem 4.5.

Lemma 4.6. Let $\varphi : Z \twoheadrightarrow X$ be a surjective map. Then, for any DG $\mathscr{G}_X$ and any $I\in\mathbf{Int}$, $\varphi^*\left(\bigvee_I \mathscr{G}_X\right)=\bigvee_I \varphi^*\mathscr{G}_X$.

Proof. Fix $z,z'\in Z$ (it is possible that $z=z'$). Note that $\bigvee_I\mathscr{G}_X$ is the union $\cup_{t\in I}\mathscr{G}_X(t)$. We have that $\{z,z'\}\in\varphi^*\left(\bigvee_I\mathscr{G}_X\right)$ iff $\{\varphi(z),\varphi(z')\}\in\bigvee_I\mathscr{G}_X$ iff $\exists t\in I$, $\{\varphi(z),\varphi(z')\}\in\mathscr{G}_X(t)$ iff $\exists t\in I$, $\{z,z'\}\in\varphi^*\mathscr{G}_X(t)$ iff $\{z,z'\}\in\bigvee_I\varphi^*\mathscr{G}_X$. □

Proof of Theorem 4.5. Reflexivity and symmetry of $d_{\mathrm{I}}^{\mathrm{dynG}}$ are clear and thus we only show the triangle inequality: Let X,Y and W be some finite sets and let $\mathscr{G}_X,\mathscr{G}_Y$ and $\mathscr{G}_W$ be DGs over the three sets respectively. We wish to prove that $d_{\mathrm{I}}^{\mathrm{dynG}}(\mathscr{G}_X,\mathscr{G}_W)\leq d_{\mathrm{I}}^{\mathrm{dynG}}(\mathscr{G}_X,\mathscr{G}_Y)+d_{\mathrm{I}}^{\mathrm{dynG}}(\mathscr{G}_Y,\mathscr{G}_W)$. Let $0<\varepsilon_1,\varepsilon_2<\infty$, and suppose that there are an ε_1-tripod $R_1:\ X \xleftarrow{\varphi_X} Z_1 \xrightarrow{\varphi_Y} Y$ between $\mathscr{G}_X$ and $\mathscr{G}_Y$ and an ε_2-tripod $R_2:\ Y \xleftarrow{\psi_Y} Z_2 \xrightarrow{\psi_W} W$ between $\mathscr{G}_Y$ and $\mathscr{G}_W$. It suffices to prove that $R_2\circ R_1$ is an $(\varepsilon_1+\varepsilon_2)$-tripod between $\mathscr{G}_X$ and $\mathscr{G}_W$. Let $I\in\mathbf{Int}$. Since R_1 is an ε_1-tripod between $\mathscr{G}_X$ and $\mathscr{G}_Y$, we have $\bigvee_I\varphi_X^*\mathscr{G}_X\leq\bigvee_{I^{\varepsilon_1}}\varphi_Y^*\mathscr{G}_Y$. Since R_2 is an ε_2-tripod between $\mathscr{G}_Y$ and $\mathscr{G}_W$, we have $\bigvee_{I^{\varepsilon_1}}\psi_Y^*\mathscr{G}_Y\leq\bigvee_{I^{\varepsilon_1+\varepsilon_2}}\psi_W^*\mathscr{G}_W$. Therefore, by Lemma 4.6,

$$\bigvee_I \pi_1^*\varphi_X^*\mathscr{G}_X\leq\bigvee_{I^{\varepsilon_1}}\pi_1^*\varphi_Y^*\mathscr{G}_Y=\bigvee_{I^{\varepsilon_1}}\pi_2^*\psi_Y^*\mathscr{G}_Y\leq\bigvee_{I^{\varepsilon_1+\varepsilon_2}}\pi_2^*\psi_W^*\mathscr{G}_W.$$

By symmetry we also have $\bigvee_I\pi_2^*\psi_W^*\mathscr{G}_W\leq\bigvee_{I^{\varepsilon_1+\varepsilon_2}}\pi_1^*\varphi_X^*\mathscr{G}_X$. Since $I\in\mathbf{Int}$ is arbitrary, we have shown that $R_2\circ R_1$ is an $(\varepsilon_1+\varepsilon_2)$-tripod between $\mathscr{G}_X$ and $\mathscr{G}_W$, as desired. □

Given a DG $\mathscr{G}_X:\mathbf{R}\to\mathrm{Graph}(X)$, let $\mathrm{crit}(\mathscr{G}_X)$ denote the set of points of discontinuity, i.e. critical points (cf. Definition 2.17).

Theorem 4.7 (Complexity of $d_{\mathrm{I}}^{\mathrm{dynG}}$)**.** Fix $\rho\in(1,6)$. Then, it is not possible to compute a ρ-approximation to $d_{\mathrm{I}}^{\mathrm{dynG}}(\mathscr{G}_X,\mathscr{G}_Y)$ between DGs in time polynomial in $|X|,|Y|,|\mathrm{crit}(\mathscr{G}_X)|$, and $|\mathrm{crit}(\mathscr{G}_Y)|$, unless $P=NP$.

We prove Theorem 4.7 in Appendix A.2 by showing that certain NP-hard instances of the Gromov-Hausdorff distance between finite metric spaces can be reduced to the computation of the interleaving distance $d_{\mathrm{I}}^{\mathrm{dynG}}$ between DGs.

Remark 4.8 (When is $d_{\mathrm{I}}^{\mathrm{dynG}}\leq\varepsilon$)**.** In Definition 4.4, the condition $d_{\mathrm{I}}^{\mathrm{Graph}(Z)}(\varphi_X^*\mathscr{G}_X,\varphi_Y^*\mathscr{G}_Y)\leq\varepsilon$ with respect to the tripod $R:\ X \xleftarrow{\varphi_X} Z \xrightarrow{\varphi_Y} Y$ is equivalent to the following: For $(x,y),(x',y')\in R$,

(i) if $x\in V_X(t)$, then there exists $s\in[t]^\varepsilon:=[t-\varepsilon,t+\varepsilon]$ such that $y\in V_Y(s)$.

(ii) if $\{x,x'\}\in E_X(t)$, then there exists $s\in[t]^\varepsilon$ such that $\{y,y'\}\in E_Y(s)$.

Furthermore, the two statements obtained by exchanging the roles of X and Y in the above two items also hold.

A sufficient condition for a pair of DGs to be ε-interleaved is described in the following example.

Example 4.9. Fix $\varepsilon\geq 0$. Let $\mathscr{G}_X$ and $\mathscr{G}_Y$ be two DGs such that for every $x,x'\in X$ (resp. every $y,y'\in Y$), for any time interval I of length ε, there exists $t\in I$ such that the edge $\{x,x'\}$ (resp. $\{y,y'\}$) is present at $\mathscr{G}_X(t)$ (resp. $\mathscr{G}_Y(t)$). Then, $d_{\mathrm{I}}^{\mathrm{dynG}}(\mathscr{G}_X,\mathscr{G}_Y)\leq\varepsilon$. Indeed, by invoking Remark 2.18 (iii), it can be checked that *any* tripod R between X and Y is an ε-tripod between $\mathscr{G}_X$ and $\mathscr{G}_Y$.

4.2 Interleaving distance between formigrams

In this section we introduce the interleaving distance between formigrams. This metric quantifies the structural difference between two grouping/disbanding behaviors over time. We also show that this metric dovetails with other celebrated metrics, which makes the summarization pipeline that is illustrated in Figure 1 is entirely stable; see Remark 4.12, Proposition 4.13, Corollary 4.16, and Theorem 4.17.

Let X and Z be any two sets and let $P_X \in \mathrm{SubPart}(X)$. For any map $\varphi : Z \to X$, the *pullback* $P_Z := \varphi^* P_X$ of P_X via φ is the subpartition of Z defined as $P_Z = \{\varphi^{-1}(B) : B \in P_X\}$. Let θ_X be a formigram over X and assume that φ is surjective. Then the *pullback* of θ_X via φ is the formigram $\theta_Z := \varphi^*\theta_X$ over Z defined as $\theta_Z(t) = \varphi^*\theta_X(t)$ for all $t \in \mathbf{R}$.

Definition 4.10 (Comparison of formigrams via pullbacks)**.** Consider a tripod $R : X \xleftarrow{\varphi_X} Z \xrightarrow{\varphi_Y} Y$.

(i) Let $P_X \in \mathrm{SubPart}(X)$ and $P_Y \in \mathrm{SubPart}(Y)$. we write $P_X \leq_R P_Y$ if $\varphi_X^* P_X \leq \varphi_Y^* P_Y$ in the poset $\mathrm{SubPart}(Z)$.
(ii) Let θ_X, θ_Y be any two formigrams. we write $\theta_X \leq_R \theta_Y$ if for all $t \in \mathbf{R}$, $\varphi_X^*\theta_X(t) \leq \varphi_Y^*\theta_Y(t)$ in $\mathrm{SubPart}(Z)$.

Let us recall that a formigram θ_X can be viewed as a constructible cosheaf $\mathbf{Int} \to \mathrm{SubPart}(X)$ (Remark 2.18 (ii)); this cosheaf sends each $I \in \mathbf{Int}$ to $\bigvee_I \theta_X := \bigvee\{\theta_X(t) : t \in I\}$. We now utilize both the interleaving distance between cosheaves (Definition 2.13) and the notion of tripod for quantifying the degree of difference between two formigrams over possibly different underlying sets.

Definition 4.11. Let θ_X and θ_Y be two formigrams. A tripod $R : X \xleftarrow{\varphi_X} Z \xrightarrow{\varphi_Y} Y$ is called an *ε-tripod between θ_X and θ_Y* if $d_{\mathrm{I}}^{\mathrm{SubPart}(Z)}(\varphi_X^*\theta_X, \varphi_Y^*\theta_Y) \leq \varepsilon$. The *interleaving distance* between formigrams θ_X and θ_Y is defined as

$$d_{\mathrm{I}}^{\mathrm{F}}(\theta_X, \theta_Y) = \min\{\varepsilon \geq 0 : \text{there exists an } \varepsilon\text{-tripod between } \theta_X \text{ and } \theta_Y\}.$$

If there is no ε-tripod between θ_X and θ_Y for any $\varepsilon \geq 0$, then we declare $d_{\mathrm{I}}^{\mathrm{F}}(\theta_X, \theta_Y) = +\infty$.

$d_{\mathrm{I}}^{\mathrm{F}}$ is is an extended pseudo metric on formigrams, which can be proved in a similar way to $d_{\mathrm{I}}^{\mathrm{dynG}}$.

Remark 4.12. (i) For unlabeled formigrams $\theta, \theta' : \mathbf{Int} \to \mathbf{Part}$ (cf. Definition 2.15), the interleaving distance $d_{\mathrm{I}}^{\mathbf{Part}}(\theta, \theta')$ (cf. Definition 2.13) can easily be infinite and thus might not be useful in practice; it is not difficult to check that $d_{\mathrm{I}}^{\mathbf{Part}}(\theta, \theta')$ is finite only if the colimits of θ and θ' have the same cardinality. In this respect, by Remark 3.6, $d_{\mathrm{I}}^{\mathrm{F}}$ can also be viewed as a practical metric between unlabeled formigrams by defining

$$d_{\mathrm{I}}^{\mathrm{F}}(\theta, \theta') := d_{\mathrm{I}}^{\mathrm{F}}(\theta_X, \theta_Y) \tag{2}$$

where $\theta = \mathscr{U}_L^X \circ \theta_X$ and $\theta' = \mathscr{U}_L^Y \circ \theta_Y$. The choices of the labeling sets X and Y do not affect the RHS of equation (2) and thus $d_{\mathrm{I}}^{\mathrm{F}}(\theta, \theta')$ is well-defined.

(ii) $d_{\mathrm{I}}^{\mathrm{F}}$ between dendrograms agrees with (twice) the Gromov-Hausdorff distance between their canonically associated ultrametrics (cf. Proposition A.6).

$d_{\mathrm{I}}^{\mathrm{F}}$ is more discriminative than the interleaving distance for Reeb graphs (cf. Remark 2.21).

Proposition 4.13. For any two formigrams θ_X and θ_Y, we have

$$d_{\mathrm{I}}^{\mathrm{R}}(\mathrm{Reeb}(\theta_X), \mathrm{Reeb}(\theta_Y)) \leq d_{\mathrm{I}}^{\mathrm{F}}(\theta_X, \theta_Y).$$

In the appendix, we define a distance $d_{\mathrm{I}}^{\omega\mathrm{R}}$ between weighted Reeb graphs which mediates between $d_{\mathrm{I}}^{\mathrm{F}}$ and $d_{\mathrm{I}}^{\mathrm{R}}$ (cf. Theorem B.3 and Remark 6.38).

Example 4.14. Since θ_X and θ_Y in Example 3.13 have the same (un)weighted Reeb graph, they are not discriminated by the interleaving distance between (un)weighted Reeb graphs. However, $d_{\mathrm{I}}^{\mathrm{F}}(\theta_X, \theta_Y) = 1$. Indeed, any tripod R between X and Y fails to be an ε-tripod between θ_X and θ_Y for $\varepsilon < 1$ and the tripod $R : X \xleftarrow{\varphi_X} Z \xrightarrow{\varphi_Y} Y$ which is defined as follows is a 1-tripod: Let $Z = \{(x_1, y_1), (x_2, y_2), (x_2, y_3)\} \subset X \times Y$ and let φ_X and φ_Y be the canonical projections to the first coordinate and the second coordinate, respectively.

Let us recall from Definition 2.2 that the underlying set of $P \in \mathrm{SubPart}(X)$ is defined as $\bigcup P$. When $x \in X$ belongs to $\bigcup P$, we denote the block containing x by $[x]$. The following remark describes an if-and-only-if condition for a tripod to be an ε-tripod between formigrams.

Remark 4.15. Let θ_X, θ_Y be any two formigrams and consider a tripod $R:\ X \xleftarrow{\varphi_X} Z \xrightarrow{\varphi_Y} Y$. Then the condition $d_{\mathrm{I}}^{\mathrm{SubPart}(Z)}(\varphi_X^*\theta_X, \varphi_Y^*\theta_Y) \leq \varepsilon$ holds if and only if the following hold: for any $I \in \mathbf{Int}$,

(i) If $(x,y) \in R$, x belongs to the underlying set of $\bigvee_I \theta_X$ then y belongs to the underlying set of $\bigvee_{I^\varepsilon} \theta_Y$.

(ii) If $(x,y),(x',y') \in R$, whenever $[x] = [x']$ in $\bigvee_I \theta_X$, it holds that $[y] = [y']$ in $\bigvee_{I^\varepsilon} \theta_Y$.

Also, the two statements obtained by exchanging the roles of X and Y in the above two items hold.

Proof of Proposition 4.13. Let $R:\ X \xleftarrow{\varphi_X} Z \xrightarrow{\varphi_Y} Y$ be an ε-tripod between θ_X and θ_Y. For $I \in \mathbf{Int}$, let us define the set map $f_{R,I} : \bigvee_I \theta_X \to \bigvee_{I^\varepsilon} \theta_Y$ as $f_{R,I}([x]) := [y] \in \bigvee_{I^\varepsilon} \theta_Y$ where $(x,y) \in R$ (this map is well-defined by Remark 4.15). Also, define $g_{R,I} : \bigvee_I \theta_Y \to \bigvee_{I^\varepsilon} \theta_X$ in a similar way. The collections $f_R := \{f_{R,I}\}_{I \in \mathbf{Int}}$ and $g_R := \{g_{R,I}\}_{I \in \mathbf{Int}}$ form an ε-interleaving pair between $\mathrm{Reeb}(\theta_X)$ and $\mathrm{Reeb}(\theta_Y)$, thus completing the proof. □

Corollary 4.16. For any two formigrams θ_X and θ_Y, we have

$$d_{\mathrm{B}}(\mathrm{barc}_{\mathbf{ZZ}}(\theta_X), \mathrm{barc}_{\mathbf{ZZ}}(\theta_Y)) \leq 2 \cdot d_{\mathrm{I}}^{\mathrm{F}}(\theta_X, \theta_Y).$$

Proof. The claim directly follows from Theorem 2.22 and Proposition 4.13. □

Summarizing DGs into formigrams via the path components functor π_0 (Definition 3.10) is stable:

Theorem 4.17. Let θ_X and θ_Y be the formigrams of two DGs $\mathscr{G}_X$ and $\mathscr{G}_Y$ respectively. Then,

$$d_{\mathrm{I}}^{\mathrm{F}}(\theta_X, \theta_Y) \leq d_{\mathrm{I}}^{\mathrm{dynG}}(\mathscr{G}_X, \mathscr{G}_Y).$$

This inequality is tight (cf. Remark 6.37 (i)).

Proof. Let $\varepsilon \geq 0$ and let $R:\ X \xleftarrow{\varphi_X} Z \xrightarrow{\varphi_Y} Y$ be an ε-tripod between $\mathscr{G}_X$ and $\mathscr{G}_Y$. We prove that R is also an ε-tripod between the formigrams θ_X and θ_Y. By symmetry, it suffices to show that $\bigvee_I \theta_X \leq_R \bigvee_{I^\varepsilon} \theta_Y$. Let $z \in Z$ and let $x := \varphi_X(z)$, and $y := \varphi_Y(z)$. Fix $t \in \mathbf{R}$. Suppose that x is in the underlying set of $\bigvee_I \theta_X$. Since $\bigvee_I \mathscr{G}_X \leq_R \bigvee_{I^\varepsilon} \mathscr{G}_Y$, we have $y \in \cup_{s \in I^\varepsilon} V_Y(s)$, which is the underlying set of $\bigvee_{I^\varepsilon} \theta_Y$. Pick another $z' \in Z$ and let $x' := \varphi_X(z')$ and $y' := \varphi_Y(z')$. Assume that x, x' belong to the same block of $\theta_X(t)$, meaning that there is a sequence $x = x_0, x_1, \ldots, x_n = x'$ in X such that $\{x_i, x_{i+1}\} \in E_X(t)$ for $0 \leq i \leq n-1$. For each $1 \leq i \leq n-1$, pick $y_i \subset Y$ such that $(x_i, y_i) \in R$. Since R is an ε-tripod between $\mathscr{G}_X$ and $\mathscr{G}_Y$, we have $\{y_i, y_{i+1}\} \in \bigcup_{s \in I^\varepsilon} E_Y(s)$ (Remark 4.8). Then, y, y' belong to the same connected component of the graph $\bigcup_{I^\varepsilon} \mathscr{G}_Y$ and in turn, by Lemma 4.6, the same block of $\bigvee_{I^\varepsilon} \theta_Y$. □

Remark 4.18. By Remark 4.12 (ii), constant factor approximations to $d_{\mathrm{I}}^{\mathrm{F}}$ cannot be obtained in polynomial time (Theorem A.7). The lower bound for $d_{\mathrm{I}}^{\mathrm{F}}$ given by Proposition 4.13 can also lead to difficult computational problems (e.g. the graph-isomorphism problem [33, Section 5]). Hence, computing the lower bound for $d_{\mathrm{I}}^{\mathrm{F}}$ given by Corollary 4.16 is a realistic approach to comparing formigrams. Another tractable lower bound for $d_{\mathrm{I}}^{\mathrm{F}}$ is introduced in the next section; Theorem 6.35, which can sometimes be more discriminative than the lower bounds in Proposition 4.13 and Corollary 4.16.

5 Categorical aspects of $\mathrm{SubPart}(X)$, Part and set

In this section we establish a few categorical results that will be useful in later sections: We show that (1) the unlabeling functor preserves limits and colimits of connected diagrams (cf. Proposition 5.1) and that (2) the composition of the three functors in Definition 2.9 preserves colimits of connected diagrams (cf. Proposition 5.4). Lastly, we compute coimages in the category **Part** (cf. Proposition 5.8).

5.1 (Co)limit preserving properties of unlabeling and collapsing functors

Let X be a nonempty finite set. The unlabeling functor $\mathscr{U}_L^X : \mathrm{SubPart}(X) \to \mathbf{Part}$ (Definition 2.9 (i)) preserves limits and colimits of connected diagrams in $\mathrm{SubPart}(X)$:

Proposition 5.1. Let $\mathbf{P}$ be a connected poset. For any $\theta_X : \mathbf{P} \to \mathrm{SubPart}(X)$, we have $\mathscr{U}_L^X\left(\varprojlim \theta_X\right) \cong \varprojlim \mathscr{U}_L^X(\theta_X)$ and $\mathscr{U}_L^X\left(\varinjlim \theta_X\right) \cong \varinjlim \mathscr{U}_L^X(\theta_X)$.

The proof is rather straightforward and hence we omit it.

Definition 5.2. Let $P, Q \in \mathrm{SubPart}(X)$ such that $P \leq Q$. The *canonical map* $P \to Q$ is the unique map which sends each block $B \in P$ to the *unique* block $C \in Q$ such that $B \subset C$. In other words, the canonical map is the image of $P \leq Q$ via the three functors in Definition 2.9.

Definition 5.3. The *collapsing functor* $\mathscr{C} : \mathrm{SubPart}(X) \to \mathbf{set}$ is defined as the composition of the three functors in Definition 2.9, i.e. $\mathscr{U}_\omega \circ \mathscr{A} \circ \mathscr{U}_L^X$. Namely, $\mathscr{C}$ sends each $P \in \mathrm{SubPart}(X)$ to $P \in \mathrm{ob}(\mathbf{set})$ and each morphism $P \leq Q$ in $\mathrm{SubPart}(X)$ to the canonical map $P \to Q$.

The collapsing functor preserves the colimit of any diagram in $\mathrm{SubPart}(X)$ indexed by a *connected* poset (Definition 2.10 (iii)). For example, let $X := \{x_1, x_2, x_3, x_4\}$ and consider the diagram $\theta_X : \{1 \leq 2 \geq 3 \leq 4\} \to \mathrm{SubPart}(X)$ defined as

$$\{x_1|x_2|x_3|x_4\} \leq \{x_1x_2|x_3x_4\} \geq \{x_1|x_2|x_3x_4\} \leq \{x_1|x_2x_3x_4\}.$$

Then, $\varinjlim \theta_X = \{x_1x_2x_3x_4\} \in \mathrm{SubPart}(X)$ and $\mathscr{C}\left(\varinjlim \theta_X\right) = \{\{x_1, x_2, x_3, x_4\}\} \in \mathrm{ob}(\mathbf{set})$, which is the colimit of the set diagram

$$\{\{x_1\},\{x_2\},\{x_3\},\{x_4\}\} \to \{\{x_1, x_2\},\{x_3, x_4\}\} \leftarrow \{\{x_1\},\{x_2\},\{x_3, x_4\}\} \to \{\{x_1\},\{x_2, x_3, x_4\}\}$$

where every map in the cocone is a canonical map. We omit the proof of the following proposition.

Proposition 5.4. Let $\mathbf{P}$ a connected poset. For any $\theta_X : \mathbf{P} \to \mathrm{SubPart}(X)$, we have $\mathscr{C}\left(\varinjlim \theta_X\right) \cong \varinjlim \mathscr{C}(\theta_X)$.

We remark that the collapsing functor $\mathscr{C}$ does *not* preserve limits (which is actually a consequence that the agglomeration functor $\mathscr{A}$ does not preserve limits). For example, let $Y = \{y_1, y_2\}$ and consider the diagram $\theta_Y : \{1 \leq 2 \geq 3\} \to \mathrm{SubPart}(Y)$ given by $\{y_1\} \leq \{y_1y_2\} \geq \{y_2\}$. Then, $\varprojlim \theta_Y = \emptyset$ which is the greatest lower bound of $\{y_1\},\{y_1y_2\},\{y_2\}$ in $\mathrm{SubPart}(Y)$. However, $\mathscr{C}(\theta_X)$ is represented as the set diagram $\{\bullet\} \to \{\bullet\} \leftarrow \{\bullet\}$ and thus $\varprojlim \mathscr{C}(\theta_X)$ contains a single element.

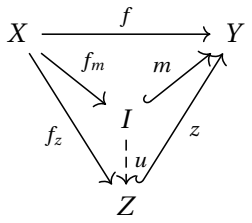
5.2 (Co)images in the category of partitions

The goal of this section is to compute coimages in **Part** (cf. Proposition 5.8).

Images and coimages in category theory [62]. A morphism $f : a \to b$ is said to be a *monomorphism* (*mono* in short) if f is left-cancellative: for any morphisms $k_1, k_2 : c \to a$, if $f \circ k_1 = f \circ k_2$, then $k_1 = k_2$. Such f is written as $f : a \hookrightarrow b$ and a is called a *subobject* of b. On the other hand, a right-cancellative morphism $g : a \to b$ is said to be an *epimorphism* (*epi* in short), written as $g : a \twoheadrightarrow b$, and b is called a *quotient object* of a.

The *image* of a morphism $f : X \to Y$ is defined as the smallest subobject of Y which f factors through.

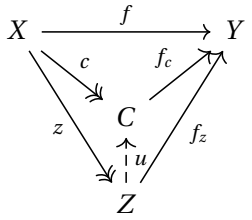
Definition 5.5 (Images)**.** Given a morphism $f : X \to Y$, an *image* of f (if it exists) is a mono $m : I \hookrightarrow Y$ such that there is a morphism $f_m : X \to I$ such that $f = m \circ f_m$, for any mono $z : Z \hookrightarrow Y$ and a morphism $f_z : X \to Z$ with $f = z \circ f_z$, there is a unique morphism $u : I \to Z$ such that $m = z \circ u$.



The object I will be sometimes denoted by $\mathrm{im}(f)$.

The *coimage* of a morphism is the dual notion of the image of a morphism. In many categories (such as the category of sets, the category of groups, the category of rings, or the category of vector spaces, and etc.), the coimage is canonically isomorphic to the image, often called the *first isomorphism theorem*. However, in the category **Part**, those two are turned out to be different in general.

Definition 5.6 (Coimages)**.** Given a morphism $f : X \to Y$, a coimage of f (if it exists) is an epi $c : X \to C$ such that there is a morphism $f_c : C \to Y$ with $f = f_c \circ c$, for any epi $z : X \to Z$ for which there is a map $f_z : Z \to Y$ with $f = f_z \circ z$, there is a unique map $u : Z \to C$ such that $c = u \circ z$.



Images and coimages in Part. It is not difficult to check that every morphism $f : (X, P_X) \to (Y, P_Y)$ in **Part** is a mono. On the other hand, we have the following characterization of epis in **Part**.

Proposition 5.7. A morphism $f : (X, P_X) \to (Y, P_Y)$ in **Part** is an epi if and only if $f : X \hookrightarrow Y$ is surjective (hence f is bijective).

We remark that the bijectivity of $f : X \to Y$ does not imply that f is an isomorphism in between (X, P_X) and (Y, P_Y).

Proof. For the forward direction, we prove the contrapositive. Suppose that f is not surjective, i.e. there exists $y \in Y$ to which no $x \in X$ is mapped via f. Let $Z = \{z_1, z_2\}$. Let $k_1, k_2 : Y \to Z$ be any pair of maps such that they differ only at y, i.e. $k_1 = k_2$ on $Y \setminus \{y\}$ and $k_1(y) \neq k_2(y)$. Then both k_1 and k_2 are morphisms from (Y, P_Y) to $(Z, \{z_1 z_2\})$. Although $k_1 \circ f = k_2 \circ f$, we do not have that $k_1 = k_2$. Hence, f is not an epi.

We prove the backward direction. Consider any two morphisms $k_1, k_2 : (Y, P_Y) \to (Z, P_Z)$ such that $k_1 \circ = k_2 \circ f$. Let $y \in Y$. Since f is surjective, there exists $x \in X$ such that $f(x) = y$. Hence, $k_1 \circ f(x) = k_2 \circ f(x)$ implies $k_1(y) = k_2(y)$. Since y was arbitrarily chosen in Y, we have that $k_1 = k_2$. □

Consider any morphism $f : (X, P_X) \to (Y, P_Y)$ in **Part**. Let $f^{-1}(P_Y) := \{f^{-1}(B) : B \in P_Y\}$ which is a partition of X. Notice that the identity map id_X on X is a morphism from (X, P_X) to $(X, f^{-1}(P_Y))$. Now we will see that, in the category **Part**, the image is not isomorphic to the coimage in general.

Proposition 5.8. For any morphism $f : (X, P_X) \to (Y, P_Y)$ in **Part**,

(i) f itself is an image of f.
(ii) The morphism $\mathrm{id}_X : (X, P_X) \to (X, f^{-1}(P_Y))$, the identity set map on X, is a coimage of f.

Proof. Item (i) directly follows from the fact that f is a mono. We prove Item (ii). Since $\mathrm{id}_X : X \to X$ is bijective, by Proposition 5.7, id_X is an epi from (X, P_X) to $(X, f^{-1}(P_Y))$. Note also that f is a morphism from $(X, f^{-1}(P_Y))$ to (Y, P_Y) with the obvious identity $f \circ \mathrm{id}_X = f$. Assume that there exists a pair of an epi $z : (X, P_X) \twoheadrightarrow (Z, P_Z)$ and a morphism $f_z : (Z, P_Z) \to (Y, P_Y)$ such that $f = f_z \circ z$. Since z is an epi, the set map $z : X \to Z$ must be bijective. The proof ends by observing that the inverse $z^{-1} : Z \to X$ is the *unique* morphism u from (Z, P_Z) to $(X, f^{-1}(P_Y))$ such that $\mathrm{id}_X = u \circ z$. □

Example 5.9. Consider $i : (\{x_1, x_2\}, \{x_1|x_2\}) \to (\{x_1, x_2, x_3\}, \{x_1x_2x_3\})$ where i is the canonical inclusion $\{x_1, x_2\} \hookrightarrow \{x_1, x_2, x_3\}$. The coimage of i is the morphism $\mathrm{id}_{\{x_1,x_2\}} : (\{x_1, x_2\}, \{x_1|x_2\}) \to (\{x_1, x_2\}, \{x_1x_2\})$.

6 Summarizing formigrams via Möbius inversion

In this section we describe two novel summaries of formigrams: *maximal group diagrams* (cf. Figure 2 (C)) and *persistence clustergrams* (cf. Figure 1 (G)); Definitions 6.16 and 6.27.

In Section 6.1 we review the Möbius inversion formula for a function from a locally finite poset. In Section 6.2, we introduce a notion of *silhouette*[6] for a group-valued map from a poset; this notion allows us to have the summarization process that is illustrated as the arrow from (G) to (H) in Figure 1. In Section 6.3, we show that the celebrated notion of *maximal groups* by Buchin et al. [15] is an instance of the generalized persistence diagrams considered in [53, 67]. Namely, we prove that maximal groups can be obtained by computing the Möbius inversion of a suitably defined rank function. In Section 6.4, we introduce persistence clustergrams, which can be regarded as being "dual" to maximal group diagrams. In Section 6.5 and Section 6.6, we consider the silhouette of a persistence clustergram and establish its stability.

Convention 6.1. In Section 6 we only consider formigrams with finite support whose critical points are contained in $\mathbf{Z}$ (cf. Definitions 2.17 and 3.5). We will not distinguish between the real interval $\langle a, b\rangle$ and $\langle a, b\rangle_{\mathbf{ZZ}} \in \mathbf{Int}(\mathbf{ZZ})$ for any $a \le b$ in $\mathbf{Z}$ (cf. Notation 2.12).

6.1 Möbius inversion of a function on a poset

We review the Möbius inversion formula for a function f on a locally finite poset [72]. In a nutshell, Möbius inversion is a discrete analogue of the derivative of a real-valued map from calculus. For example, given a map $f : \mathbf{Z} \to \mathbf{R}$ (where $\mathbf{Z}$ is equipped with the canonical order), its Möbius inversion $f' : \mathbf{Z} \to \mathbf{R}$ is defined as $f'(n) = f(n) - f(n-1)$ for $n \in \mathbf{Z}$, capturing the change of f at the point n relative to the value of f at the point $n-1$. More generally, we can define Möbius inversion of a function on any locally finite poset.

Definition 6.2. A poset $\mathbf{P}$ is said to be *locally finite* if for all $p, q \in \mathbf{P}$ with $p \le q$ the set $\{r \in \mathbf{P} : p \le r \le q\}$ is finite.

Let $\mathbf{P}$ be a locally finite poset. The *Möbius function* $\mu_{\mathbf{P}} : \mathbf{P} \times \mathbf{P} \to \mathbf{Z}$ of $\mathbf{P}$ is defined recursively as

$$\mu_{\mathbf{P}}(p, q) := \begin{cases} 1, & p = q, \\ -\sum_{p \le r < q} \mu_{\mathbf{P}}(p, r), & p < q, \\ 0, & \text{otherwise.} \end{cases} \tag{3}$$

Example 6.3. Let $\mathbf{P} := \mathbf{Int}(\mathbf{ZZ})$ (Definition 2.11). Then,

$$\mu_{\mathbf{P}}(I, J) = \begin{cases} 1, & I = J \text{ or } I \subsetneq J \text{ with } |J \setminus I| = 2, \\ -1, & I \subsetneq J \text{ with } |J \setminus I| = 1, \\ 0, & \text{otherwise.} \end{cases}$$

[6] Silhouettes in this paper have no relation with the *persistence silhouettes* in [24].

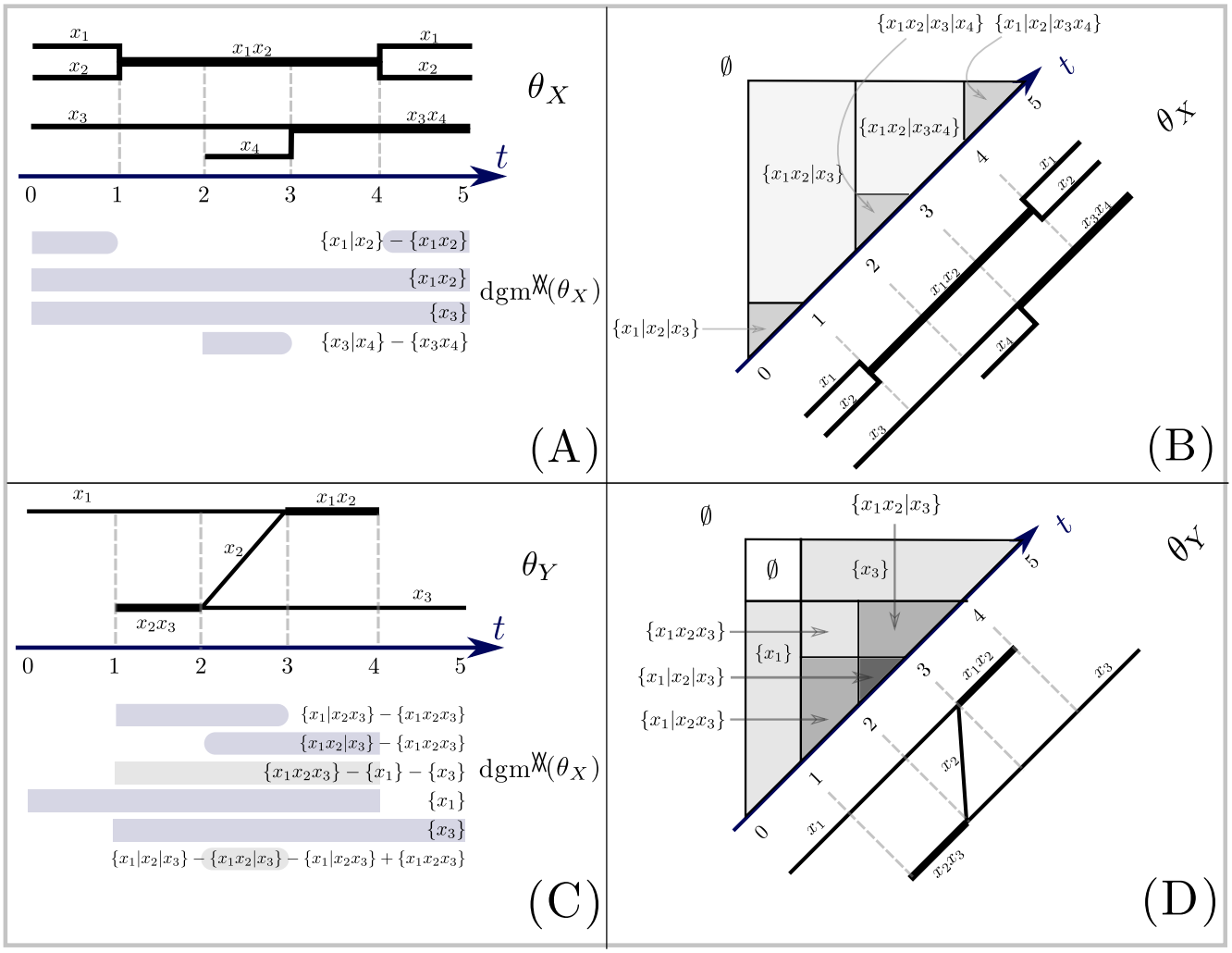


Figure 9: (A) A formigram θ_X over the set $X := \{x_1, x_2, x_3, x_4\}$ with support $[0,5]$ (i.e. union of the lifespans of all points) and the persistence clustergram $\mathrm{dgm}^{\mathbb{W}}(\theta_X)$. (B) An illustration of $\mathbb{W}\theta_X : \mathbf{Int} \to \mathrm{SubPart}(X)$ for θ_X in (A). The persistence clustergram $\mathrm{dgm}^{\mathbb{W}}(\theta_X)$ in (A) is the Möbius inversion of $\mathbb{W}\theta_X$. (C) A formigram θ_Y over $Y := \{x_1, x_2, x_3\}$ and its persistence clustergram. Grey intervals carry silhouette values that are either negative or zero; -1 for $\{x_1x_2x_3\} - \{x_1\} - \{x_3\}$ and 0 for $\{x_1|x_2|x_3\} - \{x_1x_2|x_3\} - \{x_1|x_2x_3\} + \{x_1x_2x_3\}$. (D) An illustration of $\mathbb{W}\theta_Y : \mathbf{Int} \to \mathrm{SubPart}(X)$ for θ_Y in (C). The persistence clustergram $\mathrm{dgm}^{\mathbb{W}}(\theta_Y)$ in (C) is the Möbius inversion of this $\mathbb{W}\theta_Y$.

We are interested in carrying out Möbius inversion of abelian-group-valued maps defined on a given poset. Let G be an abelian group. For any $m \in \mathbf{Z}_+$ and $x \in G$, we will interchangeably use $m \cdot x$ and $x \cdot m$ to denote $\underbrace{x + \cdots + x}_{m \text{ terms}}$. For a negative $m \in \mathbf{Z}$, we will also use $m \cdot x$ or $x \cdot m$ to denote $-((-m) \cdot x)$.

Theorem 6.4 (Möbius inversion formula)**.** Let $\mathbf{P}$ be a locally finite poset and let G be an abelian group. Suppose that for a function $f : \mathbf{P} \to G$, there exists $p \in \mathbf{P}$ such that $f(q) = 0$ unless $q \geq p$. Then, a function $g : \mathbf{P} \to G$ satisfies $f(q) = \sum_{r \leq q} g(r)$ for all $q \in \mathbf{P}$ if and only if $g(q) = \sum_{r \leq q} f(r) \cdot \mu_{\mathbf{P}}(r, q)$ for all $q \in \mathbf{P}$. We will often write $g = f'$.

A difference between this theorem and [72, Proposition 2 (p.344)] is that the codomain of the functions f and g is an abelian group, whereas the codomain is a field in [72]. Nevertheless, the verbatim proof in [72] works in our setting. In [67, 53], Möbius inversion of abelian-group-valued functions is considered in order to obtain *generalized persistence diagrams*.

Notation 6.5 (Neighborhood extension)**.** Let $I \in \mathbf{Int}(\mathbf{ZZ})$.

(i) By I^- we denote $I \cup \{(i, j)\} \in \mathbf{Int}(\mathbf{ZZ})$ where $(i, j) \in \mathbf{ZZ}$ is the "lower-left" neighborhood of I in $\mathbf{ZZ}$. For example, for $I = (-1, 1]_{\mathbf{ZZ}}$ (cf. Figure 3), we have $I^- = [-1, 1]_{\mathbf{ZZ}}$.
(ii) By I^+ we denote $I \cup \{(i', j')\} \in \mathbf{Int}(\mathbf{ZZ})$ where $(i', j') \in \mathbf{ZZ}$ is the "upper-right" neighborhood of I in $\mathbf{ZZ}$. For example, for $I = (-1, 1]_{\mathbf{ZZ}}$, we have $I^+ = (-1, 2)_{\mathbf{ZZ}}$.
(iii) By $I^\pm$ we denote $I^- \cup I^+$.

The example below directly follows from Example 6.3, Theorem 6.4, and the following fact: *For the opposite poset $\mathbf{P}^{\mathrm{op}}$ of $\mathbf{P}$, the Möbius function $\mu_{\mathbf{P}^{\mathrm{op}}}$ is obtained by $\mu_{\mathbf{P}^{\mathrm{op}}}(p, q) = \mu_{\mathbf{P}}(q, p)$ for all $p, q \in \mathbf{P}$* [72, p.345].

Example 6.6. Assume that for a function $f : \mathbf{Int}(\mathbf{ZZ}) \to G$, there exists $J_0 \in \mathbf{Int}(\mathbf{ZZ})$ such that $f(I) = 0$ unless $J_0 \supset I$. Let $g : \mathbf{Int}(\mathbf{ZZ}) \to G$ be such that $f(I) = \sum_{J \supset I} g(J)$ for all $I \in \mathbf{Int}(\mathbf{ZZ})$. Then,

$$f'(I) = g(I) = f(I) - f(I^-) - f(I^+) + f(I^\pm) \quad \text{for all } I \in \mathbf{Int}(\mathbf{ZZ}).$$

Note that (1) this formula is reminiscent of the original definition of *persistence diagrams* [28, 38] and (2) this formula was utilized in [53] to define generalized persistence diagrams for functors indexed by $\mathbf{ZZ}$.

6.2 Silhouettes and formal sums of clusters

We introduce the notion of the *silhouette* of a free-abelian-group valued map on a poset. Let A be a nonempty finite set. By $\mathbf{Z}A$ we denote the free abelian group generated by A. This means that any element in $\mathbf{Z}A$ is a formal sum of elements from A with integer coefficients.

Remark 6.7. The map $|-| : \mathbf{Z}A \to \mathbf{Z}$ that sends $\sum_{i=1}^{\ell} m_i a_i$ ($m_i \in \mathbf{Z}$, $a_i \in A$) to $\sum_{i=1}^{\ell} m_i$ is a group homomorphism.

In the rest of this section let $\mathbf{P}$ be a locally finite poset.

Definition 6.8 (Support and silhouette)**.** Let G be an abelian group. Consider a map $f : \mathbf{P} \to G$.

(i) The *support* of f is defined as $\mathrm{supp}(f) := \{p \in \mathbf{P} : f(p) \neq 0 \in G\}$.
(ii) Assume that $G = \mathbf{Z}A$. The *silhouette* $\left|f\right| : \mathbf{P} \to \mathbf{Z}$ of f is defined as follows. For $p \in \mathbf{P}$ if $f(p) = \sum_{i=1}^{\ell} m_i a_i$ ($m_i \in \mathbf{Z}$, $a_i \in A$), then $\left|f\right|(p) := \sum_{i=1}^{\ell} m_i$.

Given an $f : \mathbf{P} \to \mathbf{Z}A$, $\mathrm{supp}(\left|f\right|)$ is contained in $\mathrm{supp}(f)$ but the converse is not always true. For example, if $f(p) = a_1 - a_2$ with $a_1 \neq a_2$, then $p \in \mathrm{supp}(f)$ but $p \notin \mathrm{supp}(\left|f\right|)$.

Notation 6.9. We will often represent $f : \mathbf{P} \to G$ by the set $\{(p, f(p)) : p \in \mathrm{supp}(f)\}$. In particular, when $G = \mathbf{Z}$ and $\mathrm{im}(f) \subset \{0, 1\}$, f will be identified with $\mathrm{supp}(f)$.

The silhouette, as an operation, commutes with Möbius inversion over any locally finite poset:

Proposition 6.10. Given a map $f : \mathbf{P} \to \mathbf{Z}A$, let f' be the Möbius inversion of f, i.e. for all $p \in \mathbf{P}$, $f'(p) = \sum_{q \le p} f(q) \cdot \mu_{\mathbf{P}}(q,p)$. Then, the Möbius inversion of $\left|f\right| : \mathbf{P} \to \mathbf{Z}$ equals $\left|f'\right|$, i.e. $\left|f\right|' = \left|f'\right|$.

Proof. Let $p \in \mathbf{P}$. We have:

$$\begin{aligned} \left|f'\right|(p) &= \left| \sum_{q \le p} f(q) \cdot \mu_{\mathbf{P}}(q,p) \right| && \text{by Definition 6.8 (ii)} \\ &= \sum_{q \le p} \left|f\right|(q) \cdot \mu_{\mathbf{P}}(q,p) && \text{by Remark 6.7} \\ &= \left|f\right|'(p). \end{aligned}$$

□

In the rest of the paper, the basis A of the free abelian group $\mathbf{Z}A$ will be $\mathrm{pow}(X)$, the power set of some finite set X.

Example 6.11. Let $X := \{x_1, x_2, x_3\}$ and assume that a given map $f : \mathbf{Int}(\mathbf{ZZ}) \to \mathbb{Z}\mathrm{pow}(X)$ satisfies

$$\begin{cases} f((1,2)_{\mathbf{ZZ}}) &= \{x_1\} + \{x_2\} + \{x_3\}, \\ f([1,2)_{\mathbf{ZZ}}) &= \{x_1\} + \{x_2, x_3\}, \\ f((1,2]_{\mathbf{ZZ}}) &= \{x_1, x_2\} + \{x_3\}, \\ f([1,2]_{\mathbf{ZZ}}) &= \{x_1, x_2, x_3\}. \end{cases} \tag{4}$$

Then, from Example 6.6, we have

$$f'((1,2)_{\mathbf{ZZ}}) = \{x_1\} + \{x_2\} + \{x_3\} - (\{x_1\} + \{x_2, x_3\}) - (\{x_1, x_2\} + \{x_3\}) + \{x_1, x_2, x_3\},$$

and thus $\left|f'\right|((1,2)_{\mathbf{ZZ}}) = 1 + 1 + 1 - (1+1) - (1+1) + 1 = 0$. Next we consider $\left|f\right| : \mathbf{Int}(\mathbf{ZZ}) \to \mathbf{Z}$. By equations in (4)

$$\left|f\right|((1,2)_{\mathbf{ZZ}}) = 3, \quad \left|f\right|([1,2)_{\mathbf{ZZ}}) = \left|f\right|((1,2]_{\mathbf{ZZ}}) = 2, \quad \left|f\right|([1,2]_{\mathbf{ZZ}}) = 1.$$

Again from Example 6.6, we have $\left|f\right|'((1,2)_{\mathbf{ZZ}}) = 3 - 2 - 2 + 1 = 0$ which equals $\left|f'\right|((1,2)_{\mathbf{ZZ}})$.

We define a natural inclusion $\iota : \mathrm{SubPart}(X) \hookrightarrow \mathbb{Z}\mathrm{pow}(X)$ as follows. For any $P = \{B_i\}_{i=1}^{\ell} \in \mathrm{SubPart}(X)$, let $\iota(P) := \sum_{i=1}^{\ell} 1 \cdot B_i$. Let us also define a natural left-inverse $\Pi : \mathbb{Z}\mathrm{pow}(X) \to \mathrm{SubPart}(X)$ of ι as follows.

Definition 6.12 (Left-inverse to $\iota : \mathrm{SubPart}(X) \hookrightarrow \mathbb{Z}\mathrm{pow}(X)$)**.** Let $g \in \mathbb{Z}\mathrm{pow}(X)$ be any nonzero element that is given as $\sum_{i=1}^{\ell} m_i B_i$ ($m_i (\neq 0) \in \mathbf{Z}$) where $B_i \neq B_j$ for $i \neq j$. Then, $\Pi(g)$ is defined as the finest common coarsening $\bigvee \{\{B_i\}\}_{i=1}^{n}$. The trivial element $0 \in \mathbb{Z}\mathrm{pow}(X)$ is sent to $\emptyset$ via Π.

For example, if $X := \{x_1, x_2, x_3\}$, Π sends $\{x_1, x_2\} + \{x_2, x_3\} \in \mathbb{Z}\mathrm{pow}(X)$ to $\{\{x_1, x_2\}\} \vee \{\{x_2, x_3\}\} = \{\{x_1, x_2, x_3\}\} \in \mathrm{SubPart}(X)$.

6.3 Maximal group diagrams

Buchin et al. defined the concept of *maximal groups*[7] for a set $\mathscr{X}$ of trajectories in Euclidean space [15] (cf. Remark 6.18). We observe that maximal groups are totally determined by the formigram induced by the δ-connectivity dynamic graph of the set of trajectories (cf. Example 3.2), which enables us to prove that maximal groups are obtained by Möbius inversion (cf. Theorem 6.17). A corollary is that the collection of all maximal groups of $\mathscr{X}$ contains the same information as the formigram θ induced by $\mathscr{X}$ (cf. Remark 6.18).

[7] In this section *groups* do not stand for groups in abstract algebra. See Remark 6.18.

Definition 6.13. Let θ_X be a formigram over X. A subset $G \subset X$ is called a *group* over an interval $I_G \subset \mathbf{R}$ if for all $t \in I$, there exists $B_t \in \theta_X(t)$ such that $G \subset B_t$. A group H *covers* group G if $G \subset H$ and $I_G \subset I_H$.

Definition 6.14. Let θ_X be a formigram and let $G \subset X$ be a group over $I_G \subset \mathbf{R}$. Then, G is said to be a *maximal group* (over I_G) if there is no group $H \subset X$ that covers G.

Let us recall the natural injection $\iota : \mathrm{SubPart}(X) \hookrightarrow \mathbb{Z}\mathrm{pow}(X)$ which sends $\{B_i\}_{i=1}^{\ell} \in \mathrm{SubPart}(X)$ to $\sum_{i=1}^{\ell} 1 \cdot B_i$, a formal sum of blocks of P. In what follows, $\{B_i\}_{i=1}^{\ell} \in \mathrm{SubPart}(X)$ will be identified with $\sum_{i=1}^{\ell} 1 \cdot B_i$.

Definition 6.15. Let θ_X be a formigram. The $\bigwedge$*-rank function* $\bigwedge\theta_X : \mathbf{Int}(\mathbf{ZZ}) \to \mathrm{SubPart}(X)$ is defined as $I \mapsto \bigwedge_I \theta_X := \bigwedge\{\theta_X(i,j) : (i,j) \in I\}$. By Convention 6.1, when $I = \langle a, b\rangle_{\mathbf{ZZ}}$, we have $\bigwedge_I \theta_X = \bigwedge_{t \in \langle a,b\rangle} \theta_X(t)$.

For $I \in \mathbf{Int}(\mathbf{ZZ})$, note that $\bigwedge_I \theta_X$ is a collection of groups over I. In particular, $G \in \bigwedge_I \theta_X$ is a maximal group if there is no group $G' \subset X$ covering G over either I^- or I^+ (cf. Notation 6.5). Let $\mathrm{dgm}^{\wedge}(\theta_X)$ be the Möbius inversion of $\bigwedge\theta_X$ over $\mathbf{Int}(\mathbf{ZZ})^{\mathrm{op}}$ (cf. Example 6.6). This means that for all $I \in \mathbf{Int}(\mathbf{ZZ})$

$$\mathrm{dgm}^{\wedge}(\theta_X)(I) := \bigwedge_{I} \theta_X - \bigwedge_{I^+} \theta_X - \bigwedge_{I^-} \theta_X + \bigwedge_{I^{\pm}} \theta_X, \tag{5}$$

where these sums and subtractions should be interpreted as operations in $\mathbb{Z}\mathrm{pow}(X)$. Let us recall the map $\Pi : \mathbb{Z}\mathrm{pow}(X) \to \mathrm{SubPart}(X)$ from Definition 6.12.

Definition 6.16. The *maximal group diagram* of θ_X is defined as $\Pi \circ \mathrm{dgm}^{\wedge}(\theta_X) : \mathbf{Int}(\mathbf{ZZ}) \to \mathrm{SubPart}(X)$. We will simply write $\Pi\mathrm{dgm}^{\wedge}(\theta_X)$ for $\Pi \circ \mathrm{dgm}^{\wedge}(\theta_X)$.

We adapt Notation 6.9 as follows. For $I \in \mathbf{Int}(\mathbf{ZZ})$, if $\Pi\mathrm{dgm}^{\wedge}(\theta_X)(I)$ contains a block $G \subset X$, then we write $(I, G) \in \Pi\mathrm{dgm}^{\wedge}(\theta_X)$. The following theorem says that $\Pi\mathrm{dgm}^{\wedge}(\theta_X)$ encodes all the maximal groups of θ_X. See Figures 10 (A) and (B) for examples; any pair $(I, G) \in \Pi\mathrm{dgm}^{\wedge}(\theta_X)$ is depicted as the interval I annotated by G.

Theorem 6.17. Let θ_X be a formigram. A subset $G \subset X$ is a maximal group of θ_X on an interval $I \subset \mathbf{R}$ if and only if $(I, G) \in \Pi\mathrm{dgm}^{\wedge}(\theta_X)$.

Proof. Fix *any* $G \in \bigwedge_I \theta_X$. Since $\bigwedge_{I^+} \theta_X \leq \bigwedge_I \theta_X$, either (a) $G \in \bigwedge_{I^+} \theta_X$ or (b) there exists the subcollection $\{H_j \in \bigwedge_{I^+} \theta_X : H_j \subset G\}$ of $\bigwedge_{I^+} \theta_X$ which does not include G. Similarly, since $\bigwedge_{I^-} \theta_X \leq \bigwedge_I \theta_X$, there are the two analogous cases: (a') $G \in \bigwedge_{I^-} \theta_X$, or (b') there exists the subcollection $\{K_j \in \bigwedge_I \theta_X : K_j \subset G\}$ which does not include G. In combination, there are the four possible cases: (aa'), (ab'), (ba'), and (bb'). Among these, observe that G appears in the subpartition $\Pi\mathrm{dgm}^{\wedge}(\theta_X)(I)$ only in case (bb'), i.e. when G is a maximal group over I. In the other three cases, $\Pi\mathrm{dgm}^{\wedge}(\theta_X)(I)$ does not contain G nor any of its subsets. The claim follows. □

Remark 6.18. Let X be a set of trajectories in Euclidean space. In [15], a *group* of X is defined according to three different parameters. For any positive $m \in \mathbf{Z}$ and $\varepsilon, \delta \in \mathbf{R}_+$, a set $G \subset X$ is said to form an (m, ε, δ)*-group* during a time interval I if and only if (1) G contains at least m points, (2) the length of I is not less than ε and (3) for any two points $x, x' \in G$ and any time $t \in I$, there is a chain $x = x_0, x_1, \ldots, x_n = x'$ of points in X such that any two consecutive ones are at distance $\leq \delta$ at time t. Note that (1) *groups are totally determined by the formigram* θ_X *induced by the* δ*-connectivity dynamic graph on* X, and that (2) for any positive $m \in \mathbf{Z}$ and any $\varepsilon \in \mathbf{R}_+$ the collection of (m, ε, δ)-groups is the subcollection of $(1, 0, \delta)$-groups. Therefore, we restrict our attention to maximal $(1, 0, \delta)$-groups which are exactly the maximal groups of θ_X in Definition 6.14.

Example 6.19. Assume that the formigram θ_X in Figure 10 (B) is obtained from some three trajectories x_1, x_2 and x_3 in Euclidean space as described in Remark 6.18 (cf. Example 3.2 and Definition 3.10). Figure 11 is another representation of the maximal group diagram of θ_X.

Consider any $\mathbf{R}$-indexed module M (cf. Section 2.3). Then, for any $t \in \mathbf{R}$, the dimension of $M(t)$ equals the total multiplicity of those intervals I in the barcode of M which contain t. We will establish an analogous result for $\theta_X : \mathbf{R} \to \mathrm{SubPart}(X)$. Let us observe that for any nonempty $B \in \mathrm{pow}(X)$, we have that $\{B\} \in \mathrm{SubPart}(X)$.

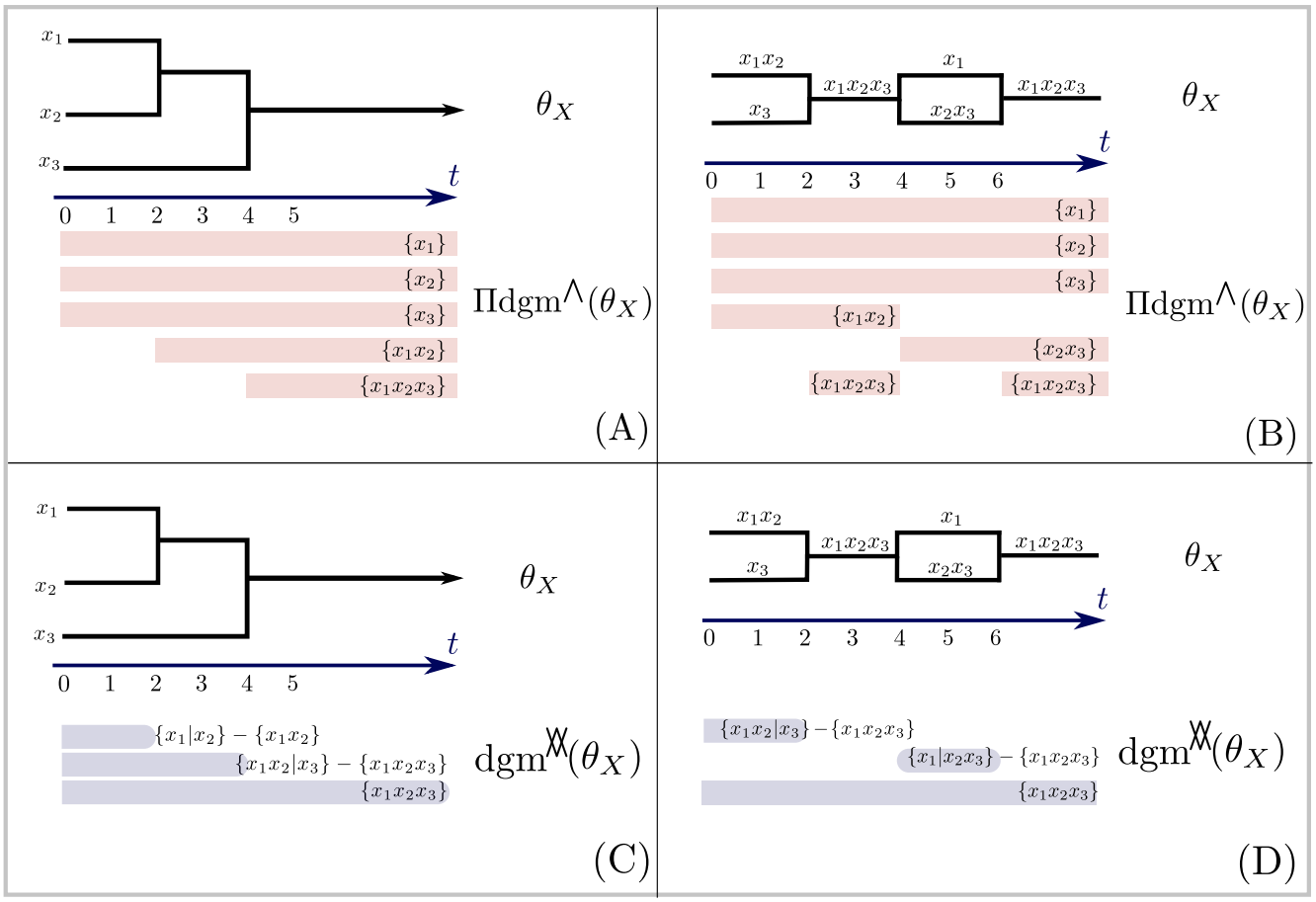


Figure 10: (A) and (B) depict maximal group diagrams (cf. Definition 6.16) while (C) and (D) depict persistence clustergrams (cf. Definition 6.27).

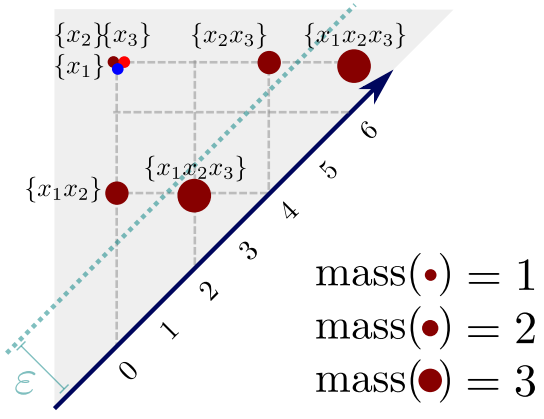


Figure 11: The maximal group diagram in Figure 10 (B) is represented as an annotated standard persistence diagram [28] ($[a,b] \in \mathbf{Int}$ is identified with $(a,b) \in \mathbf{R}^{\text{op}} \times \mathbf{R}$). In the 3-tuple (m,ε,δ) of parameters for maximal groups (cf. Remark 6.18), m corresponds to the minimal size of maximal groups (depicted as the "mass" of points above), and ε corresponds to the minimal duration of maximal groups. By the monotonicity of maximal groups (cf. Remark 6.20), the masses of points near the diagonal line $y = x$ tend to be relatively large.

Remark 6.20 (Monotonicity of maximal groups and completeness)**.** By Theorem 6.17 and the definition of maximal groups, $\Pi\mathrm{dgm}^{\bigwedge}(\theta_X)$ satisfies a *monotonicity property*: if $B \subset B'$ with $(I,B),(I',B') \in \Pi\mathrm{dgm}^{\bigwedge}(\theta_X)$, then $I \supset I'$. This in turn implies that, for $t \in \mathbf{R}$, $\theta_X(t)$ is equal to

$$\bigvee\{\{B\} \in \mathrm{pow}(X) \setminus \{\emptyset\} : \text{there exists } I \ni t \text{ such that } (I,\{B\}) \in \Pi\mathrm{dgm}^{\bigwedge}(\theta_X)\}.$$

Therefore, we can recover a formigram θ_X from its maximal group diagram $\Pi\mathrm{dgm}^{\bigwedge}(\theta_X)$.

Example 6.21. Consider the formigram depicted in Figure 10 (B). Note that $\theta_X(5) = \{x_1|x_2x_3\}$ and the blocks corresponding to the four intervals containing $t = 5$ are $\{x_1\},\{x_2\},\{x_3\}$ and $\{x_2x_3\}$. We have that

$$\theta_X(5) = \{x_1|x_2x_3\} = \bigvee\{\{x_1\},\{x_2\},\{x_3\},\{x_2x_3\}\}.$$

Let us characterize the silhouette of the maximal group diagram of a dendrogram (cf. Remark 3.7).

Example 6.22. Let θ_X be a dendrogram, and let $G \subset X$. If there exists $t \in \mathbf{R}$ such that $G \in \theta_X(t)$, then define $b(G) := \min\{t \in \mathbf{R} : G \subset \theta_X(t)\}$. Then, the silhouette of $\Pi\mathrm{dgm}^{\bigwedge}(\theta_X)$ amounts to the set

$$\{[b(G),\infty) : \text{there exists } t \in \mathbf{R} \text{ such that } G \in \theta_X(t)\} \text{ (cf. Notation 6.9)}.$$

For example, consider the dendrogram θ_X over $X := \{x_1,x_2,x_3\}$ that is depicted in Figure 10 (A). Since

$$\bigcup_{t\in\mathbf{R}} \theta_X(t) = \{\{x_1\},\{x_2\},\{x_3\},\{x_1,x_2\},\{x_1,x_2,x_3\}\},$$

the silhouette of $\Pi\mathrm{dgm}^{\bigwedge}(\theta_X)$ consists of the five half-infinite intervals whose left endpoints are $b(\{x_1\})$, $b(\{x_2\})$, $b(\{x_3\})$, $b(\{x_1,x_2\})$, and $b(\{x_1,x_2,x_3\})$.

Remark 6.23 below motivates us to consider a different summary of a formigram, leading to the next section.

Remark 6.23. (i) The maximal group diagram can drastically change under perturbations of an input formigram *with respect to* $d_{\mathrm{I}}^{\mathrm{F}}$ (for example, see Figure 12). This is not unexpected since the distance $d_{\mathrm{I}}^{\mathrm{F}}$ utilizes the join operation $\bigvee$ on subpartitions to quantify the difference between formigrams whereas the maximal group diagram is extracted from the $\bigwedge$-rank function (Definition 6.15).

(ii) The silhouette of the maximal group diagram almost always looks completely different from the barcode of θ_X (Definition 3.12 (iv)); for example, observe that the silhouettes of $\Pi\mathrm{dgm}^{\bigwedge}(\theta_X)$ in Figure 10 (A),(B) are completely different from the silhouettes of $\mathrm{dgm}^{\bigwedge\!\!\bigvee}(\theta_X)$ in Figure 10 (C),(D). The latter silhouettes are actually the zigzag barcodes of the respective formigrams, as it will turn out in the next section (cf. Theorem 6.30).

6.4 Persistence clustergrams

In this section we define the persistence clustergram of a formigram. When a given formigram θ_X is saturated, its persistence clustergram can be regarded as an "annotated" zigzag barcode of θ_X (cf. Figure 1 (C)). We begin by defining the $\bigwedge\!\!\bigvee$-rank function of a formigram ($\bigwedge\!\!\bigvee$ is a fusion of $\bigwedge$ and $\bigvee$, as will be clear below). The Möbius inversion of the $\bigwedge\!\!\bigvee$-rank function of θ_X will be the persistence clustergram of θ_X.

Let θ_X be a formigram. For $I \in \mathbf{Int}$, we define $\bigwedge\!\!\bigvee_I \theta_X$ as the partition of the underlying set $X'(\subset X)$ of $\bigwedge_I \theta_X$ that is obtained by restricting the equivalence relation induced by $\bigvee_I \theta_X$ to X'. In other words,

$$\bigwedge\!\!\bigvee_I \theta_X = \left\{B \cap X' : B \in \bigvee_I \theta_X \text{ and } B \cap X' \neq \emptyset\right\}. \tag{6}$$

Note that when θ_X is saturated, $\bigwedge\!\!\bigvee_I \theta_X = \bigvee_I \theta_X$ for any interval $I \subset \mathrm{supp}(\theta_X)$.

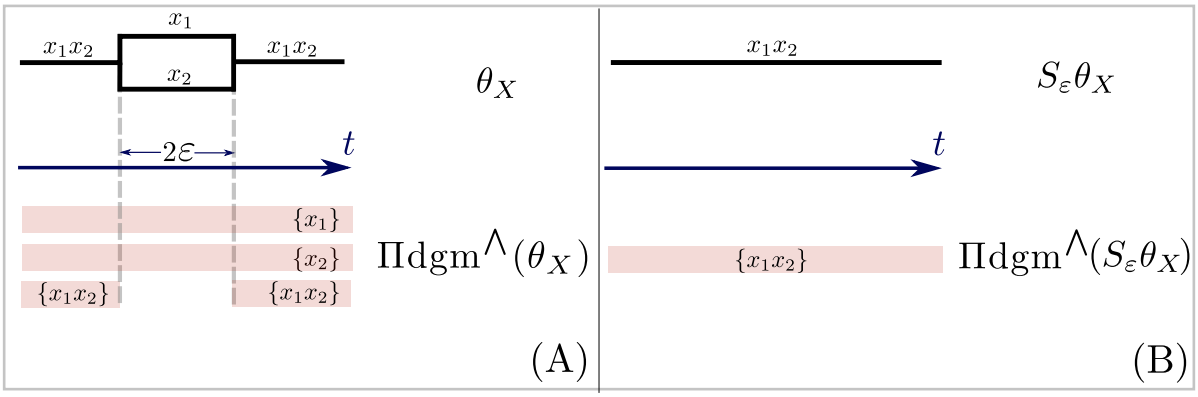


Figure 12: (A) The formigram θ_X over $X := \{x_1, x_2\}$ such that $\theta_X(t) = \{x_1|x_2\}$ for $t \in (0, 2\varepsilon)$ and $\theta_X(t) = \{x_1x_2\}$ for $t \in \mathbf{R} \setminus (0, \varepsilon)$. (B) The ε-smoothing of θ_X (Definition 2.23). The bottleneck distance between the silhouettes of $\Pi\mathrm{dgm}^{\wedge}(\theta_X)$ and $\Pi\mathrm{dgm}^{\wedge}(S_\varepsilon\theta_X)$ is ∞, whereas $d_1^{\mathrm{F}}(\theta_X, S_\varepsilon\theta_X) = \varepsilon$.

	Nature of $F : \mathbf{P} \to \mathbf{C}$	**P**	**C**	$\mathrm{rk}(F)(I)$	Representation of $\mathrm{rk}(F)(I)$
(i)	Sublevelset persistence [28]	**R**	**vec**	$\mathrm{coim}\left(\varprojlim F\|_I \to \varinjlim F\|_I\right)$	An integer (dimension)
(ii)	Levelset persistence [18]	**Int**			
(iii)	Merge tree [63]	**R**	**set**		An integer (cardinality)
(iv)	Reeb graph [33]	**Int**			
(v)	Unlabeled dendrogram [19]	**R**	**Part**		An integer partition
(vi)	Unlabeled formigram	**Int**			

Table 4: $\mathrm{rk}(F)(I)$ denotes the *rank* of the functor F over an interval $I \subset \mathbf{R}$ up to isomorphism [53, Definition 3.5]. In each of rows (i)-(iv), the *coimage* of $\varprojlim F|_I \to \varinjlim F|_I$ can be replaced by the *image* of $\varprojlim F|_I \to \varinjlim F|_I$, since they are isomorphic. However, it is not the case in row (v) nor in row (vi); see Proposition 5.8.

Definition 6.24. Let θ_X be a formigram. The $\mathbb{X}$*-rank function* $\mathbb{X}\theta_X : \mathbf{Int}(\mathbf{ZZ}) \to \mathrm{SubPart}(X)$ of θ_X is defined by $I \mapsto \mathbb{X}_I\theta_X$.

Remark 6.25. In the category **Part** (cf. Definition 2.7), the pair $(\bigcup(\mathbb{X}_I\theta_X), \mathbb{X}_I\theta_X)$ is the *coimage* of the morphism $(\bigcup(\bigwedge_I\theta_X), \bigwedge_I\theta_X) \to (\bigcup(\bigvee_I\theta_X), \bigvee_I\theta_X)$ which is given by the inclusion $\bigcup(\bigwedge_I\theta_X) \hookrightarrow \bigcup(\bigvee_I\theta_X)$ (cf. Proposition 5.8). In this respect, the $\mathbb{X}$-rank function is a rendition of the *generalized rank invariant* from [53]. Table 4 clarifies the analogy.

Example 6.26. Consider the formigram depicted in Figure 9 (A). For $I := [0,5]$, we have $\bigwedge_I\theta_X = \{x_1|x_2|x_3\}$, $\bigvee_I\theta_X = \{x_1x_2|x_3x_4\}$, and $\mathbb{X}_I\theta_X = \{x_1x_2|x_3\}$. Note that whereas the $\wedge$-rank function classifies x_1 and x_3 into different clusters over I, the $\mathbb{X}$-rank function puts x_1 and x_3 into the same cluster over I. The $\mathbb{X}$-rank function $\mathbb{X}\theta_X$ is completely depicted in Figure 9 (B).

Definition 6.27. Let θ_X be a formigram. The *persistence clustergram* $\mathrm{dgm}^{\mathbb{X}}(\theta_X) : \mathbf{Int}(\mathbf{ZZ}) \to \mathbb{Z}\mathrm{pow}(X)$ is defined as the Möbius inversion of $\mathbb{X}\theta_X$ over the poset $\mathbf{Int}(\mathbf{ZZ})^{\mathrm{op}}$. Namely, for all $I \in \mathbf{Int}(\mathbf{ZZ})$,

$$\mathrm{dgm}^{\mathbb{X}}(\theta_X)(I) := \mathbb{X}_I\theta_X - \mathbb{X}_{I^+}\theta_X - \mathbb{X}_{I^-}\theta_X + \mathbb{X}_{I^\pm}\theta_X. \tag{7}$$

By the following remark, $\mathrm{dgm}^{\mathbb{X}}$ is a complete invariant of formigrams.

Remark 6.28. By Theorem 6.4, for any $I \in \mathbf{Int}(\mathbf{ZZ})$, we have that $\mathbb{X}_I\theta_X = \sum_{J \supset I} \mathrm{dgm}^{\mathbb{X}}(\theta_X)(J)$. In particular, for any $t \in \mathbf{R}$, $\theta_X(t) = \mathbb{X}_{[t,t]}\theta_X = \sum_{J \ni t} \mathrm{dgm}^{\mathbb{X}}(\theta_X)(J)$. Thus θ_X can be recovered from $\mathrm{dgm}^{\mathbb{X}}(\theta_X)$.

Whereas the H_0 barcode or the underlying merge tree is not a complete invariant of a dendrogram, the persistence clustergram of a dendrogram is a complete invariant.

Example 6.29 (Persistence clustergram of dendrograms)**.** Consider the dendrogram θ_X over $X := \{x_1, x_2, x_3\}$ which is depicted as in Figure 10 (C). Then, $\mathrm{dgm}^{\text{⨳}}(\theta_X)$ consists of the three elements (cf. Notation 6.9)

$$([0,2), \{x_1|x_2\} - \{x_1x_2\}),\ ([0,4), \{x_1x_2|x_3\} - \{x_1x_2x_3\}),\ ([0,\infty), \{x_1x_2x_3\}), \tag{8}$$

as illustrated in the figure. Invoking Remark 6.28, let us compute $\theta_X(1) = \sum_{I \ni 1} \mathrm{dgm}^{\text{⨳}}(\theta_X)(I)$. Since the silhouette of $\mathrm{dgm}^{\text{⨳}}(\theta_X)$ is $\{[0,2), [0,4), [0,\infty)\}$, and $1 \in \mathbf{R}$ belongs to all of $[0,2), [0,4)$ and $[0,\infty)$ we have:

$$\begin{aligned}\theta_X(1) &= \mathrm{dgm}^{\text{⨳}}(\theta_X)[0,2) + \mathrm{dgm}^{\text{⨳}}(\theta_X)[0,4) + \mathrm{dgm}^{\text{⨳}}(\theta_X)[0,\infty) \\ &= (\{x_1|x_2\} - \{x_1x_2\}) + (\{x_1x_2|x_3\} - \{x_1x_2x_3\}) + \{x_1x_2x_3\} \\ &= \{x_1|x_2|x_3\}.\end{aligned}$$

Also, the silhouette $\{[0,2), [0,4), [0,\infty)\}$ of $\mathrm{dgm}^{\text{⨳}}(\theta_X)$ coincides with the zigzag barcode of θ_X. This is not merely a coincidence, as we will see in the following theorem.

Theorem 6.30. If θ_X is a *saturated* formigram (Definition 3.8), then the barcode of θ_X is equal to the silhouette $\left|\mathrm{dgm}^{\text{⨳}}(\theta_X)\right|$ of $\mathrm{dgm}^{\text{⨳}}(\theta_X)$ (cf. Figures 1 (F),(G),(H) and 10 (C),(D)).

We prove this theorem in Appendix A.4 by harnessing results from [53].

Corollary 6.31. If θ_X is a *saturated* formigram, the silhouette $\left|\mathrm{dgm}^{\text{⨳}}(\theta_X)\right| : \mathbf{Int}(\mathbf{ZZ}) \to \mathbf{Z}$ is nonnegative.

Example 6.32. When a formigram is not saturated, the silhouette of its persistence clustergram is not necessarily the same as the barcode of θ_X. See Figure 9 (C) for an illustrative example.

Since $\mathrm{dgm}^{\text{⨳}}$ is a complete invariant of formigrams, the distance $d_{\mathrm{I}}^{\mathrm{F}}$ between formigrams can also be viewed as a distance between their persistence clustergrams. Since computing $d_{\mathrm{I}}^{\mathrm{F}}$ is NP-hard, it is desirable to find many computable lower bounds for $d_{\mathrm{I}}^{\mathrm{F}}$. One such lower bound is the bottleneck distance between the barcodes of formigrams (cf. Corollary 4.16). One additional lower bound based on persistence clustergrams is proposed in the next section.

6.5 Persistent cluster counting functor

We define the *persistent cluster counting functor* of a formigram θ_X as the silhouette of $\text{⨳}\theta_X$. We will see later that persistent cluster counting functors of formigrams can be used for discriminating formigrams which cannot be discriminated by the underlying Reeb graphs of formigrams. Throughout this section, X will denote nonempty finite sets. Convention 6.1 still applies in this section.

For $P \in \mathrm{SubPart}(X)$, $|P|$ denotes the number of blocks in P. By viewing P as the formal sum $\sum_{B \in P} 1 \cdot B \in \mathbb{Z}\mathrm{pow}(X)$, this notation is consistent with the notation $|-|$ which is defined in Remark 6.7.

Definition 6.33. The *persistent cluster counting functor* of a formigram θ_X is the map $|\text{⨳}\theta_X| : \mathbf{Int}(\mathbf{ZZ}) \to \mathbf{Z}_+$ defined by $I \mapsto |\text{⨳}_I\theta_X|$.

For $t \in \mathbf{R}$, $|\text{⨳}\theta_X|(t,t) = |\theta_X(t)|$, the number of the blocks in $\theta_X(t)$. The value $|\text{⨳}\theta_X|(I)$ in Definition 6.33 is the number of *independent* groups over I (cf. Definition 6.13); Two groups G_1 and G_2 over an interval I are called independent if there is no pair of $x_1 \in G_1$ and $x_2 \in G_2$ such that x_1 and x_2 belong to the same block of $\theta_X(t)$ for some $t \in I$. The independence of G_1 and G_2 is stronger condition than $G_1 \cap G_2 = \emptyset$. If G_1 and G_2 are not independent, then they are called *dependent*. For the equivalence relation generated by dependence, the value $|\text{⨳}\theta_X|(I) = \text{⨳}_I\theta_X$ is the number of equivalence classes of groups over I. Note that $|\text{⨳}\theta_X|$ is analogous to the rank invariant of $\mathbf{R}$-indexed and $\mathbf{ZZ}$-indexed modules [22, 28, 53].

We have that

$$\left|\divideontimes\theta_X\right|(I) = \sum_{J\supset I}\left|\mathrm{dgm}^{\divideontimes}(\theta_X)\right|(J) \tag{9}$$

by Theorem 6.4 and Proposition 6.10. In Appendix A.5 we also prove that $|\divideontimes\theta_X|$ can be obtained from the unlabeled formigram of θ_X (cf. Definition 3.12 (i)); see Proposition A.10. This establishes the arrow (C)→(H) in Figure 1, invoking that $|\divideontimes\theta_X|$ and $\left|\mathrm{dgm}^{\divideontimes}(\theta_X)\right|$ can recover each other.

6.6 Stability of the persistent cluster counting functor

Convention 6.1 still applies in this section. For any two intervals $I \subset J$, the number of independent maximal groups over I is greater than equal to that of J, i.e. $\left|\divideontimes_J\theta_X\right| \le |\divideontimes_I\theta_X|$. This monotonicity allows us to quantify the difference between two persistent cluster counting functors via the so-called *erosion distance*.

Definition 6.34 ([67, 68])**.** Let $Y_1, Y_2 : \mathbf{Int} \to \mathbf{Z}_+$ be any two order-reversing maps. The *erosion distance* between Y_1 and Y_2 is defined as

$$d_{\mathrm{E}}(Y_1,Y_2) := \inf\left\{\varepsilon\in[0,\infty) : \text{for all } I\in\mathbf{Int},\ Y_i(I)\le Y_j(I^{\varepsilon}),\ \text{for } i,j\in\{1,2\}\right\}.$$

Throughout this section, X and Y will denote nonempty finite sets. Persistent cluster counting functor enjoys stability:

Theorem 6.35. For any two formigrams θ_X and θ_Y, we have

$$d_{\mathrm{E}}\left(\left|\divideontimes\theta_X\right|,\left|\divideontimes\theta_Y\right|\right) \le d_{\mathrm{I}}^{\mathrm{F}}(\theta_X,\theta_Y).$$

We prove this theorem at the end of this section. Invoking Proposition 4.17, this theorem implies that DGs can be summarized into persistent cluster counting functors with a guarantee of stability. Example 6.36 below shows that persistent cluster counting functors can sometimes be more discriminative than the Reeb graph of formigrams (cf. Definition 3.12).

Example 6.36. Consider the two DGs $\mathscr{G}_X = (V_X(\cdot), E_X(\cdot))$ and $\mathscr{G}_Y = (V_Y(\cdot), E_Y(\cdot))$ over $X := \{x_1, x_2\}$ and $Y := \{y_1\}$ respectively given as follows (cf. Figure 13 (A)):

$$V_X(t)\cup E_X(t) = \begin{cases} \{\{x_1\}\}, & t\in[0,1)\cup(2,3] \\ \{\{x_1\},\{x_2\},\{x_1,x_2\}\}, & t\in[1,2] \\ \emptyset, & \text{otherwise,}\end{cases} \qquad V_Y(t)\cup E_Y(t) = \begin{cases} \{\{y_1\}\}, & t\in[0,3] \\ \emptyset, & \text{otherwise.}\end{cases}$$

Let θ_X and θ_Y be the formigrams of $\mathscr{G}_X$ and $\mathscr{G}_Y$, respectively (cf. Definition 3.10 and Figure 13 (B)). Then $|\divideontimes\theta_X|, |\divideontimes\theta_Y| : \mathbf{Int} \to \mathbf{Z}_+$ are described in Figure 13 (C). By Definition 6.34, we have $d_{\mathrm{E}}(|\divideontimes\theta_X|, |\divideontimes\theta_Y|) = 1$ (More details are provided below). Note that these two DGs cannot be discriminated by computing their Reeb graphs nor their zigzag barcodes.

Remark 6.37. (i) The inequalities in Theorems 4.17 and 6.35 are *tight*. For the DGs $\mathscr{G}_X, \mathscr{G}_Y$ and formigrams θ_X, θ_Y in Example 6.36, we have that $d_{\mathrm{I}}^{\mathrm{dynG}}(\mathscr{G}_X,\mathscr{G}_Y) = d_{\mathrm{I}}^{\mathrm{F}}(\theta_X,\theta_Y) = 1$. Indeed, $X \xleftarrow{\pi_1} \{(x_1,y_1),(x_2,y_1)\} \xrightarrow{\pi_2} Y$ (where π_1 and π_2 are the canonical projections) is a 1-tripod between $\mathscr{G}_X$ and $\mathscr{G}_Y$, and also between θ_X and θ_Y.

(ii) Assume that θ_X, θ_Y are two formigrams with the same n critical points. Once $|\divideontimes\theta_X|$ and $|\divideontimes\theta_Y|$ are computed, computing $d_{\mathrm{E}}(|\divideontimes\theta_X|, |\divideontimes\theta_Y|)$ via *ordinary binary search* requires the (expected) cost $O(n^2\log n)$, see [54, Section 5].

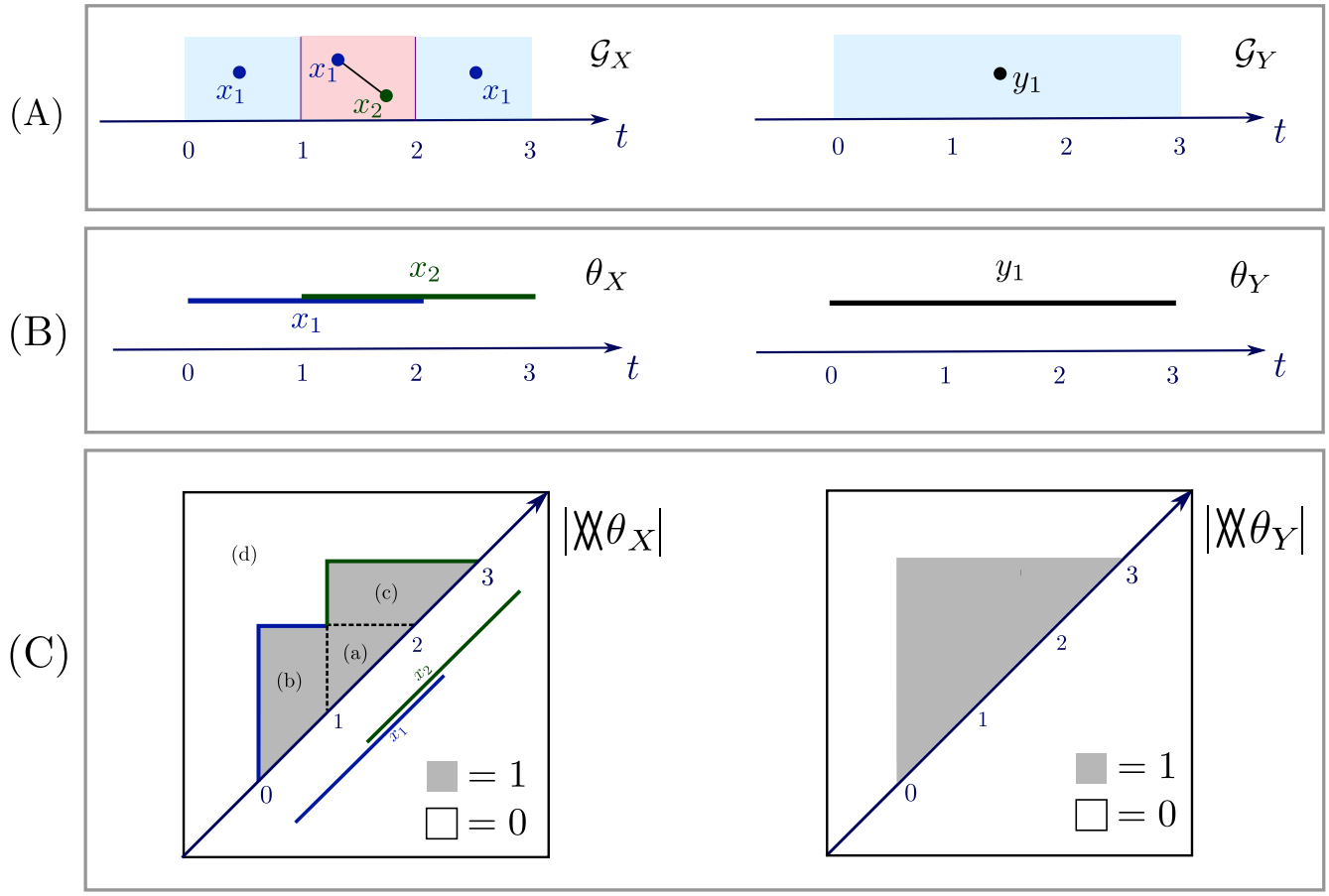


Figure 13: The summarization process of the two DGs $\mathscr{G}_X$ and $\mathscr{G}_Y$ from Example 6.36.

Details for Example 6.36. Let us compute the formigram θ_X induced from $\mathscr{G}_X$ (cf. Definition 3.10):

$$\theta_X(t) = \begin{cases} \{\{x_1\}\}, & t \in [0,1) \\ \{\{x_1, x_2\}\}, & t \in [1,2] \\ \{\{x_2\}\}, & t \in (2,3] \\ \emptyset, & t \in \mathbf{R} \setminus [1,3] \end{cases} \quad \text{(cf. Figure 13 (B))}.$$

Next we compute $|\!\!\bigwedge \theta_X| : \mathbf{Int} \to \mathbf{Z}_+$ (cf. Figure 13 (C)). Note that

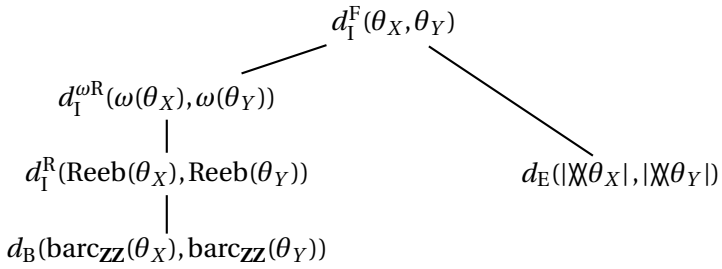
$$\bigwedge_{[s,t]} \theta_X = \begin{cases} \{\{x_1, x_2\}\}, & 1 \le s \le t \le 2, \quad \text{Region (a)} \\ \{\{x_1\}\}, & s \in [0,1) \text{ and } s \le t \le 2, \quad \text{Region (b)} \\ \{\{x_2\}\}, & t \in (2,3] \text{ and } 1 < s \le t, \quad \text{Region (c)} \\ \emptyset, & \text{otherwise}, \quad \text{Region (d)}, \end{cases}$$

where regions (a),(b),(c), and (d) are marked in Figure 13 (C). Notice that the cardinality of $\bigwedge_{[s,t]} \theta_X$ is 1 for $[s,t]$ in regions (a),(b) and (c). Thus, we directly have that $|\!\!\bigwedge \theta_X|\,[s,t] = 1$ for $[s,t] \in \mathbf{Int}$ in these regions. Also, since $\bigwedge_{[s,t]} \theta_X$ is empty for $[s,t]$ in region (d), we also have that $|\!\!\bigwedge \theta_X|\,[s,t] = 0$ for $[s,t]$ in region (d). Similarly, one can compute $\theta_Y : \mathbf{R} \to \mathrm{SubPart}(Y)$ and $|\!\!\bigwedge \theta_Y| : \mathbf{Int} \to \mathbf{Z}_+$ as

$$\theta_Y(t) = \begin{cases} \{y_1\}, & t \in [0,3] \\ \emptyset, & \text{otherwise}, \end{cases} \quad \text{and} \quad \left|\!\!\bigwedge \theta_Y\right|[s,t] = \begin{cases} 1, & 0 \le s \le t \le 3 \\ 0, & \text{otherwise}. \end{cases} \quad \text{(see Figure 13 (B),(C))}$$

Observe from Figure 13 (C) that $d_{\mathrm{E}}(|\!\!\bigwedge \theta_X|, |\!\!\bigwedge \theta_Y|) = 1$. □

Remark 6.38. In general, we have the following "poset of distances":



where the distance $d_{\mathrm{I}}^{\omega\mathrm{R}}$ between weighted Reeb graphs is defined in Appendix B. When θ_X and θ_Y are *saturated formigrams*, we have the following totally ordered hierarchy:

$$d_{\mathrm{I}}^{\mathrm{F}}(\theta_X, \theta_Y) \ge d_{\mathrm{I}}^{\omega\mathrm{R}}(\omega(\theta_X), \omega(\theta_Y)) \ge d_{\mathrm{I}}^{\mathrm{R}}(\mathrm{Reeb}(\theta_X), \mathrm{Reeb}(\theta_Y)) \ge d_{\mathrm{B}}(\mathrm{barc}_{\mathbf{ZZ}}(\theta_X), \mathrm{barc}_{\mathbf{ZZ}}(\theta_Y)) \ge d_{\mathrm{E}}(\left|\!\!\bigwedge \theta_X\right|, \left|\!\!\bigwedge \theta_Y\right|).$$

The last inequality follows from Theorem 6.30 and the well-known inequality $d_{\mathrm{B}} \ge d_{\mathrm{E}}$ for (standard) persistence diagrams [59, 67].

Proof of Theorem 6.35. If $d_{\mathrm{I}}^{\mathrm{F}}(\theta_X, \theta_Y) = +\infty$, there is nothing to prove. For some $\varepsilon \in \mathbf{R}_+$, assume that $R : X \xleftarrow{\varphi_X} Z \xrightarrow{\varphi_Y} Y$ is an ε-tripod between θ_X and θ_X (cf. Definition 4.11). Fix $I \in \mathbf{Int}$ and we will only prove that $|\!\!\bigwedge \theta_X|\,(I^\varepsilon) \le |\!\!\bigwedge \theta_Y|\,(I)$. If $\bigwedge_{I^\varepsilon} \theta_X$ is empty, then $|\!\!\bigwedge \theta_X|\,(I^\varepsilon) = 0$ by definition and hence there is nothing to prove. Suppose that $\bigwedge_{I^\varepsilon} \theta_X$ is nonempty. We show that there are two set maps $\psi_1 : \bigwedge_{I^\varepsilon} \theta_X \to \bigwedge_I \theta_Y$ and $\psi_2 : \bigvee_I \theta_Y \to \bigvee_{I^\varepsilon} \theta_X$ which make the following diagram commutes.

$$\begin{array}{ccc} \bigwedge_{I^\varepsilon} \theta_X & \xrightarrow{\phi^X(I^\varepsilon)} & \bigvee_{I^\varepsilon} \theta_X \\ {\scriptstyle \psi_1}\downarrow & & \uparrow{\scriptstyle \psi_2} \\ \bigwedge_I \theta_Y & \xrightarrow{\phi^Y(I)} & \bigvee_I \theta_Y. \end{array}$$

Here the maps $\phi^X(I^\varepsilon)$ and $\phi^Y(I)$ are the canonical maps in $\mathrm{SubPart}(X)$ and $\mathrm{SubPart}(Y)$, respectively (cf. Definition 5.2). Indeed, if we have such maps ψ_1 and ψ_2, then we have:

$$\left|\bigtimes\theta_X\right|(I^\varepsilon) = \left|\mathrm{im}\left(\phi^X(I^\varepsilon)\right)\right| \leq \left|\mathrm{im}\left(\phi^Y(I)\right)\right| = \left|\bigtimes\theta_Y\right|(I),$$

as desired.

Let us construct two such maps ψ_1 and ψ_2. First, define set maps $f : X \to Y$ and $g : Y \to X$ such that

$$\{(x, f(x)) : x \in X\} \cup \{(g(y), y) : y \in Y\} \subset R, \tag{10}$$

which is possible since φ_X and φ_Y are surjective (cf. Notation 4.2). We now construct the map $\psi_1 : \bigwedge_{I^\varepsilon}\theta_X \to \bigwedge_I \theta_Y$. Let $B \in \bigwedge_{I^\varepsilon}\theta_X$ and pick any $x \in B$. By definition of $\bigwedge_{I^\varepsilon}\theta_X$, this implies that x is in the underlying set of $\theta_X(t)$ for *all* $t \in I^\varepsilon$.

We claim that the lifespan $I_{f(x)}$ of $f(x) \in Y$ in the formigram θ_Y contains the interval $I =: [s,t]$. Since $I_{f(x)}$ is an interval in $\mathbf{R}$ (cf. Definition 3.5), it suffices to prove that $I_{f(x)}$ contains some $\alpha \in (-\infty, s]$ and $\beta \in [t, \infty)$. Invoking that R is an ε-tripod between θ_X and θ_Y, we have that

$$\theta_X(s-\varepsilon) \leq_R \bigvee_{[s-\varepsilon]^\varepsilon} \theta_Y = \bigvee_{[s-2\varepsilon, s]} \theta_Y. \tag{11}$$

Also, since x is in the underlying set of $\theta_X(s-\varepsilon)$ and $(x, f(x)) \in R$ (from inclusion (10)), relation (11) implies that the element $f(x) \in Y$ must be in the underlying set of $\bigvee_{[s-2\varepsilon,s]}\theta_Y$ (cf. Remark 4.15 (i)). This implies that there exists $\alpha \in [s-2\varepsilon, s]$ such that y is in the underlying set of $\theta_Y(\alpha)$. Hence, α belongs to $I_{f(x)}$. Similarly, one can also check that there exists $\beta \in [t, t+2\varepsilon]$ such that $\beta \in I_{f(x)}$. Therefore, we have that $I \subset I_{f(x)}$.

This inclusion implies that $\bigwedge_I \theta_Y$ contains a block C which in turn contains $f(x)$. We define ψ_1 as the map sending B to C. Note that the definition of ψ_1 depends on the choice of a representative element x for each block B in $\bigwedge_{I^\varepsilon}\theta_X$.

Next, by invoking that R is an ε-tripod between θ_X and θ_Y, inclusion (10), and Remark 4.15 (ii), we define the map $\psi_2 : \bigvee_I \theta_Y \to \bigvee_{I^\varepsilon}\theta_X$ as follows: for each $C \in \bigvee_I \theta_Y$, let $\psi_2(C)$ be the unique block $B \in \bigvee_{I^\varepsilon}\theta_X$ containing the image of C via the map $g : Y \to X$.

It remains to verify that $\phi^X(I^\varepsilon) = \psi_2 \circ \phi^Y(I) \circ \psi_1$. Pick any block $B \in \bigwedge_{I^\varepsilon}\theta_X$. Since $\phi^X(I^\varepsilon)$ is the canonical map in $\mathrm{SubPart}(X)$, B is sent to the unique block $B' \in \bigvee_{I^\varepsilon}\theta_X$ containing the whole block B. Now, let $x \in B$ be the representative element which was used for defining ψ_1. Via ψ_1, the block B is sent to the block $C \in \bigwedge_I \theta_Y$ containing $f(x)$. Then, the map $\phi^Y(I)$ sends C to the unique block $C' \in \bigvee_I \theta_Y$ containing $f(x)$ (and the whole block C). From Remark 4.15 (ii), we have that $\bigvee_I \theta_Y \leq_R \bigvee_{I^\varepsilon}\theta_X$. Thus, by inclusion (10), we conclude that ψ_2 sends $C'(\ni f(x))$ to the block $B'(\ni x)$, completing the proof. □

7 Analysis of dynamic metric spaces (DMSs)

Our work is motivated by the desire to construct a well-defined summarization tool of clustering behavior of time-varying metric data, which is modeled as *dynamic metric spaces (DMSs)*. In Section 7.1, we define DMSs. In Section 7.2, we establish a sufficient condition for DMSs to be converted into DGs via the Rips graph functor (cf. Proposition 7.5). This enables us to produce summaries of DMSs such as those which are illustrated in Figure 1.[8] In Section 7.3, we define the *λ-slack interleaving distance* $d_{\mathrm{I},\lambda}^{\mathrm{dynM}}$ between DMSs. Although this metric was utilized in [54], all properties of $d_{\mathrm{I},\lambda}^{\mathrm{dynM}}$ mentioned therein are proved in this paper, including the fact that $d_{\mathrm{I},\lambda}^{\mathrm{dynM}}$ is a metric.

[8] In [55, Section 5], DMSs generated by *Boid* [69] were successfully classified by the bottleneck distance on their zigzag barcodes (cf. Figure 1 (F)).

7.1 DMSs

In this section we introduce definitions pertaining to our model for dynamic metric spaces (DMSs). In particular, *tameness* (cf. Definition 7.4) is a crucial requirement on DMSs, which permits transforming DMSs into DGs via the Rips graph functor (cf. Proposition 7.13), thus subsequently into formigrams, persistence clustergrams, Reeb graphs, and barcodes.

Definition 7.1 ([54])**.** A *dynamic metric space* is a pair $\gamma_X = (X, d_X(\cdot))$ where X is a nonempty finite set and $d_X : \mathbf{R} \times X \times X \to \mathbf{R}_+$ satisfies:

(i) For every $t \in \mathbf{R}$, $\gamma_X(t) = (X, d_X(t))$ is a pseudo-metric space.
(ii) For any $x, x' \in X$ with $x \neq x'$ the function $d_X(\cdot)(x, x') : \mathbf{R} \to \mathbf{R}_+$ is not identically zero.
(iii) For fixed $x, x' \in X$, $d_X(\cdot)(x, x') : \mathbf{R} \to \mathbf{R}_+$ is continuous.

We refer to t as the *time* parameter.

We remark that a DMS γ_X is not just a continuous curve in the Gromov-Hausdorff space [25], but it also keeps track of the identities of points in X. Item (ii) is assumed to avoid redundancy; otherwise there could be two points which are forever identified.

Example 7.2. An example is given by n particles/animals moving continuously inside an environment $\Omega \subset \mathbf{R}^d$ where particles are allowed to coalesce. If the n trajectories are $p_1(t), \ldots, p_n(t) \in \mathbf{R}^d$, then let $P := \{1, \ldots, n\}$ and define a DMS $\gamma_P := (P, d_P(\cdot))$ as follows: for $t \in \mathbf{R}$ and $i, j \in \{1, \ldots, n\}$, let $d_P(t)(i, j) := \|p_i(t) - p_j(t)\|$, where $\|\cdot\|$ denotes the Euclidean norm. Buchin et al. considered this setting [15].

We now introduce a notion of *equality* between two DMSs.

Definition 7.3. Let $\gamma_X = (X, d_X(\cdot))$ and $\gamma_Y = (Y, d_Y(\cdot))$ be two DMSs. We say that γ_X and γ_Y are *isomorphic* if there exists a bijection $\varphi : X \to Y$ such that φ is an isometry between $\gamma_X(t)$ and $\gamma_Y(t)$ across all $t \in \mathbf{R}$.

7.2 From DMSs to DGs

We introduce a notion of *tame DMS* which will ultimately ensure that the Rips graph functor induces DGs satisfying our definition (cf. Definition 3.1 and Example 3.2). A continuous function $f : \mathbf{R} \to \mathbf{R}$ is called *tame*, if for any $c \in \mathbf{R}$ and any finite interval $I \subset \mathbf{R}$, the set $f^{-1}(c) \cap I \subset \mathbf{R}$ has only finitely many connected components (and is possibly empty). Elementary functions including polynomial functions (in particular, constant functions), piecewise linear functions with locally finitely many critical points are tame.

Definition 7.4. A DMS $\gamma_X = (X, d_X(\cdot))$ is said to be *tame* if for any $x, x' \in X$ the function $d_X(\cdot)(x, x') : \mathbf{R} \to \mathbf{R}_+$ is tame.

For $\delta \geq 0$ and for any finite metric space (X, d_X), let $\mathscr{R}^1_\delta(X, d_X)$ be the 1-skeleton of the δ-Rips complex of X, i.e. a simple graph over the vertex set X with the edge set $E_X = \{\{x, x'\} \subset X : d_X(x, x') \leq \delta \text{ and } x \neq x'\}$.

Proposition 7.5. Let γ_X be a *tame* DMS over X and let $\delta \geq 0$. Then, by defining $\mathscr{R}^1_\delta(\gamma_X)(t) := \mathscr{R}^1_\delta(\gamma_X(t))$ for $t \in \mathbf{R}$, $\mathscr{R}^1_\delta(\gamma_X) : \mathbf{R} \to \mathrm{Graph}(X)$ is a saturated DG over X.

The proof of Proposition 7.5 is given in Appendix A.6.1. Let γ_X be a tame DMS over X. By Proposition 7.5 and Definition 3.10, one can obtain a formigram $\theta_X := \pi_0\left(\mathscr{R}^1_\delta(\gamma_X)\right)$.

7.3 The λ-slack interleaving distance between DMSs

The main goal of this section is to introduce a $[0,\infty)$-parametrized family $\left\{d_{\mathrm{I},\lambda}^{\mathrm{dynM}}\right\}_{\lambda\in[0,\infty)}$ of extended metrics for DMSs. Each metric in this family is a hybrid between the Gromov-Hausdorff distance [16] and the interleaving distance [23, 33]. We obtain a stability result with respect to the most stringent metric (the metric corresponding to $\lambda = 0$) in the family (cf. Theorem 7.14).

Definition 7.6. Let $\varepsilon \geq 0$. Given any map $d : X \times X \to \mathbf{R}$, by $d+\varepsilon$ we denote the map from $X \times X$ to $\mathbf{R}$ defined by $(d+\varepsilon)(x,x') = d(x,x') + \varepsilon$ for all $(x,x') \in X \times X$.

Definition 7.7. Given any DMS $\gamma_X = (X, d_X(\cdot))$ and any interval $I \subset \mathbf{R}$, define the map $\bigvee_I d_X : X \times X \to \mathbf{R}_+$ by $\left(\bigvee_I d_X\right)(x,x') := \min_{t\in I} d_X(t)(x,x')$ for all $(x,x') \in X \times X$.

Given any map $d : X \times X \to \mathbf{R}$, let Z be any set and let $\varphi : Z \to X$ be any map. Then, we define the pullback $\varphi^* d : Z \times Z \to \mathbf{R}$ of d under φ by

$$\varphi^* d(z,z') := d\left(\varphi(z), \varphi(z')\right)$$

for all $(z,z') \in Z \times Z$. Consider any two functions $d_1 : X \times X \to \mathbf{R}$ and $d_2 : Y \times Y \to \mathbf{R}$. Given a tripod $R:\ X \xleftarrow{\varphi_X} Z \xrightarrow{\varphi_Y} Y$ between X and Y, by $d_1 \leq_R d_2$ we mean $\varphi_X^* d_1(z,z') \leq \varphi_Y^* d_2(z,z')$ for all $(z,z') \in Z \times Z$.

Recall that for any $t \in \mathbf{R}$, $[t]^\varepsilon := [t-\varepsilon, t+\varepsilon]$.

Definition 7.8 (λ-distortion of a tripod)**.** Fix $\lambda \geq 0$. Let $\gamma_X = (X, d_X(\cdot))$ and $\gamma_Y = (Y, d_Y(\cdot))$ be any two DMSs. Let $R:\ X \xleftarrow{\varphi_X} Z \xrightarrow{\varphi_Y} Y$ be a tripod between X and Y such that

$$\text{for all } t \subset \mathbf{R},\ \bigvee_{[t]^\varepsilon} d_X \leq_R d_Y(t) + \lambda\varepsilon \text{ and } \bigvee_{[t]^\varepsilon} d_Y \leq_R d_X(t) + \lambda\varepsilon. \tag{12}$$

We call any such R a (λ,ε)-*tripod* between γ_X and γ_Y. Define the λ-*distortion* $\mathrm{dis}_\lambda^{\mathrm{dyn}}(R)$ of R to be the infimum of those $\varepsilon \geq 0$ for which R is a $(\lambda,\varepsilon)-$tripod.

Example 7.9. For $\lambda > 0$, $\mathrm{dis}_\lambda^{\mathrm{dyn}}(R)$ takes into account both spatial and temporal distortion of the tripod R between γ_X and γ_Y:

(i) (Spatial distortion) Let $a, b \geq 0$. For the two metric spaces $(X, d_{X,a}) = \left(\{x,x'\}, \left(\begin{smallmatrix} 0 & a \\ a & 0 \end{smallmatrix}\right)\right)$ and $(X, d_{X,b}) = \left(\{x,x'\}, \left(\begin{smallmatrix} 0 & b \\ b & 0 \end{smallmatrix}\right)\right)$, consider the two *constant* DMSs $\gamma_{X,a} \equiv (X, d_{X,a})$ and $\gamma_{X,b} \equiv (X, d_{X,b})$. Take the tripod $R : X \xleftarrow{\mathrm{id}_X} X \xrightarrow{\mathrm{id}_X} X$. Then, for $\lambda > 0$, it is easy to check that $\mathrm{dis}_\lambda^{\mathrm{dyn}}(R) = \frac{|a-b|}{\lambda}$.

(ii) (Temporal distortion) Fix $\tau \geq 0$. Let $\gamma_X = (X, d_X(\cdot))$ be any DMS and define any continuous map $\alpha : \mathbf{R} \to \mathbf{R}$ such that $\|\alpha - \mathrm{id}_{\mathbf{R}}\|_\infty \leq \tau$. Define the DMS $\gamma_X \circ \alpha := (X, d_X(\alpha(\cdot)))$, i.e. for $t \in \mathbf{R}$, $\gamma_X \circ \alpha(t) = (X, d_X(\alpha(t)))$. Take the tripod $R : X \xleftarrow{\mathrm{id}_X} X \xrightarrow{\mathrm{id}_X} X$. Then, for any $\lambda \geq 0$, it is easy to check that $\mathrm{dis}_\lambda^{\mathrm{dyn}}(R) \leq \tau$.

Remark 7.10. In Definition 7.8, if R is a (λ,ε)-tripod, then R is also a (λ,ε')-tripod for any $\varepsilon' > \varepsilon$: Fix any $t \subset \mathbf{R}$. If for some $\varepsilon \geq 0$, $\bigvee_{[t]^\varepsilon} d_X \leq_R d_Y(t) + \lambda\varepsilon$, then for any $\varepsilon' > \varepsilon$,

$$\bigvee_{[t]^{\varepsilon'}} d_X \leq \bigvee_{[t]^\varepsilon} d_X \leq_R d_Y(t) + \lambda\varepsilon < d_Y(t) + \lambda\varepsilon'.$$

Now we introduce a family of metrics for DMSs.

Definition 7.11 (The λ-slack interleaving distance between DMSs)**.** For each $\lambda \geq 0$, we define the λ-*slack interleaving distance* between any two DMSs $\gamma_X = (X, d_X(\cdot))$ and $\gamma_Y = (Y, d_Y(\cdot))$ as

$$d_{\mathrm{I},\lambda}^{\mathrm{dynM}}(\gamma_X, \gamma_Y) := \min_R \mathrm{dis}_\lambda^{\mathrm{dyn}}(R)$$

where the minimum ranges over all tripods between X and Y. For simplicity, when $\lambda = 0$, we write $d_{\mathrm{I}}^{\mathrm{dynM}}$ instead of $d_{\mathrm{I},0}^{\mathrm{dynM}}$. If $d_{\mathrm{I}}^{\mathrm{dynM}}(\gamma_X, \gamma_Y) \leq \varepsilon$ for some $\varepsilon \geq 0$, then we say that γ_X and γ_Y are ε-*interleaved* or simply *interleaved*. By definition, it is clear that for all $\lambda > 0$, $d_{\mathrm{I},\lambda}^{\mathrm{dynM}} \leq d_{\mathrm{I}}^{\mathrm{dynM}}$.

For $r>0$, we call any DMS $\gamma_X=(X,d_X(\cdot))$ *$r-$bounded* if the distance between any pair of points in X does not exceed r across all $t\in\mathbf{R}$. If γ_X is $r-$bounded for some $r>0$, then γ_X is said to be simply *bounded*.

Theorem 7.12. For each $\lambda\geq 0$, $d_{\mathrm{I},\lambda}^{\mathrm{dynM}}$ is an extended metric between DMSs modulo isomorphism. In particular, for $\lambda>0$, $d_{\mathrm{I},\lambda}^{\mathrm{dynM}}$ is a metric between bounded DMSs modulo isomorphism.

The proof of Theorem 7.12 together with details pertaining to the following facts are deferred to Appendix A.6.2:

(i) For $\lambda>0$, $d_{\mathrm{I},\lambda}^{\mathrm{dynM}}$ generalizes the Gromov-Hausdorff distance (cf. Remark A.14).
(ii) The metrics $d_{\mathrm{I},\lambda}^{\mathrm{dynM}}$, for different $\lambda>0$, are bilipschitz-equivalent (cf. Proposition A.15).
(iii) In Proposition D.1 we will elucidate a link between $d_{\mathrm{I}}^{\mathrm{dynM}}$ and the Gromov-Hausdorff distance. This link will be useful for determining the computational complexity of $d_{\mathrm{I}}^{\mathrm{dynM}}$ (cf. Theorem 7.15).

In the rest of this section, we discuss several properties of $d_{\mathrm{I}}^{\mathrm{dynM}}$.

Stability results. The following proposition provides a gateway for extending the stability results that are illustrated in Figure 1 to the setting of DMSs.

Proposition 7.13 (Stability of summarizing DMSs into DGs)**.** Let $\gamma_X=(X,d_X(\cdot))$ and $\gamma_Y=(Y,d_Y(\cdot))$ be any tame DMSs. Fix any $\delta\geq 0$. Consider saturated DGs $\mathscr{G}_X:=\mathscr{R}_\delta^1(\gamma_X),\mathscr{G}_Y:=\mathscr{R}_\delta^1(\gamma_Y)$, as in Proposition 7.5. Then,

$$d_{\mathrm{I}}^{\mathrm{dynG}}(\mathscr{G}_X,\mathscr{G}_Y)\leq d_{\mathrm{I}}^{\mathrm{dynM}}(\gamma_X,\gamma_Y).$$

Proof. The proof follows from the fact that for any $\varepsilon\geq 0$, any $(0,\varepsilon)$-tripod R between γ_X and γ_Y (Definition 7.11) is also an ε-tripod between $\mathscr{G}_X$ and $\mathscr{G}_Y$ (cf. Definition 4.4). □

A priori Proposition 7.13 does not seem to be a satisfactory stability theorem in that the RHS can be infinity in many cases in comparison with the LHS. Nevertheless, this 'weak' stability seems to be the most we can expect for the mapping [DMSs] $\mapsto$ [DGs] via the Rips graph functor because DMSs change continuously over time (cf. Definition 7.1 (iii)) whereas DGs are discontinuous in the sense that edges appear and disappear over time.

Proposition 7.13 together with Theorem 2.22, Proposition 4.13 and Theorem 4.17 directly imply:

Theorem 7.14. Let $\gamma_X=(X,d_X(\cdot))$ and $\gamma_Y=(Y,d_Y(\cdot))$ be any two tame DMSs. Fix any $\delta\geq 0$. Consider the saturated formigrams $\theta_X:=\pi_0\left(\mathscr{R}_\delta^1(\gamma_X)\right)$ and $\theta_Y:=\pi_0\left(\mathscr{R}_\delta^1(\gamma_Y)\right)$. [9] Then,

$$d_{\mathrm{B}}\left(\mathrm{barc}_{\mathbf{ZZ}}(\theta_X),\mathrm{barc}_{\mathbf{ZZ}}(\theta_Y)\right)\leq 2\,d_{\mathrm{I}}^{\mathrm{dynM}}(\gamma_X,\gamma_Y).$$

We discuss the generalization of Theorem 7.14 to higher dimensional homology barcodes in Appendix E.

Computational complexity $d_{\mathrm{I}}^{\mathrm{dynM}}$. A DMS $\gamma_X=(X,d_X(\cdot))$ is said to be *piecewise linear* if for all $x,x'\in X$, the function $d_X(\cdot)(x,x):\mathbf{R}\to\mathbf{R}_+$ is piecewise linear. We denote by S_X the set of all breakpoints of all distance functions $d_X(\cdot)(x,x')$, $x,x'\in X$.

Theorem 7.15 (Complexity of $d_{\mathrm{I}}^{\mathrm{dynM}}$)**.** Fix $\rho\in(1,6)$ and let γ_X and γ_Y be piecewise linear DMSs. Then, it is not possible to compute a ρ-approximation to $d_{\mathrm{I}}^{\mathrm{dynM}}(\gamma_X,\gamma_Y)$ in time depending polynomially on $|X|,|Y|,|S_X|$, and $|S_Y|$, unless $P=NP$.

Theorem 7.15 will be proved in Appendix D. More examples about $d_{\mathrm{I}}^{\mathrm{dynM}}$ are provided in Appendix D as well. The theorem above indicates that computing the lower bound for $d_{\mathrm{I}}^{\mathrm{dynM}}$ given by Theorem 7.14 is a realistic approach to comparing DMSs, especially when one is interested in a specific spatial scale.

[9] These are formigrams by Proposition 7.5 and Definition 3.10.

8 Conclusion

We have established a stable mathematical framework for summarizing dynamic graphs, which often arise as discrete representations of spatiotemporal data. The evolution of connected components of a dynamic graph is fully encoded in a *formigram*, a constructible cosheaf over $\mathbf{R}$ valued in the lattice of subpartitions.[10] The lattice structure of subpartitions of a given set has been indispensable for obtaining:

(i) the formigram interleaving distance $d_{\mathrm{I}}^{\mathrm{F}}$ which is more discriminative than the well-known Reeb graph interleaving distance.
(ii) the maximal group diagram and persistence clustergram which are complete and visualizable invariants of formigrams (and thus more discriminative invariants than the Reeb graph of a formigram).

Note that we can directly extend the definitions of the maximal group diagram and the persistence clustergram to *any* cellular cosheaf over a topological space other than $\mathbf{R}$ [30]. Indeed, our two main ingredients, Möbius inversion and the lattice structure of subpartitions, do not depend on any specific property of $\mathbf{R}$. Exploring this extension in relation to *Reeb spaces* [66] is left for future work. Extending the functorial pipeline in the left column of Figure 1 to the entire diagram is also left for the future [60]. Devising a bottleneck-type distance which can directly measure the difference between persistence clustergrams or between maximal group diagrams is of independent interest.

A Details and Proofs

A.1 Bottleneck distance

Recall that injective partial functions are referred to as *matchings*. We use $\sigma : A \nrightarrow B$ to denote a matching $\sigma \subset A \times B$ between sets A and B. The canonical projections of σ onto A and B are denoted by $\mathrm{coim}(\sigma)$ and $\mathrm{im}(\sigma)$, respectively.

Many equivalent expressions for the *bottleneck distance* have been given in the TDA literature. We adopt the following form from [5]: Recall Notation 2.12. Letting $\mathscr{A}$ be a multiset of intervals in $\mathbf{R}$ and $\varepsilon \geq 0$,

$$\mathscr{A}^{\varepsilon} := \{\langle b, d\rangle \in \mathscr{A} : b + \varepsilon < d\} = \{I \in \mathscr{A} : [t, t+\varepsilon] \subset I \text{ for some } t \in \mathbf{R}\}.$$

Note that $\mathscr{A}^0 = \mathscr{A}$.

Definition A.1 ([5])**.** Let $\mathscr{A}$ and $\mathscr{B}$ be multisets of intervals in $\mathbf{R}$. We define a δ-matching between $\mathscr{A}$ and $\mathscr{B}$ to be a matching $\sigma : \mathscr{A} \nrightarrow \mathscr{B}$ such that $\mathscr{A}^{2\delta} \subset \mathrm{coim}(\sigma)$, $\mathscr{B}^{2\delta} \subset \mathrm{im}(\sigma)$, and if $\sigma\langle b, d\rangle = \langle b', d'\rangle$, then

$$\langle b, d\rangle \subset \langle b' - \delta, d' + \delta\rangle, \qquad \langle b', d'\rangle \subset \langle b - \delta, d + \delta\rangle.$$

with the convention $+\infty + \delta = +\infty$ and $-\infty - \delta = -\infty$. We define the bottleneck distance d_{B} by

$$d_{\mathrm{B}}(\mathscr{A}, \mathscr{B}) := \inf\{\delta \in [0, \infty) : \exists \delta\text{-matching between } \mathscr{A} \text{ and } \mathscr{B}\}.$$

We declare $d_{\mathrm{B}}(\mathscr{A}, \mathscr{B}) = +\infty$ when there is no δ-matching between $\mathscr{A}$ and $\mathscr{B}$ for any $\delta \in [0, \infty)$.

A.2 Proof of Theorem 4.7

We recall the *Gromov-Hausdorff distance* between metric spaces. Let (X, d_X) and (Y, d_Y) be any two metric spaces and let $R : X \xleftarrow{\varphi_X} Z \xrightarrow{\varphi_Y} Y$ be a tripod between X and Y. Then, the *distortion* of R is defined as

$$\mathrm{dis}(R) := \sup_{z, z' \in Z} \left| d_X\left(\varphi_X(z), \varphi_X(z')\right) - d_Y\left(\varphi_Y(z), \varphi_Y(z')\right) \right|.$$

[10] In the preprint of this work, we also considered formigrams derived from *directed* dynamic graphs [51].

Definition A.2 (Gromov-Hausdorff distance [16, Section 7.3])**.** Let (X,d_X) and (Y,d_Y) be any two compact metric spaces. Then,

$$d_{\mathrm{GH}}((X,d_X),(Y,d_Y)) = \frac{1}{2}\inf_R \mathrm{dis}(R)$$

where the infimum is taken over all tripods R between X and Y. In particular, any tripod R between X and Y is said to be an ε-*tripod* between (X,d_X) and (Y,d_Y) if $\mathrm{dis}(R)\leq\varepsilon$.

Proposition A.3. Let (X,d_X) and (Y,d_Y) be any two finite metric spaces. Then, there exist two DGs $\mathscr{G}_X = (V_X(\cdot),E_X(\cdot))$ and $\mathscr{G}_Y = (V_Y(\cdot),E_Y(\cdot))$ corresponding to (X,d_X) and (Y,d_Y) respectively such that

$$d_{\mathrm{I}}^{\mathrm{dynG}}(\mathscr{G}_X,\mathscr{G}_Y) = 2\cdot d_{\mathrm{GH}}((X,d_X),(Y,d_Y)).$$

Proof. Let T be the diameter of (X,d_X). For $t\in\mathbf{R}$, we define:

$$V_X(t) := \begin{cases}\emptyset, & t\notin[0,T]\\ X, & t\in[0,T],\end{cases} \quad E_X(t) := \begin{cases}\emptyset, & t\notin[0,T]\\ \{\{x,x'\}\subset X : x\neq x' \text{ and } d_X(x,x')\leq t\}, & t\in[0,T].\end{cases}$$

We define $\mathscr{G}_X$ by $t\mapsto(V_X(t),E_X(t))$. Define $\mathscr{G}_Y$ similarly. We show that $d_{\mathrm{I}}^{\mathrm{dynG}}(\mathscr{G}_X,\mathscr{G}_Y)\geq 2\cdot d_{\mathrm{GH}}((X,d_X),(Y,d_Y))$. To this end, suppose that for some $\varepsilon\geq 0$, $R:\ X \xleftarrow{\varphi_X} Z \xrightarrow{\varphi_Y} Y$ is any ε-tripod between $\mathscr{G}_X$ and $\mathscr{G}_Y$ (Definition 4.4). Then, by the construction of $\mathscr{G}_X,\mathscr{G}_Y$, it must hold that $\left|d_X\left(\varphi_X(z),\varphi_X(z')\right)-d_Y\left(\varphi_Y(z),\varphi_Y(z')\right)\right|\leq\varepsilon$ for all $z,z'\in Z$. The other inequality $d_{\mathrm{I}}^{\mathrm{dynG}}(\mathscr{G}_X,\mathscr{G}_Y)\leq 2\cdot d_{\mathrm{GH}}((X,d_X),(Y,d_Y))$ can be similarly proved. □

Definition A.4. An *ultrametric space* is a metric space (X,d) in which the following ultra-triangle inequality holds: for all $x,y,z\in X$,

$$d(x,z)\leq\max\{d(x,y),d(y,z)\}.$$

If (X,d) were a pseudometric, then d is called an ultra-pseudometric.

Proof of Theorem 4.7 Pick any two ultrametric spaces (X,u_X) and (Y,u_Y). Then, by Proposition A.3, there exist DGs $\mathscr{G}_X = (V_X(\cdot),E_X(\cdot))$ and $\mathscr{G}_Y = (V_Y(\cdot),E_Y(\cdot))$ such that the interleaving distance between $\mathscr{G}_X$ and $\mathscr{G}_Y$ is identical to twice the Gromov-Hausdorff distance $\Delta := d_{\mathrm{GH}}((X,u_X),(Y,u_Y))$ between (X,u_X) and (Y,u_Y). However, according to [75, Corollary 3.8], Δ cannot be approximated within any factor less than 3 in polynomial time, unless $P=NP$. The author shows this by observing that any instance of the 3-partition problem can be reduced to an instance of the bottleneck ∞-Gromov-Hausdorff distance (∞-BGHD) problem between ultrametric spaces (cf. [75, p.865]). The proof follows. □

A.3 Details about Remark 4.18

Remark A.5 (Interleaving between dendrograms)**.** When θ_X,θ_Y are dendrograms over sets X and Y respectively, let $R:\ X \xleftarrow{\varphi_X} Z \xrightarrow{\varphi_Y} Y$ be an ε-tripod between θ_X and θ_Y. Since both θ_X and θ_Y get coarser as $t\in\mathbf{R}$ increases, the interleaving condition in Definition 4.11 can be rewritten as follows: for all $t\in\mathbf{R}$ it holds that $\theta_X(t)\leq_R\theta_Y(t+\varepsilon)$ and $\theta_Y(t)\leq_R\theta_X(t+\varepsilon)$ (cf. Definition 4.10).

Let X be a finite set and let θ_X be a dendrogram over X (cf. Remark 3.7). Recall from [19] that this θ_X induces a canonical ultra-pseudometric $u_X: X\times X\to\mathbf{R}_+$ on X (cf. Definition A.4) defined by

$$u_X(x,x') := \inf\{\varepsilon\geq 0 : x,x' \text{ belong to the same block of } \theta_X(\varepsilon)\} \tag{13}$$

Proposition A.6. Given any two dendrograms θ_X,θ_Y over sets X,Y, respectively, let u_X,u_Y be the canonical ultra-pseudometrics on X and Y, respectively. Then, $d_{\mathrm{I}}^{\mathrm{F}}(\theta_X,\theta_Y) = 2\,d_{\mathrm{GH}}((X,u_X),(Y,u_Y))$.

Proof. We first show that the LHS $\geq$ the RHS. Let $\varepsilon \geq 0$ and let $R:\ X \xleftarrow{\varphi_X} Z \xrightarrow{\varphi_Y} Y$ be any ε-tripod between the two dendrograms θ_X and θ_Y. Let $(x,y),(x',y') \in R$ and let $t := u_X(x,x')$. This implies that x, x' belong to the same block of the partition $\theta_X(t)$. Since $\theta_X(t) \leq_R \bigvee_{[t]^\varepsilon} \theta_Y = \theta_Y(t+\varepsilon)$, y and y' must belong to the same block of $\theta_Y(t+\varepsilon)$, and in turn this implies that $u_Y(y,y') \leq t+\varepsilon = u_X(x,x')+\varepsilon$. By symmetry, we also have $u_Y(y,y') \leq u_X(x,x')+\varepsilon$ and in turn $\left|u_X(x,x') - u_Y(y,y')\right| \leq \varepsilon$. By Definition A.2, this implies that $d_{\mathrm{GH}}((X,u_X),(Y,u_Y)) \leq \varepsilon/2$.

Next, we prove the opposite inequality. Let $R:\ X \xleftarrow{\varphi_X} Z \xrightarrow{\varphi_Y} Y$ be a tripod between X and Y such that $\mathrm{dis}(R) = \varepsilon$. it suffices to show that for all $t \in \mathbf{R}$, $\theta_X(t) \leq_R \theta_Y(t+\varepsilon)$ and $\theta_Y(t) \leq_R \theta_X(t+\varepsilon)$. By symmetry, we only prove that $\theta_X(t) \leq_R \theta_Y(t+\varepsilon)$ for all $t \in \mathbf{R}$. For $t<0$, since $\theta_X(t) = \emptyset$, $\theta_X(t) \leq_R \theta_Y(t+\varepsilon)$ trivially holds. Now pick any $t \geq 0$ and pick any $(x,y),(x',y') \in R$. Assume that x, x' belong to the same block of $\theta_X(t)$, implying that $u_X(x,x') \leq t$. Since $\left|u_X(x,x') - u_Y(y,y')\right| \leq \varepsilon$, we know $u_Y(y,y') \leq t+\varepsilon$, and hence y, y' belong to the same block of $\theta_Y(t+\varepsilon)$. Therefore, $\theta_X(t) \leq_R \theta_Y(t+\varepsilon)$ for all $t \in \mathbf{R}$. □

Theorem A.7 (Complexity of computing $d_{\mathrm{I}}^{\mathrm{F}}$)**.** Fix $\rho \in (1,6)$. It is not possible to obtain a ρ approximation to the distance $d_{\mathrm{I}}^{\mathrm{F}}(\theta_X,\theta_Y)$ between formigrams in time polynomially depending on $|X|, |Y|, |\mathrm{crit}(\theta_X)|, |\mathrm{crit}(\theta_Y)|$ unless $P = NP$.

Proof. Pick any two dendrograms and invoke Proposition A.6 to reduce the problem to the computation of the Gromov-Hausdorff distance between the ultra-pseudometric spaces associated to the dendrograms. The rest of the proof follows along the same lines as that of Theorem 4.7. □

A.4 Proof of Theorem 6.30

Theorem 6.30 will directly follow from Theorem A.9 below.

We explicitly represent the colimit of $M : \mathbf{ZZ} \to \mathbf{set}$ as follows. For $k, l \in \mathbf{ZZ}$, assume that $x \in M(k)$ and $y \in M(l)$. We write $x \sim y$ if k and l are comparable and one of x and y is mapped to the other via the internal map between $M(k)$ and $M(l)$. The colimit of M is the pair $(C, (i_k)_{k\in\mathbf{ZZ}})$ described as follows:

$$C := \left(\coprod_{k\in\mathbf{ZZ}} M(k) \right) / \approx, \tag{14}$$

where $\approx$ is the equivalence relation generated by the relations $x_k \sim x_l$ for $x_k \in M(k)$ and $x_l \in M(l)$ with k, l being comparable. For the quotient map $q : \coprod_{k\in\mathbf{ZZ}} M(k) \to C$, each i_k is the composition $M_k \hookrightarrow \coprod_{k\in\mathbf{ZZ}} M(k) \xrightarrow{q} C$.

Let $I \in \mathbf{Int}(\mathbf{ZZ})$. For any functor $N : I \to \mathbf{set}$, we can construct the limit and colimit of N in the same way; namely, in the above description, replace M and $\mathbf{ZZ}$ by N and I, respectively. **In what follows, we use this explicit construction whenever considering colimits of (interval restrictions of) ZZ-indexed set-diagrams.**

Definition A.8. Let $I \in \mathbf{Int}(\mathbf{ZZ})$ and let $N : I \to \mathbf{set}$ by any functor. Let $c \in \varinjlim N$. We define the *support* of c as

$$\mathrm{supp}(c) := \{k \in I : \exists x_k \in N_k,\ i_k(x_k) = c\}.$$

In particular, if $\mathrm{supp}(c) = I$, we call c a *full component* of the functor N.

Given $M : \mathbf{ZZ} \to \mathbf{set}$ and $I \in \mathbf{Int}(\mathbf{ZZ})$, we denote the number of *full components* of $M|_I$ by $\mathrm{full}(M|_I)$. Recall Notation 6.5.

Theorem A.9 ([53, Corollary 4.10])**.** For any functor $M : \mathbf{ZZ} \to \mathbf{set}$, the multiplicity of I in $\mathrm{barc}(\mathscr{F} \circ M)$ is

$$\mathrm{full}(M|_I) - \mathrm{full}(M|_{I^+}) - \mathrm{full}(M|_{I^-}) + \mathrm{full}(M|_{I^\pm}).$$

Proof of Theorem 6.30. By Proposition 6.10, for every $I \in \mathbf{Int}(\mathbf{ZZ})$,

$$\left|\mathrm{dgm}^{\bigwedge}(\theta_X)\right|(I) = \left|\bigwedge_I \theta_X\right| - \left|\bigwedge_{I^+} \theta_X\right| - \left|\bigwedge_{I^-} \theta_X\right| + \left|\bigwedge_{I^\pm} \theta_X\right|.$$

Therefore, by Theorem A.9, it suffices to show that $\left|\bigwedge_J \theta_X\right| = \mathrm{full}(\mathrm{Reeb}(\theta_X)|_J)$ for all $J \in \mathbf{Int}(\mathbf{ZZ})$. If $J \in \mathbf{Int}(\mathbf{ZZ})$ is not a subset of $\mathrm{supp}(\theta_X)$, then clearly $0 = \left|\bigwedge_J \theta_X\right| = \mathrm{full}(\mathrm{Reeb}(\theta_X)|_J)$. Now assume that $J \in \mathbf{Int}(\mathbf{ZZ})$ is contained in $\mathrm{supp}(\theta_X)$. Then, since θ_X is saturated, $\bigwedge_J \theta_X = \bigvee_J \theta_X$. Also, $\left|\bigvee_J \theta_X\right|$ is equal to the number of full components of $\mathrm{Reeb}(\theta_X)|_J$, completing the proof. □

A.5 From unlabeled formigrams to persistent cluster counting functors

Let θ_X be a formigram. We shall prove that the persistent counting functor $|\divideontimes\theta_X|$ (cf. Definition 6.33) can be obtained from the unlabeled formigram of θ_X (cf. Definition 3.12 (i)).

Proposition A.10. Let θ be the unlabeled formigram of θ_X. For any $I \in \mathbf{Int}(\mathbb{ZZ})$, consider the canonical limit-to-colimit morphism $\varphi_I : \varprojlim \theta|_I \to \varinjlim \theta|_I$ in the category **Part**. Then, $\mathrm{coim}(\varphi_I) \cong (\bigcap_{t\in I}\theta_X(t), \divideontimes_I \theta_X)$.

Proof. By Proposition 5.1, $\varprojlim \theta|_I \cong \bigwedge_I \theta_X$ and $\varinjlim \theta|_I \cong \bigvee_I \theta_X$, and the morphism φ_I in **Part** is the inclusion $\bigcap_{t\in I}\bigcup\theta_X(t) \hookrightarrow \bigcup_{t\in I}\bigcup\theta_X(t)$. Now by Proposition 5.8 (ii) the desired isomorphism follows. □

Proposition A.10 implies that we can extract $|\divideontimes\theta_X|$ from θ: Namely, $|\divideontimes\theta_X|(I) = |\divideontimes_I\theta_X|$ equals the number of blocks in the second entry of $\mathrm{coim}(\varphi_I)$. Reciprocally, one may wonder whether $|\divideontimes\theta_X|$ contains enough information to reconstruct θ. That is not true; there exists a pair of formigrams which have identical persistent cluster functor, whereas their underlying weighted/unweighted Reeb graphs are different. This implies that their unlabeled formigrams are also different.

A.6 Details from Section 7

A.6.1 Details from Section 7.2

Proof of Proposition 7.5. Clearly, $\mathscr{R}^1_\delta(\gamma_X)$ is a function $\mathbf{R} \to \mathrm{Graph}(X)$. We show that $\mathscr{R}^1_\delta(\gamma_X)$ is cosheaf-inducing (Definition 2.17). First we prove that locally $\mathscr{R}^1_\delta(\gamma_X)$ admits only finitely many points of discontinuity (those points are called critical points). Let $I \subset \mathbf{R}$ be any nonempty finite interval. For $i, j \in X := \{1, \dots, n\}$, let $f_{i,j} := d_X(\cdot)(i,j) : \mathbf{R} \to \mathbf{R}_+$. Note that discontinuity points of $\mathscr{R}^1_\delta(\gamma_X)$ can occur only at endpoints of connected components of the set ${f_{i,j}}^{-1}(\delta)$ for some $i, j \in X$. Fix any $i, j \in X$. Then, by Definition 7.4, the set ${f_{i,j}}^{-1}(\delta) \cap I$ has only finitely many connected components and thus there are only finitely many endpoints arising from those components. Since the set X is finite, this implies that $\mathscr{R}^1_\delta(\gamma_X)$ can have only finitely many points of discontinuity in I. Fix any point $c \in \mathbf{R}$ on which $\mathscr{R}^1_\delta(\gamma_X)$ is discontinuous. Consider the following two subsets of $X \times X$:

$$A(c,\delta) := \{(i,j) : \ i < j \in X,\ d_X(c)(i,j) \le \delta\},$$

$$B(c,\delta) := \{(i,j) : \ i < j \in X,\ d_X(c)(i,j) > \delta\}.$$

The continuity of $d_X(\cdot)(i,j)$ for each $(i,j) \in X \times X$ guarantees that there exists $\varepsilon > 0$ such that

$$B(t,\delta) \supset B(c,\delta) \quad \text{for all } t \in (c-\varepsilon, c+\varepsilon)$$

and in turn

$$A(t,\delta) \subset A(c,\delta) \quad \text{for all } t \in (c-\varepsilon, c+\varepsilon)$$

since $A(t,\delta) \cup B(t,\delta) = \{(i,j) : i < j \in X\}$ for all $t \in \mathbf{R}$. This implies that the graph $\mathscr{R}^1_\delta(\gamma_X(c))$ contains $\mathscr{R}^1_\delta(\gamma_X(t))$ as a subgraph for each $t \in (c-\varepsilon, c+\varepsilon)$.

□

A.6.2 Details from Section 7.3

Details about $d_{\mathrm{I},\lambda}^{\mathrm{dynM}}$. We investigate further properties of the metrics in the family $\left\{d_{\mathrm{I},\lambda}^{\mathrm{dynM}}\right\}_{\lambda\in[0,\infty)}$. In particular, a discussion about stable invariants of DMSs with respect to the metrics $d_{\mathrm{I},\lambda}^{\mathrm{dynM}}$ for $\lambda > 0$ can be found in [54].

Remark A.11. Let $\lambda > 0$. The distance $d_{\mathrm{I},\lambda}^{\mathrm{dynM}}$ between any two bounded DMSs is finite. More specifically, for any r-bounded DMSs $\gamma_X = (X, d_X(\cdot))$ and $\gamma_Y = (Y, d_Y(\cdot))$ for some $r > 0$, any tripod R between X and Y is a $(\lambda, \frac{r}{\lambda})$-tripod between γ_X and γ_Y. This implies that

$$d_{\mathrm{I},\lambda}^{\mathrm{dynM}}(\gamma_X, \gamma_Y) \le \frac{r}{\lambda}.$$

Definition A.12 (Equivalent tripods)**.** Let X, Y be any two sets. For any two tripods $R:\ X \xleftarrow{\varphi_X} Z \xrightarrow{\varphi_Y} Y$ and $S:\ X \xleftarrow{\psi_X} Z \xrightarrow{\psi_Y} Y$ between X and Y, we say that R and S are *equivalent* if $(x,y)\in R$ if and only if $(x,y)\in S$.

Remark A.13. Let $\gamma_X=(X,d_X(\cdot))$ and $\gamma_Y=(Y,d_Y(\cdot))$ be any two DMSs. Suppose that R and S are equivalent tripods between X and Y (Definition A.12). Then, it is not difficult to check that for any $\lambda,\varepsilon\geq 0$, R is a (λ,ε)-tripod between γ_X and γ_Y if and only if S is a (λ,ε)-tripod between γ_X and γ_Y.

Proof of Theorem 7.12. We prove the triangle inequality. Take any DMSs γ_X,γ_Y and γ_W over X,Y and W, respectively. For some $\varepsilon,\varepsilon'>0$, let $R_1:\ X \xleftarrow{\varphi_X} Z_1 \xrightarrow{\varphi_Y} Y$ and $R_2:\ Y \xleftarrow{\psi_Y} Z_2 \xrightarrow{\psi_W} W$ be any (λ,ε)-tripod between γ_X and γ_Y and (λ,ε')-tripod between γ_Y and γ_W (Definition 7.8), respectively. Consider the set $Z:=\left\{(z_1,z_2)\in Z_1\times Z_2:\varphi_Y(z_1)=\psi_Y(z_2)\right\}$ and let $\pi_1:Z\to Z_1$ and $\pi_2:Z\to Z_2$ be the canonical projections to the first and the second coordinate, respectively. Define the tripod $R_2\circ R_1$ between X and W as in equation (1). It is not difficult to check that $R_2\circ R_1$ is a $(\lambda,\varepsilon+\varepsilon')$-tripod between γ_X and γ_W and thus we have $d_{\mathrm{I},\lambda}^{\mathrm{dynM}}(\gamma_X,\gamma_W)\leq d_{\mathrm{I},\lambda}^{\mathrm{dynM}}(\gamma_X,\gamma_Y)+d_{\mathrm{I},\lambda}^{\mathrm{dynM}}(\gamma_Y,\gamma_W)$.

Next assume that $d_{\mathrm{I},\lambda}^{\mathrm{dynM}}(\gamma_X,\gamma_Y)=0$. We outline the proof of the fact that γ_X and γ_Y are isomorphic (Definition 7.3). Because there are only finitely many tripods between X and Y up to equivalence (Definition A.12), $d_{\mathrm{I},\lambda}^{\mathrm{dynM}}(\gamma_X,\gamma_Y)=0$ implies that there must be a certain tripod $R:\ X \xleftarrow{\varphi_X} Z \xrightarrow{\varphi_Y} Y$ between X and Y such that R becomes an (λ,ε)-tripod between γ_X and γ_Y for *any* $\varepsilon>0$. In order to show that γ_X and γ_Y are isomorphic, one needs to prove that that R is in fact $(\lambda,0)$-tripod. After that, invoke Definition 7.1, (ii) and (iii) to verify that the multivalued map $\varphi_Y\circ\varphi_X^{-1}:X\rightrightarrows Y$ is in fact a bijection from X to Y.

Lastly, by Remark A.11, for $\lambda>0$, $d_{\mathrm{I},\lambda}^{\mathrm{dynM}}$ is finite between bounded DMSs. □

Remark A.14 (For $\lambda>0$, $d_{\mathrm{I},\lambda}^{\mathrm{dynM}}$ generalizes the Gromov-Hausdorff distance)**.** Let $\lambda>0$. Given any two constant DMSs $\gamma_X\equiv(X,d_X)$ and $\gamma_Y\equiv(Y,d_Y)$, the value $d_{\mathrm{I},\lambda}^{\mathrm{dynM}}(\gamma_X,\gamma_Y)$ equals the Gromov-Hausdorff distance between (X,d_X) and (Y,d_Y) up to multiplicative constant $\frac{\lambda}{2}$. Indeed, for any tripod $R:\ X \xleftarrow{\varphi_X} Z \xrightarrow{\varphi_Y} Y$ between X and Y, condition (12) reduces to

$$\left|d_X\left(\varphi_X(z),\varphi_X(z')\right)-d_Y\left(\varphi_Y(z),\varphi_Y(z')\right)\right|\leq\lambda\varepsilon\ \text{ for all } z,z'\in Z.$$

Therefore,

$$d_{\mathrm{GH}}((X,d_X),(Y,d_Y))=\frac{\lambda}{2}\cdot d_{\mathrm{I},\lambda}^{\mathrm{dynM}}(\gamma_X,\gamma_Y).$$

We have the following bilipschitz-equivalence relation between the metrics $d_{\mathrm{I},\lambda}^{\mathrm{dynM}}$ for different $\lambda>0$.

Proposition A.15 (Bilipschitz-equivalence)**.** For all $0<\lambda<\lambda'$,

$$d_{\mathrm{I},\lambda'}^{\mathrm{dyn}}\leq d_{\mathrm{I},\lambda}^{\mathrm{dynM}}\leq\frac{\lambda'}{\lambda}\cdot d_{\mathrm{I},\lambda'}^{\mathrm{dyn}}.$$

Proof. Fix any two DMSs γ_X and γ_Y over X and Y. That $d_{\mathrm{I},\lambda'}^{\mathrm{dynM}}(\gamma_X,\gamma_Y)\leq d_{\mathrm{I},\lambda}^{\mathrm{dynM}}(\gamma_X,\gamma_Y)$ follows from the observation that any (λ,ε)-tripod R between γ_X and γ_Y is also a (λ',ε)-tripod (Definition 7.8). We next prove $d_{\mathrm{I},\lambda}^{\mathrm{dynM}}(\gamma_X,\gamma_Y)\leq\frac{\lambda'}{\lambda}\cdot d_{\mathrm{I},\lambda'}^{\mathrm{dyn}}(\gamma_X,\gamma_Y)$. For some $\varepsilon\geq 0$ let R be any (λ',ε)-tripod between γ_X and γ_Y. It suffices to show that R is also a $(\lambda,\frac{\lambda'}{\lambda}\varepsilon)$-tripod. Fix any $t\in T$. Then,

$$\bigvee_{[t]^{\left(\frac{\lambda'}{\lambda}\varepsilon\right)}}d_X\leq\bigvee_{[t]^{\varepsilon}}d_X\leq_R d_Y(t)+\lambda'\varepsilon=d_Y(t)+\lambda\left(\frac{\lambda'}{\lambda}\varepsilon\right).$$

By symmetry, we also have $\bigvee_{[t]^{\left(\frac{\lambda'}{\lambda}\varepsilon\right)}}d_Y\leq_R d_X(t)+\lambda\left(\frac{\lambda'}{\lambda}\varepsilon\right)$, as desired. □

B Distance between weighted Reeb graphs

In this section we introduce a distance between weighted Reeb graphs which mediates between $d_{\mathrm{I}}^{\mathrm{F}}$ and $d_{\mathrm{I}}^{\mathrm{R}}$ (cf. Definition 2.15 and Table 3).

Proposition B.1 (Realization as an unlabeled formigram)**.** For any weighted Reeb graph $F : \mathbf{Int} \to \omega\mathbf{set}$, there exists an unlabeled formigram $\theta : \mathbf{Int} \to \mathbf{Part}$ such that $F \cong \mathscr{A} \circ \theta$.

The proof is rather trivial and thus we omit it. In general, a realization of a weighted Reeb graph as an unlabeled formigram is not unique; see Example 3.13. Proposition B.1 allows us to define the following dissimilarity measure on weighted Reeb graphs. From equation (2), recall how to define $d_{\mathrm{I}}^{\mathrm{F}}$ between unlabeled formigrams. For all weighted Reeb graphs $F, G : \mathbf{Int} \to \omega\mathbf{set}$, we define:

$$W(F,G) := \inf\{\varepsilon \in [0,\infty] : \text{there exist } \theta,\theta' : \mathbf{Int} \to \mathbf{Part} \text{ s.t. } F \cong \mathscr{A} \circ \theta, \text{ and } G \cong \mathscr{A} \circ \theta',\ d_{\mathrm{I}}^{\mathrm{F}}(\theta,\theta') = \varepsilon\}. \tag{15}$$

Since a realization of a weighted Reeb graph as an unlabeled formigram is not necessarily unique, we have to possibly take into account multiple realizations of F and G to compute $W(F,G)$. This leads to the fact that W does not necessarily satisfy the triangle inequality and thus we consider the *maximal sub-dominant metric* of W [21] as a metric on weighted Reeb graphs:

Definition B.2 (Metric on weighted Reeb graphs)**.** For any two weighted Reeb graphs $F, G : \mathbf{Int} \to \omega\mathbf{set}$,

$$d_{\mathrm{I}}^{\omega\mathrm{R}}(F,G) := \inf\left\{ \sum_{i=0}^{m-1} W(F_i, F_{i+1}) : \ F = F_1, \dots, F_m = G \text{ is a sequence in } \mathbf{Int}^{\omega\mathbf{set}} \right\}.$$

$d_{\mathrm{I}}^{\omega\mathrm{R}}$ is the greatest metric on weighted Reeb graphs among those upper bounded by W. $d_{\mathrm{I}}^{\omega\mathrm{R}}$ mediates between $d_{\mathrm{I}}^{\mathrm{F}}$ and $d_{\mathrm{I}}^{\mathrm{R}}$:

Theorem B.3. For any two formigrams θ_X and θ_Y, let $\omega(\theta_X)$ and $\omega(\theta_Y)$ be their weighted Reeb graphs. Then,

$$d_{\mathrm{I}}^{\mathrm{R}}(\mathrm{Reeb}(\theta_X), \mathrm{Reeb}(\theta_Y)) \leq d_{\mathrm{I}}^{\omega\mathrm{R}}(\omega(\theta_X), \omega(\theta_Y)) \leq d_{\mathrm{I}}^{\mathrm{F}}(\theta_X, \theta_Y). \tag{16}$$

Proof. From the definition of $d_{\mathrm{I}}^{\mathrm{R}}$ and Proposition 4.13, we have that

$$d_{\mathrm{I}}^{\mathrm{R}}(\mathrm{Reeb}(\theta_X), \mathrm{Reeb}(\theta_Y)) \leq W(\omega(\theta_X), \omega(\theta_Y)).$$

Since $d_{\mathrm{I}}^{\omega\mathrm{R}}$ is the greatest metric on weighted Reeb graphs among those upper bounded by W, the left inequality in (16) follows. The right inequality in (16) directly follows from the definition of $d_{\mathrm{I}}^{\omega\mathrm{R}}$. □

$d_{\mathrm{I}}^{\omega\mathrm{R}}$ is strictly less discriminative than $d_{\mathrm{I}}^{\mathrm{F}}$ whereas strictly more discriminative than $d_{\mathrm{I}}^{\mathrm{R}}$:

Example B.4. (i) Consider θ_X and θ_Y in Example 3.13. Since the underlying weighted Reeb graphs of θ_X and θ_Y are isomorphic, their distance in $d_{\mathrm{I}}^{\omega\mathrm{R}}$ is zero. However, by Remark 4.12 (i), we have that $d_{\mathrm{I}}^{\mathrm{F}}(\mathscr{U}_L^X \circ \theta_X, \mathscr{U}_L^Y \circ \theta_Y) = d_{\mathrm{I}}^{\mathrm{F}}(\theta_X, \theta_Y) > 0$.

(ii) Let F and G be weighted Reeb graphs depicted in Figure 14. Their unweighted Reeb graphs $\mathscr{A} \circ F$ and $\mathscr{A} \circ G$ are clearly isomorphic and thus $d_{\mathrm{I}}^{\mathrm{R}}(\mathscr{A} \circ F, \mathscr{A} \circ G) = 0$. On the other hand, $d_{\mathrm{I}}^{\omega\mathrm{R}}(F,G) = 1/2$; this follows from the observation that both F and G are uniquely realized (up to natural isomorphism) by unlabeled formigrams θ and θ', which leads to $d_{\mathrm{I}}^{\omega\mathrm{R}}(F,G) = d_{\mathrm{I}}^{\mathrm{F}}(\theta,\theta')$. Also, it is not difficult to check that $d_{\mathrm{I}}^{\mathrm{F}}(\theta,\theta') = 1/2$.

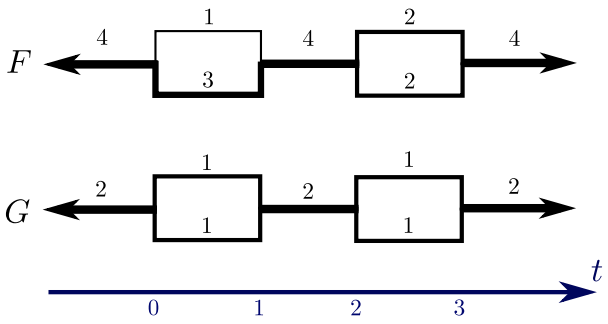


Figure 14: Two weighted Reeb graphs in Example B.4 (ii).

C Smoothing formigrams

The goal of this section is to establish a few basic properties of smoothing of formigrams. In particular, we reveal its effect on the zigzag barcodes of formigrams and its compatibility with smoothing of Reeb graphs in [33]; see Propositions C.2 and C.5.

Recall that a formigram θ_X will be regarded as either a cosheaf-inducing function $\mathbf{R} \to \mathrm{SubPart}(X)$ or a constructible cosheaf $\mathbf{Int} \to \mathrm{SubPart}(X)$ (cf. Definition 3.5, Remark 2.18 (i) and (ii)). By Definition 2.23 and Proposition 2.25, a smoothing operation on formigrams can be induced via the join operation on subpartitions. Namely, $S_\varepsilon\theta_X$ sends each $I \in \mathbf{Int}$ to $\bigvee_{I^\varepsilon} \theta_X := \bigvee\{\theta_X(t) : t \in I^\varepsilon\}$.

Remark C.1 (Comparison with robust grouping structure)**.** The use of the join operation is an important element that distinguishes our notion of smoothing from the *robust grouping structure* in [15]. In particular, given a dynamic metric space (DMS), the induced formigram of this DMS (which is obtained by combining Definition 3.10 and Proposition 7.5) can be smoothed out using the join operation. We emphasize that this smoothing operation is *intrinsic* in contrast to the robust grouping structure from [15]. Namely, our smoothing operation can be carried out *without* constructing any topological space in the spatiotemporal ambient space of the DMS as illustrated in [15, Figure 11]. One consequence of this 'intrinsicality' is that, when a dynamic *graph* is the input data (as opposed to a dynamic *metric space*), we can smooth out its induced formigram (cf. Definition 3.10), while [15] does not propose such a method. Since the coordinates of entities are not always available in applications (e.g. sensor networks [31, 32], low-cost swarm robots [73], etc.), this intrinsicality is a desirable property.

Given a formigram θ_X, Figure 15 illustrates both the relationship between $\mathrm{Reeb}(\theta_X)$ and $\mathrm{Reeb}(S_\varepsilon\theta_X)$ and the relationship between their zigzag barcodes. The following proposition precisely describes the relationship between $\mathrm{barc}_{\mathbf{ZZ}}(\theta_X)$ and $\mathrm{barc}_{\mathbf{ZZ}}(S_\varepsilon\theta_X)$. For any $r \in \mathbf{R}$, we define $-\infty + r$ to be $-\infty$.

Proposition C.2. Let θ_X be a formigram over X and let $\varepsilon \geq 0$. Then, we have the following bijection between $\mathrm{barc}_{\mathbf{ZZ}}(\theta_X)$ and $\mathrm{barc}_{\mathbf{ZZ}}(S_\varepsilon\theta_X)$ (cf. Figure 15):

$$\begin{array}{ccc|l} \mathrm{barc}_{\mathbf{ZZ}}(\theta_X) & & \mathrm{barc}_{\mathbf{ZZ}}(S_\varepsilon\theta_X) & \\ \hline (b,d) & \leftrightarrow & (b+\varepsilon, d-\varepsilon) & \text{for } -\infty \leq b \leq b+\varepsilon < d-\varepsilon \leq +\infty \\ (b,d) & \leftrightarrow & \text{Nothing} & \text{for } b < d < b+2\varepsilon. \\ [b,d) & \leftrightarrow & [b-\varepsilon, d-\varepsilon) & \\ (b,d] & \leftrightarrow & (b+\varepsilon, d+\varepsilon] & \\ [b,d] & \leftrightarrow & [b-\varepsilon, d+\varepsilon] & \end{array} \tag{17}$$

Recall the free functor $\mathscr{F} : \mathbf{set} \to \mathbf{vec}$ (cf. Definition 2.6) and the fact that any constructible cosheaf $\mathbf{Int} \to \mathbf{vec}$ is interval decomposable (cf. Proposition 2.19).

Lemma C.3. Given any constructible cosheaf $F : \mathbf{Int} \to \mathbf{set}$, the barcode of $\mathscr{F} \circ F : \mathbf{Int} \to \mathbf{vec}$ cannot include any interval of the form $[b,a]_{\mathrm{BL}} := \{(x,y) \in \mathbf{Int} : x \leq a < b \leq y\}$ for $a < b$ in $\mathbf{R}$ (cf. Figure 16).

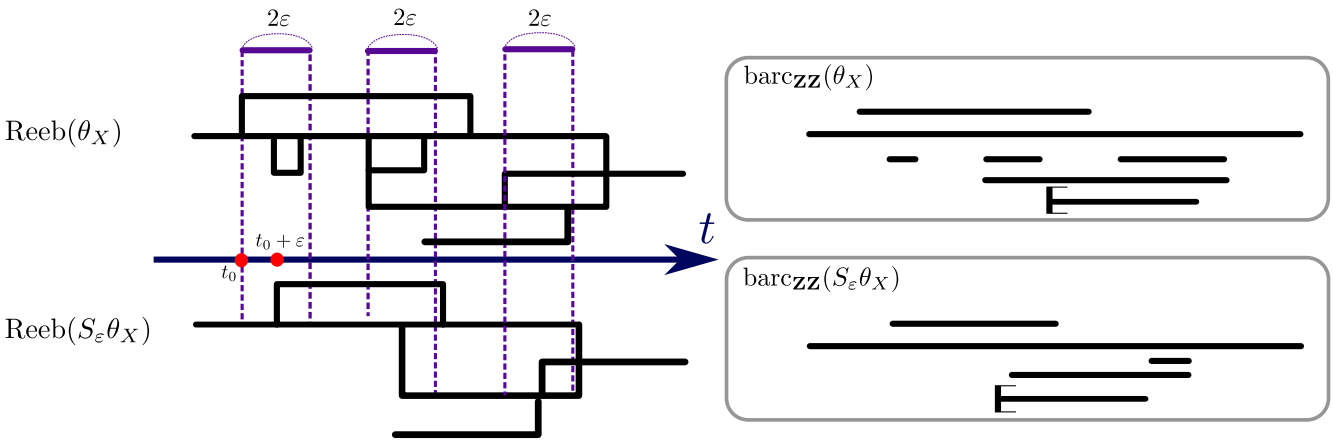


Figure 15: An illustration for Proposition C.2. **Top**: The Reeb graph of a formigram θ_X and its barcode. **Bottom**: The Reeb graph of the formigram $S_\varepsilon\theta_X$ and its barcode. Small loops in $\mathrm{Reeb}(\theta_X)$ disappear in $\mathrm{Reeb}(S_\varepsilon\theta_X)$. In the barcodes, bars with "[" on the left stand for half-closed intervals of the form $[a,b)$. Open intervals in $\mathrm{barc}_{\mathbf{ZZ}}(\theta_X)$ that are shorter than 2ε do not have corresponding intervals in $\mathrm{barc}_{\mathbf{ZZ}}(S_\varepsilon\theta_X)$. Also, disbanding and merging events in θ_X *which do not correspond to vertices on small loops in* $\mathrm{Reeb}(\theta_X)$ are replicated in $S_\varepsilon\theta_X$: disbanding events in θ_X are reflected in $S_\varepsilon\theta_X$ but with delay ε, whereas merging events in θ_X are advanced by ε. For example, observe from the graphs $\mathrm{Reeb}(\theta_X)$ and $\mathrm{Reeb}(S_\varepsilon\theta_X)$ that the disbanding event in θ_X at $t=t_0$ is delayed to $t=t_0+\varepsilon$ in $S_\varepsilon\theta_X$.

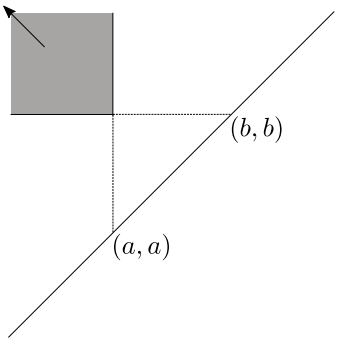


Figure 16: An illustration of $[b,a]_{\mathbf{ZZ}}$ for $a<b$ in $\mathbf{Z}$.

Proof. Since F is constructible is defined via colimits over restrictions of a zigzag diagram over $\mathbf{R}$ (cf. Definition 2.14), for any $J\in\mathbf{Int}$ and for any $x\in F(J)$, there exist $t\in J$ and $y\in F([t,t])$ such that $F([t,t]\subset J)(y)=x$. This property directly implies that the interval module $I^{[b,a]_{\mathrm{BL}}}$ cannot be a summand of $\mathscr{F}\circ F$. □

Proof of Proposition C.2. By Definitions 2.20 and 2.23, $\mathrm{barc}_{\mathbf{ZZ}}(S_\varepsilon\theta_X)$ is equal to the multiset

$$\left\{B\cap\mathbf{R}_{y=x+2\varepsilon} : B\in\mathrm{barc}(\mathscr{F}\circ F)\right\}.$$

where $\mathbf{R}_{y=x+2\varepsilon}$ is the line $y=x+2\varepsilon$ identified with the real line via the bijection $(r-\varepsilon,r+\varepsilon)\leftrightarrow r$. The table (17) is directly obtained by Lemma C.3 and the *block decomposability* of $\mathscr{F}\circ\mathscr{C}\circ\theta_X$ [11, Section 3]. □

The bijective correspondence of barcodes given in Proposition C.2 directly implies the following:

Corollary C.4. Let θ_X be any formigram over X. Then, for $\varepsilon\geq 0$,

$$d_{\mathrm{B}}\left(\mathrm{barc}_{\mathbf{ZZ}}\left(S_\varepsilon\theta_X\right),\ \mathrm{barc}_{\mathbf{ZZ}}\left(\theta_X\right)\right)\leq\varepsilon.$$

The smoothing operations defined for formigrams and Reeb graphs (cf. Definition 2.23) are compatible in the following sense:

Proposition C.5. Let θ_X be a formigram over X. Then, for any $\varepsilon \geq 0$,

$$\mathrm{Reeb}(S_\varepsilon \theta_X) = S_\varepsilon \mathrm{Reeb}(\theta_X).$$

Proof. Let $I \in \mathbf{Int}$. We have:

$$\begin{aligned}
\mathrm{Reeb}(S_\varepsilon\theta_X)(I) &= (\mathscr{C} \circ (S_\varepsilon \theta_X))(I) && \text{by Definitions 2.9 and 5.3}\\
&= \mathscr{C} \circ (S_\varepsilon \theta_X)(I) && \text{by Proposition 5.4}\\
&= \mathscr{C} \circ \theta_X(I^\varepsilon) && \text{by Definition 2.23}\\
&= (\mathscr{C} \circ \theta_X)(I^\varepsilon) && \text{by Proposition 5.4}\\
&= S_\varepsilon \mathrm{Reeb}(\theta_X)(I).
\end{aligned}$$

□

Formigrams change in a continuous manner under ε-smoothing:

Proposition C.6. For any $\varepsilon \geq 0$ and any formigram θ_X,

$$d_{\mathrm{I}}^{\mathrm{F}}(S_\varepsilon \theta_X, \theta_X) \leq \varepsilon.$$

Proof. Consider the tripod $R : X \xleftarrow{\mathrm{id}_X} X \xrightarrow{\mathrm{id}_X} X$ and check that R is an ε-tripod between $S_\varepsilon\theta_X$ and θ_X. □

The following proposition is analogous to [33, Proposition 4.14]:

Proposition C.7. For any $\varepsilon \geq 0$, S_ε is a contraction on formigrams, i.e. for any formigrams θ_X and θ_Y

$$d_{\mathrm{I}}^{\mathrm{F}}(S_\varepsilon\theta_X, S_\varepsilon\theta_Y) \leq d_{\mathrm{I}}^{\mathrm{F}}(\theta_X, \theta_Y).$$

Proof. For $\delta \geq 0$, assume that $R : X \xleftarrow{\varphi_X} Z \xrightarrow{\varphi_Y} Y$ is a δ-tripod between θ_X and θ_Y. We claim that R is also a δ-tripod between $S_\varepsilon\theta_X$ and $S_\varepsilon\theta_Y$. First, we remark that $\varphi_X^* S_\varepsilon \theta_X = S_\varepsilon \varphi_X^* \theta_X$. Indeed, for any $I \in \mathbf{Int}$, $(\varphi_X^* S_\varepsilon \theta_X)(I) = \varphi_X^*(S_\varepsilon\theta_Y(I)) = \varphi_X^*(\theta_X(I^\varepsilon)) = (S_\varepsilon \varphi_X^* \theta_X)(I)$. Therefore,

$$\begin{aligned}
S_\delta\left(\varphi_X^* S_\varepsilon \theta_X\right) &= S_\delta\left(S_\varepsilon \varphi_X^* \theta_X\right)\\
&= S_\varepsilon\left(S_\delta \varphi_X^* \theta_X\right) && \text{by Remark 2.24}\\
&\geq S_\varepsilon \varphi_Y^* \theta_Y && \text{by the choice of } R\\
&= \varphi_Y^* S_\varepsilon \theta_Y
\end{aligned}$$

and by symmetry we have $S_\delta\left(\varphi_Y^* S_\varepsilon \theta_Y\right) \geq \varphi_X^* S_\varepsilon \theta_X$, completing the proof. □

D About the 0-slack interleaving distance between DMSs

We clarify the computational complexity of $d_{\mathrm{I}}^{\mathrm{dynM}}$ (cf. Theorem 7.15) and provide a few examples of computing $d_{\mathrm{I}}^{\mathrm{dynM}}$.

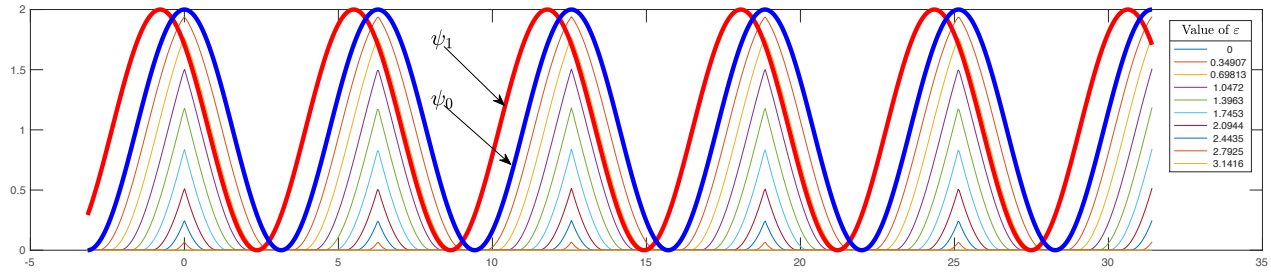


Figure 17: **The interleaving condition.** The thick blue curve and the thick red curve represent the graphs of $\psi_0(t) = 1+\cos(t)$ and $\psi_1(t) = 1+\cos(t+\pi/4)$, respectively. Fixing $\varepsilon \geq 0$, define a function $S_\varepsilon(\psi_0) : \mathbf{R} \to \mathbf{R}$ by $S_\varepsilon(\psi_0)(t) := \min_{s\in[t]^\varepsilon} \psi_0(s)$. The thin curves below the thick blue curve illustrate the graphs of $S_\varepsilon(\psi_0)$ for several different choices of ε. Note that for $\varepsilon \geq \pi/4 \simeq 0.785$, it holds that $S_\varepsilon(\psi_0) \leq \psi_1$.

Computational complexity of $d_{\mathrm{I}}^{\mathrm{dynM}}$. We relate the Gromov-Hausdorff distance between two given ultrametric spaces to the interleaving distance $d_{\mathrm{I}}^{\mathrm{dynM}}$ between certain DMSs induced by those ultrametric spaces. Then, invoking results from F. Schmiedl's PhD thesis [74, 75] we obtain the claim of Theorem 7.15.

Given a ultrametric space (X, u_X), define a DMS $\mathscr{D}(X, u_X) := (X, d_X(\cdot))$ where for all $x, x' \in X$ and for all $t \in \mathbf{R}$, $d_X(t)(x,x') := \max(0, u_X(x,x') - t)$. It is noteworthy that for any $x, x' \in X$, $d_X(\cdot)(x,x') : \mathbf{R} \to \mathbf{R}_+$ is decreasing down to zero and that $d_X(0) = u_X$, a legitimate metric (i.e. not just pseudo-metric), satisfying the second item of Definition 7.1. Furthermore, note that $\mathscr{D}(X, u_X)$ is clearly piecewise linear and that the set of breakpoints is $S_{\mathscr{D}(X,u_X)} = \{u_X(x,x'),\, x, x' \in X\}$. Recall Definition A.2.

Proposition D.1. For any two ultrametric spaces (X, u_X) and (Y, u_Y) we have

$$d_{\mathrm{I}}^{\mathrm{dynM}}(\mathscr{D}(X,u_X), \mathscr{D}(X,u_Y)) = 2\, d_{\mathrm{GH}}((X,u_X),(Y,u_Y)).$$

Proof. Let $\mathscr{D}(X,u_X) = (X, d_X(\cdot))$ and $\mathscr{D}(Y,u_Y) = (Y, d_Y(\cdot))$. Observe that for any $x, x' \in X$, any $t \in \mathbf{R}$, and any $\varepsilon \geq 0$, $\min_{s\in[t]^\varepsilon} d_X(s)(x,x') = d_X(t+\varepsilon)(x,x')$ since d_X is decreasing over time. Thus, for some $\varepsilon \geq 0$, a tripod $R:\ X \xleftarrow{\varphi_X} Z \xrightarrow{\varphi_Y} Y$ is an ε-tripod between $(X,d_X),(Y,d_Y)$ (Definition A.2) if and only if for all $z, z' \in Z$ and for all $t \in \mathbf{R}$, $d_X(t+\varepsilon)\left(\varphi_X(z),\varphi_X(z')\right) \leq d_Y(t)\left(\varphi_Y(z),\varphi_Y(z')\right)$ and $d_Y(t+\varepsilon)\left(\varphi_Y(z),\varphi_Y(z')\right) \leq d_X(t)\left(\varphi_X(z),\varphi_X(z')\right)$, if and only if for all $z, z' \in Z$ and for all $t \in \mathbf{R}$, $\max\left(0, u_X\left(\varphi_X(z),\varphi_X(z')\right) - t - \varepsilon\right) \leq \max\left(0, u_Y\left(\varphi_Y(z),\varphi_Y(z')\right) - t\right)$ and $\max\left(0, u_Y\left(\varphi_Y(z),\varphi_Y(z')\right) - t - \varepsilon\right) \leq \max\left(0, u_X\left(\varphi_X(z),\varphi_X(z')\right) - t\right)$ if and only if for all $z, z' \in Z$,

$$\left|u_X\left(\varphi_X(z),\varphi_X(z')\right) - u_Y\left(\varphi_Y(z),\varphi_Y(z')\right)\right| \leq \varepsilon,$$

completing the proof. □

Proof of Theorem 7.15 Pick any two ultrametric spaces (X, u_X) and (Y, u_Y). Then, by Proposition D.1, the interleaving distance between $\mathscr{D}(X,u_X)$ and $\mathscr{D}(Y,u_Y)$ is identical to twice the Gromov-Hausdorff distance $\Delta := d_{\mathrm{GH}}((X,u_X),(Y,u_Y))$ between (X,u_X) and (Y,u_Y). The rest of the proof follows along the same lines as that of Theorem 4.7. □

Next we discuss a few computational examples of $d_{\mathrm{I}}^{\mathrm{dynM}}$. Let $\psi : \mathbf{R} \to \mathbf{R}_+$ be any non identically zero continuous function. Then, for any finite metric space (X, d'_X) we have the DMS $\gamma_X^\psi = (X, d_X^\psi(\cdot))$ where for $t \in \mathbf{R}$, $d_X^\psi(t) := \psi(t) \cdot d'_X$.

Example D.2 (An interleaved pair of DMSs I)**.** This example refers to Figure 17. Fix the two-point metric space $(X, d_X) = \left(\{x,x'\}, \left(\begin{smallmatrix}0 & 1\\ 1 & 0\end{smallmatrix}\right)\right)$ and consider two DMSs $\gamma_X^{\psi_0} = (X, d_X^{\psi_0})$ and $\gamma_X^{\psi_1} = (X, d_X^{\psi_1})$ where, for $t \in \mathbf{R}$, $\psi_0(t) = 1+\cos(t)$, $\psi_1(t) = 1+\cos(t+\pi/4)$. Then, $\gamma_X^{\psi_0}$ and $\gamma_X^{\psi_1}$ are ε-interleaved if and only if for $i, j \in \{0,1\}$, $i \neq j$, and for all $t \in \mathbf{R}$, $S_\varepsilon(\psi_i)(t) := \min_{s\in[t]^\varepsilon} \psi_i(s) = \left(\bigvee_{[t]^\varepsilon} d_X^{\psi_i}\right)(x,x') \leq d_X^{\psi_j}(t)(x,x') = \psi_j(t)$. In fact, this inequality holds if and only if $\varepsilon \geq \pi/4$, and hence $d_{\mathrm{I}}^{\mathrm{dynM}}\left(\gamma_X^{\psi_0}, \gamma_X^{\psi_1}\right) = \pi/4$ (cf. Figure 17).

The following example generalizes the previous one.

Example D.3 (An interleaved pair of DMSs II)**.** Fix the two-point metric space $(X, d_X) = \left(\{x, x'\}, \left(\begin{smallmatrix} 0 & 1 \\ 1 & 0 \end{smallmatrix}\right)\right)$ and consider two DMSs $\gamma_X^{\psi_0} = (X, d_X^{\psi_0})$ and $\gamma_X^{\psi_1} = (X, d_X^{\psi_1})$ where, for $t \in \mathbf{R}$, $\psi_0(t) = 1 + \cos(\omega t)$, $\psi_1(t) = 1 + \cos(\omega(t+\tau))$, for fixed $\omega > 0$ and $0 < \tau < \frac{2\pi}{\omega}$. Since in this case $\psi_1(t) = \psi_0(t+\tau)$ for all t, one would expect that the interleaving distance between $\gamma_X^{\psi_0}$ and $\gamma_X^{\psi_1}$ is able to uncover the precise the value of τ. In this respect, we have: $d_{\mathrm{I}}^{\mathrm{dynM}}(\gamma_X^{\psi_0}, \gamma_X^{\psi_1}) = \min\left(\tau, \frac{2\pi}{\omega} - \tau\right) =: \eta(\omega, \tau)$.

E Higher dimensional persistent homology barcodes of dynamic metric spaces.

In this section we discuss extendibility of Theorem 7.14. The zigzag barcodes $\mathrm{barc}_{\mathbf{ZZ}}(\theta_X)$ and $\mathrm{barc}_{\mathbf{ZZ}}(\theta_Y)$ in Theorem 7.14 encodes the clustering behaviors of the given DMSs for a fixed scale $\delta \geq 0$. However, we do not need to restrict ourselves to clustering features of DMSs. Imagine that a flock of birds flies while keeping a circular arrangement from time $t = 0$ to $t = 1$. Regarding this flock as a DMS (trajectory data in $\mathbf{R}^3$), we may want to have an interval containing $[0, 1]$ in its *1-dimensional homology barcode*. This idea can actually be implemented as follows.

For a fixed $\delta \geq 0$, we substitute the Rips complex functor $\mathscr{R}_\delta$ for the Rips graph functor $\mathscr{R}_\delta^1$ in Proposition 7.13. What we obtain is a *dynamic simplicial complex or zigzag simplicial filtration*, a generalization of Definition 3.1, induced from any tame DMS γ_X. We then can apply the k-th homology functor to this zigzag simplicial filtration for each $k \geq 0$ in order to obtain a **vec**-valued constructible cosheaf over $\mathbf{R}$. This zigzag module will be a signature summarizing the time evolution of k-dimensional homological features of γ_X. By virtue of Proposition 2.19 we eventually obtain the *k-th homology barcode* $\mathrm{barc}_{\mathbf{ZZ}}\left(\mathrm{H}_k\left(\mathscr{R}_\delta(\gamma_X)\right)\right)$ of γ_X with respect to the fixed scale $\delta \geq 0$; see also [35] for the computation of $\mathrm{barc}_{\mathbf{ZZ}}\left(\mathrm{H}_k\left(\mathscr{R}_\delta(\gamma_X)\right)\right)$ for various δ. In particular, the 0-th homology barcode of the resulting zigzag module coincides with $\mathrm{barc}_{\mathbf{ZZ}}\left(\pi_0\left(\mathscr{R}_\delta^1(\gamma_X)\right)\right)$ as defined in Theorem 7.14.

A natural question is then to ask whether our stability theorem (Theorem 7.14) can be extended to higher dimensional homology barcodes:

Question E.1. For any pair of tame DMSs $\gamma_X = (X, d_X(\cdot))$ and $\gamma_Y = (Y, d_Y(\cdot))$, is it true that for any $\delta \geq 0$ and for any $k \geq 1$,

$$d_{\mathrm{B}}\left(\mathrm{barc}_{\mathbf{ZZ}}\left(\mathrm{H}_k\left(\mathscr{R}_\delta(\gamma_X)\right)\right), \mathrm{barc}_{\mathbf{ZZ}}\left(\mathrm{H}_k\left(\mathscr{R}_\delta(\gamma_Y)\right)\right)\right) \leq 2\, d_{\mathrm{I}}^{\mathrm{dynM}}\left(\gamma_X, \gamma_Y\right) ?$$

Interestingly, we found a family of counter-examples that indicates that stability, as expressed by Theorem 7.14, is a phenomenon which seems to be essentially tied to clustering (i.e. H_0) information.

Theorem E.2. For each integer $k \geq 1$ there exist two different tame DMSs γ_{X_k} and γ_{Y_k}, and $\delta_k \geq 0$ such that $d_{\mathrm{I}}^{\mathrm{dynM}}\left(\gamma_{X_k}, \gamma_{Y_k}\right) < \infty$ but such that the bottleneck distance between the barcodes of $\mathrm{H}_k\left(\mathscr{R}_{\delta_k}\left(\gamma_{X_k}\right)\right)$ and $\mathrm{H}_k\left(\mathscr{R}_{\delta_k}\left(\gamma_{Y_k}\right)\right)$ is unbounded.

Proof. Fix any $k \geq 1$. We will illustrate DMSs γ_{X_k} and γ_{Y_k} as collections of trajectories of points in $\mathbf{R}^{k+1}$, with the metric inherited from the Euclidean metric of $\mathbf{R}^{k+1}$ across all $t \in \mathbf{R}$. For $k = 1$ or $k = 2$, see Figure 18.

Define γ_{X_k} to be the constant DMS consisting of $2(k+1)$ points $\pm e_i = (0, \ldots, 0, \pm 1, 0, \ldots, 0) \in \mathbf{R}^{k+1}$ for $i = 1, 2, \ldots, k+1$. On the other hand, define γ_{Y_k} to be obtained from γ_{X_k} by substituting the still point $+e_1$ of γ_{X_k} by the oscillating point $(1 + \sin^2(t))e_1 = (1 + \sin^2(t), 0, \ldots, 0)$ for $t \in \mathbf{R}$.

It is not difficult to check that $d_{\mathrm{I}}^{\mathrm{dynM}}\left(\gamma_{X_k}, \gamma_{Y_k}\right) \leq \pi/2$. However, with the connectivity parameter $\delta = \sqrt{2}$, their barcodes of the k-th zigzag persistent homology are $\mathrm{barc}_{\mathbf{ZZ}}\left(\mathrm{H}_k\left(\mathscr{R}_\delta(X_k)\right)\right) = \{(-\infty, \infty)\}$ and $\mathrm{barc}_{\mathbf{ZZ}}\left(\mathrm{H}_k\left(\mathscr{R}_\delta(Y_k)\right)\right) = \{[n\pi, n\pi] : n \in \mathbf{Z}\}$, respectively. Therefore, $d_{\mathrm{B}}\left(\mathrm{barc}_{\mathbf{ZZ}}\left(\mathrm{H}_k\left(\mathscr{R}_\delta(X_k)\right)\right), \mathrm{barc}_{\mathbf{ZZ}}\left(\mathrm{H}_k\left(\mathscr{R}_\delta(Y_k)\right)\right)\right) = +\infty$. □

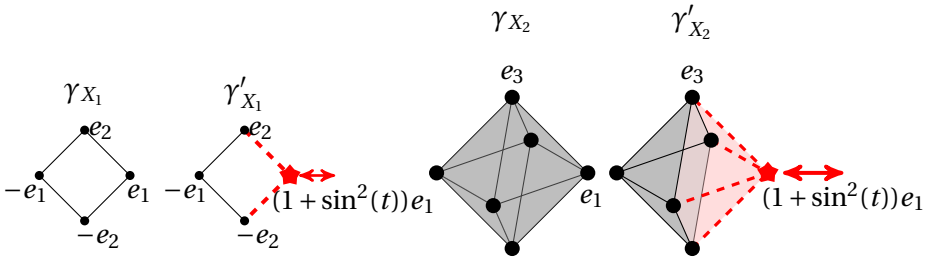


Figure 18: Pairs of DMSs $(\gamma_{X_i}, \gamma'_{X_i})$ for $i = 1,2$ such that $d_{\mathrm{I}}^{\mathrm{dynM}}\left(\gamma_{X_i}, \gamma'_{X_i}\right) \leq \pi/2$. In contrast, for $k = 1$ (or $k = 2$), the bottleneck distance between their k-dimensional zigzag-persistence barcodes is infinite for $\delta \in [\sqrt{2}, 2)$. DMS γ_{X_1}, described as the left-most figure, (γ_{X_2}, the third figure from the left) consists of four (eight) static points located at $\pm e_1 = (\pm 1, 0, 0)$ and $\pm e_2 = (0, \pm 1, 0)$ (and $\pm e_3 = (0, 0, \pm 1)$), respectively. On the other hand, DMS γ'_{X_1}, illustrated at the second from the left (γ'_{X_2}, at the right-most), contains a single oscillating point, denoted by a star shape, with trace $(1+\sin^2(t))e_1$ for $t \in \mathbf{R}$ along with three (five) static points located at $-e_1, +e_2$ and $-e_2$, (and $\pm e_3$), respectively. Then, the 1-dimensional (2-dimensional) zigzag-persistent homology barcode for γ_{X_1} (for γ_{X_2}) consists of exactly one interval $(-\infty, \infty)$, indicating the presence of a loop (a void) for all time. However, the barcode of γ'_{X_1} (γ'_{X_2}) consists of an infinite number of ephemeral intervals $[n\pi, n\pi]$, $n \in \mathbf{Z}$, indicating the on-and-off presence of a loop (a void) that exists only at $t = n\pi$ for $n \in \mathbf{Z}$ in its configuration.

References

[1] H. Adams and G. Carlsson. Evasion paths in mobile sensor networks. *The International Journal of Robotics Research*, 34(1):90–104, 2015.

[2] H. Adams, D. Ghosh, C. Mask, W. Ott, and K. Williams. Efficient evader detection in mobile sensor networks. *arXiv preprint arXiv:2101.09813*, 2021.

[3] G. Azumaya et al. Corrections and supplementaries to my paper concerning Krull-Remak-Schmidt's theorem. *Nagoya Mathematical Journal*, 1:117–124, 1950.

[4] U. Bauer, X. Ge, and Y. Wang. Measuring distance between Reeb graphs. In *Proceedings of the thirtieth annual symposium on Computational geometry*, pages 464–473, 2014.

[5] U. Bauer and M. Lesnick. Induced matchings and the algebraic stability of persistence barcodes. *Journal of Computational Geometry*, 6(2):162–191, 2015.

[6] U. Bauer, E. Munch, and Y. Wang. Strong Equivalence of the Interleaving and Functional Distortion Metrics for Reeb Graphs. In L. Arge and J. Pach, editors, *31st International Symposium on Computational Geometry (SoCG 2015)*, volume 34 of *Leibniz International Proceedings in Informatics (LIPIcs)*, pages 461–475, Dagstuhl, Germany, 2015. Schloss Dagstuhl–Leibniz-Zentrum fuer Informatik.

[7] M. Benkert, J. Gudmundsson, F. Hübner, and T. Wolle. Reporting flock patterns. *Computational Geometry*, 41(3):111–125, 2008.

[8] G. Birkhoff. *Lattice theory*, volume 25. American Mathematical Society New York, 1948.

[9] H. B. Bjerkevik. On the stability of interval decomposable persistence modules. *Discrete & Computational Geometry*, 66(1):92–121, 2021.

[10] J. Bondy and U. Murty. *Graph theory (graduate texts in mathematics)*. Springer New York, 2008.

[11] M. Botnan and M. Lesnick. Algebraic stability of zigzag persistence modules. *Algebraic & geometric topology*, 18(6):3133–3204, 2018.

[12] M. B. Botnan. Interval decomposition of infinite zigzag persistence modules. *Proceedings Of The American Mathematical Society*, 145(8):3571–3577, 2017.

[13] G. E. Bredon. *Sheaf theory*, volume 170. Springer Science & Business Media, 2012.

[14] P. Bubenik and J. A. Scott. Categorification of persistent homology. *Discrete & Computational Geometry*, 51(3):600–627, 2014.

[15] K. Buchin, M. Buchin, M. J. van Kreveld, B. Speckmann, and F. Staals. Trajectory grouping structure. *JoCG*, 6(1):75–98, 2015.

[16] D. Burago, Y. Burago, and S. Ivanov. *A Course in Metric Geometry*, volume 33 of *AMS Graduate Studies in Math*. American Mathematical Society, 2001.

[17] G. Carlsson. Topology and data. *Bulletin of the American Mathematical Society*, 46(2):255–308, 2009.

[18] G. Carlsson and V. De Silva. Zigzag persistence. *Foundations of computational mathematics*, 10(4):367–405, 2010.

[19] G. Carlsson and F. Mémoli. Characterization, stability and convergence of hierarchical clustering methods. *Journal of Machine Learning Research*, 11:1425–1470, 2010.

[20] G. Carlsson and F. Mémoli. Multiparameter hierarchical clustering methods. In *Classification as a Tool for Research*, pages 63–70. Springer, 2010.

[21] G. Carlsson and F. Mémoli. Classifying clustering schemes. *Foundations of Computational Mathematics*, 13(2):221–252, 2013.

[22] G. Carlsson and A. Zomorodian. The theory of multidimensional persistence. *Discrete & Computational Geometry*, 42(1):71–93, 2009.

[23] F. Chazal, D. Cohen-Steiner, M. Glisse, L. J. Guibas, and S. Oudot. Proximity of persistence modules and their diagrams. In *Proc. 25th ACM Sympos. on Comput. Geom.*, pages 237–246, 2009.

[24] F. Chazal, B. T. Fasy, F. Lecci, A. Rinaldo, and L. Wasserman. Stochastic convergence of persistence landscapes and silhouettes. In *Proceedings of the thirtieth annual symposium on Computational geometry*, pages 474–483, 2014.

[25] S. Chowdhury and F. Mémoli. Explicit geodesics in Gromov-Hausdorff space. *Electronic Research Announcements*, 25:48–59, 2018.

[26] N. Clause. Zigzag persistent homology and dynamic networks. https://github.com/ndag/DynGraphZZ, 2021.

[27] N. Clause and W. Kim. Spatiotemporal persistent homology computation tool. https://github.com/ndag/PHoDMSs, 2020.

[28] D. Cohen-Steiner, H. Edelsbrunner, and J. Harer. Stability of persistence diagrams. *Discrete & Computational Geometry*, 37(1):103–120, 2007.

[29] J. Curry and A. Patel. Classification of constructible cosheaves. *Theory and Applications of Categories*, 35(27):1012–1047, 2020.

[30] J. M. Curry. *Sheaves, cosheaves and applications*. University of Pennsylvania, 2014.

[31] V. De Silva and R. Ghrist. Coordinate-free coverage in sensor networks with controlled boundaries via homology. *The International Journal of Robotics Research*, 25(12):1205–1222, 2006.

[32] V. De Silva, R. Ghrist, et al. Homological sensor networks. *Notices of the American mathematical society*, 54(1), 2007.

[33] V. De Silva, E. Munch, and A. Patel. Categorified Reeb graphs. *Discrete & Computational Geometry*, 55(4):854–906, 2016.

[34] T. K. Dey and T. Hou. Computing zigzag persistence on graphs in near-linear time. In *37th International Symposium on Computational Geometry (SoCG 2021)*, volume 189 of *Leibniz International Proceedings in Informatics (LIPIcs)*, pages 30:1–30:15. Schloss Dagstuhl – Leibniz-Zentrum für Informatik, 2021.

[35] T. K. Dey and T. Hou. Updating zigzag persistence and maintaining representatives over changing filtrations. *arXiv preprint arXiv:2112.02352*, 2021.

[36] B. Di Fabio and C. Landi. The edit distance for Reeb graphs of surfaces. *Discrete & Computational Geometry*, 55(2):423–461, 2016.

[37] H. Edelsbrunner, J. Harer, et al. Persistent homology-a survey. *Contemporary mathematics*, 453:257–282, 2008.

[38] H. Edelsbrunner, D. Letscher, and A. Zomorodian. Topological persistence and simplification. *Discrete Comput. Geom.*, 28:511–533, 2002.

[39] P. Gabriel. Unzerlegbare darstellungen i. *Manuscripta mathematica*, 6(1):71–103, 1972.

[40] J. Gamble, H. Chintakunta, and H. Krim. Applied topology in static and dynamic sensor networks. In *2012 International Conference on Signal Processing and Communications (SPCOM)*, pages 1–5. IEEE, 2012.

[41] R. Ghrist and H. Riess. Cellular sheaves of lattices and the Tarski Laplacian. *arXiv preprint arXiv:2007.04099, To appear in Homology, Homotopy and Applications*, 2022.

[42] R. Gonzalez-Diaz, M.-J. Jimenez, and B. Medrano. Spatiotemporal barcodes for image sequence analysis. In *International Workshop on Combinatorial Image Analysis*, pages 61–70. Springer, 2015.

[43] J. Gudmundsson and M. van Kreveld. Computing longest duration flocks in trajectory data. In *Proceedings of the 14th annual ACM international symposium on Advances in geographic information systems*, pages 35–42. ACM, 2006.

[44] J. Gudmundsson, M. van Kreveld, and B. Speckmann. Efficient detection of patterns in 2d trajectories of moving points. *Geoinformatica*, 11(2):195–215, 2007.

[45] M. Hajij, B. Wang, C. Scheidegger, and P. Rosen. Visual detection of structural changes in time-varying graphs using persistent homology. arxiv preprint. *arXiv preprint arXiv:1707.06683*, 3, 2017.

[46] Y. Huang, C. Chen, and P. Dong. Modeling herds and their evolvements from trajectory data. In *International Conference on Geographic Information Science*, pages 90–105. Springer, 2008.

[47] S.-Y. Hwang, Y.-H. Liu, J.-K. Chiu, and E.-P. Lim. Mining mobile group patterns: A trajectory-based approach. In *PAKDD*, volume 3518, pages 713–718. Springer, 2005.

[48] N. Jardine and R. Sibson. *Mathematical taxonomy*. John Wiley & Sons Ltd., London, 1971. Wiley Series in Probability and Mathematical Statistics.

[49] H. Jeung, M. L. Yiu, X. Zhou, C. S. Jensen, and H. T. Shen. Discovery of convoys in trajectory databases. *Proceedings of the VLDB Endowment*, 1(1):1068–1080, 2008.

[50] P. Kalnis, N. Mamoulis, and S. Bakiras. On discovering moving clusters in spatio-temporal data. In *SSTD*, volume 3633, pages 364–381. Springer, 2005.

[51] W. Kim and F. Memoli. Stable signatures for dynamic graphs and dynamic metric spaces via zigzag persistence. *arXiv preprint arXiv:1712.04064v4*, 2017.

[52] W. Kim and F. Mémoli. Formigrams: Clustering summaries of dynamic data. In *Proceedings of 30th Canadian Conference on Computational Geometry (CCCG18)*, 2018.

[53] W. Kim and F. Mémoli. Generalized persistence diagrams for persistence modules over posets. *Journal of Applied and Computational Topology*, 5(4):533–581, 2021.

[54] W. Kim and F. Mémoli. Spatiotemporal persistent homology for dynamic metric spaces. *Discrete & Computational Geometry*, 66(3):831–875, 2021.

[55] W. Kim, F. Mémoli, and Z. Smith. Analysis of dynamic graphs and dynamic metric spaces via zigzag persistence. In *Topological data analysis*, pages 371–389. Springer, 2020.

[56] W. Kim, F. Mémoli, and A. Stefanou. Interleaving by parts for persistence in a poset. *arXiv preprint arXiv:1912.04366*, 2019.

[57] Z. Li, B. Ding, J. Han, and R. Kays. Swarm: Mining relaxed temporal moving object clusters. *Proceedings of the VLDB Endowment*, 3(1-2):723–734, 2010.

[58] S. Mac Lane. *Categories for the working mathematician*, volume 5. Springer Science & Business Media, 2013.

[59] A. McCleary and A. Patel. Bottleneck stability for generalized persistence diagrams. *Proceedings of the American Mathematical Society*, 148(7):3149–3161, 2020.

[60] A. McCleary and A. Patel. Edit distance and persistence diagrams over lattices. *arXiv preprint arXiv:2010.07337*, 2020.

[61] F. Mémoli. A distance between filtered spaces via tripods. *arXiv preprint arXiv:1704.03965*, 2017.

[62] B. Mitchell. *Theory of categories*, volume 17. Academic Press, 1965.

[63] D. Morozov, K. Beketayev, and G. Weber. Interleaving distance between merge trees. *Discrete and Computational Geometry*, 49:22–45, 2013.

[64] E. Munch. *Applications of persistent homology to time varying systems*. PhD thesis, Duke University, 2013.

[65] J. K. Parrish and W. M. Hamner. *Animal groups in three dimensions: how species aggregate*. Cambridge University Press, 1997.

[66] A. Patel. *Reeb spaces and the robustness of preimages*. Duke University, 2010.

[67] A. Patel. Generalized persistence diagrams. *Journal of Applied and Computational Topology*, 1(3):397–419, 2018.

[68] V. Puuska. Erosion distance for generalized persistence modules. *Homology, Homotopy and Applications*, 22(1):233–254, 2020.

[69] C. W. Reynolds. Flocks, herds and schools: A distributed behavioral model. *ACM SIGGRAPH computer graphics*, 21(4):25–34, 1987.

[70] A. Rolle and L. Scoccola. Stable and consistent density-based clustering. *arXiv preprint arXiv:2005.09048*, 2020.

[71] G. Rossetti and R. Cazabet. Community discovery in dynamic networks: a survey. *ACM Computing Surveys (CSUR)*, 51(2):1–37, 2018.

[72] G.-C. Rota. On the foundations of combinatorial theory i. theory of Möbius functions. *Probability theory and related fields*, 2(4):340–368, 1964.

[73] M. Rubenstein, C. Ahler, and R. Nagpal. Kilobot: A low cost scalable robot system for collective behaviors. In *2012 IEEE international conference on robotics and automation*, pages 3293–3298. IEEE, 2012.

[74] F. Schmiedl. *Shape matching and mesh segmentation*. PhD thesis, Technische Universität München, 2015.

[75] F. Schmiedl. Computational aspects of the Gromov–Hausdorff distance and its application in non-rigid shape matching. *Discrete & Computational Geometry*, 57(4):854–880, 2017.

[76] M. Sinhuber and N. T. Ouellette. Phase coexistence in insect swarms. *Physical review letters*, 119(17):178003, 2017.

[77] D. J. Sumpter. *Collective animal behavior*. Princeton University Press, 2010.

[78] C. M. Topaz, L. Ziegelmeier, and T. Halverson. Topological data analysis of biological aggregation models. *PloS one*, 10(5):e0126383, 2015.

[79] A. van Goethem, M. van Kreveld, M. Löffler, B. Speckmann, and F. Staals. Grouping Time-Varying Data for Interactive Exploration. In *32nd International Symposium on Computational Geometry (SoCG 2016)*, volume 51 of *Leibniz International Proceedings in Informatics (LIPIcs)*, pages 61:1–61:16. Schloss Dagstuhl–Leibniz-Zentrum fuer Informatik, 2016.

[80] M. van Kreveld, M. Löffler, F. Staals, and L. Wiratma. A refined definition for groups of moving entities and its computation. *International Journal of Computational Geometry & Applications*, 28(02):181–196, 2018.

[81] C. Vehlow, F. Beck, P. Auwärter, and D. Weiskopf. Visualizing the evolution of communities in dynamic graphs. *Computer Graphics Forum*, 34(1):277–288, 2015.

[82] M. R. Vieira, P. Bakalov, and V. J. Tsotras. On-line discovery of flock patterns in spatio-temporal data. In *Proceedings of the 17th ACM SIGSPATIAL international conference on advances in geographic information systems*, pages 286–295. ACM, 2009.

[83] Y. Wang, E.-P. Lim, and S.-Y. Hwang. Efficient algorithms for mining maximal valid groups. *The VLDB Journal—The International Journal on Very Large Data Bases*, 17(3):515–535, 2008.

[84] Wikipedia. Formicarium — Wikipedia, the free encyclopedia, 2021. [Online; accessed 12-December-2021].

[85] L. Wiratma, M. van Kreveld, M. Löffler, and F. Staals. An experimental evaluation of grouping definitions for moving entities. In *Proceedings of the 27th ACM SIGSPATIAL International Conference on Advances in Geographic Information Systems*, pages 89–98, 2019.

[86] L. Xian, H. Adams, C. M. Topaz, and L. Ziegelmeier. Capturing dynamics of time-varying data via topology. *Foundations of Data Science*, 4(1):1–36, 2022.